Continuous measurements of small systems: Feedback control, thermodynamics, entanglement

Annby-Andersson, Björn

2024

Continuous measurements of small systems

Feedback control, thermodynamics, entanglement

BJÖRN ANNBY-ANDERSSON
DEPARTMENT OF PHYSICS | FACULTY OF SCIENCE | LUND UNIVERSITY

Continuous measurements of small systems
Feedback control, thermodynamics, entanglement

Continuous measurements of small systems

Feedback control, thermodynamics, entanglement

by Björn Annby-Andersson

LUND
UNIVERSITY

Thesis for the degree of Doctor of Philosophy
Thesis advisors: Peter Samuelsson, Patrick P. Potts
Faculty opponent: Prof. Gerard J. Milburn

To be presented, with the permission of the Faculty of Science of Lund University, for public criticism at the Rydberg lecture hall (room H418, Physics Department) on Friday, the 24th of May 2024 at 9:00.

Organization
LUND UNIVERSITY

Department of Physics
Box 118
SE–221 00 Lund
Sweden

Author(s)
Björn Annby-Andersson

Document name
DOCTORAL DISSERTATION

Date of disputation
2024-05-24

Sponsoring organization

Title and subtitle
Continuous measurements of small systems: Feedback control, thermodynamics, entanglement

Abstract
Technological and scientific advancements over the past 30-40 years make it possible to fabricate nanometer-sized systems where fluctuations and quantum effects are important features. These systems can be controlled and measured with high accuracy, making them suitable for exploring fundamendal aspects of the microscopic world. This thesis makes contributions in this direction, focusing on the theory of continuous, Markovian feedback control and stochastic as well as quantum thermodynamics.

In Paper I and III, we study an implementation of Maxwell's demon in a double quantum dot. A feedback protocol, based on charge detection, transfers electrons against an external voltage bias, without performing any net work. The protocol is studied for both classical and quantum dynamics. We characterize the electronic transport properties, explore information-to-work conversion with realistic detector models, as well as the quantum-to-classical transition.

Paper II introduces a novel master equation for continuous, Markovian feedback control. This equation describes the dynamics of a quantum system and a detector with finite bandwidth. For a fast detector, the equation reduces to a Markovian master equation for the system alone. This equation can describe protocols that depend linearly as well as nonlinearly on the measured signal. For linear protocols, this equation coincides with the Wiseman-Milburn equation, illustrating a compelling connection to previous work in the field.

Paper IV investigates a specific feedback protocol for increasing the entanglement generation in an autonomous thermal machine. Under optimal conditions, we find that the protocol significantly increases the entanglement. The entanglement violates the CHSH inequality and can uphold quantum teleportation.

Paper V presents a setup for generating maximally entangled states in autonomous thermal machines. First, we show that maximal bipartite entanglement can be generated in a system of three qubits. This is later generalized to a setup of $2n - 1$ qubits.

Paper VI develops a model for Bayesian temperature estimation with continuous measurements. We study adaptive as well as non-adaptive strategies, and find that the adaptive strategy improves estimation precision.

Key words
quantum feedback control, stochastic thermodynamics, quantum thermodynamics, entanglement, Maxwell's demon, quantum dots, full counting statistics, open quantum systems, parameter estimation, stochastic processes

Classification system and/or index terms (if any)

Supplementary bibliographical information

Language
English

ISSN and key title

ISBN
978-91-8104-027-2 (print)
978-91-8104-028-9 (pdf)

Recipient's notes

Number of pages
228

Price

Security classification

Signature

Date 2024-04-05

Continuous measurements of small systems

Feedback control, thermodynamics, entanglement

by Björn Annby-Andersson

LUND
UNIVERSITY

A doctoral thesis at a university in Sweden takes either the form of a single, cohesive research study (monograph) or a summary of research papers (compilation thesis), which the doctoral student has written alone or together with one or several other author(s).

In the latter case the thesis consists of two parts. An introductory text puts the research work into context and summarizes the main points of the papers. Then, the research publications themselves are reproduced, together with a description of the individual contributions of the authors. The research papers may either have been already published or are manuscripts at various stages (in press, submitted, or in draft).

Funding information: The thesis work was financially supported by the Swedish Research Council, Grant No. 2018-03921.

Faculty of Science, Department of Physics

ISBN: 978-91-8104-027-2 (print)
ISBN: 978-91-8104-028-9 (pdf)

Printed in Sweden by Media-Tryck, Lund University, Lund 2024

Till mamma och pappa

Contents

List of publications

This thesis is based on the following publications, referred to by their Roman numerals:

I **Maxwell's demon in a double quantum dot with continuous charge detection**

Björn Annby-Andersson, Peter Samuelsson, Ville F. Maisi, and Patrick P. Potts
Phys. Rev. B 101, 165404 (2020)

II **Quantum Fokker-Planck Master Equation for Continuous Feedback Control**

Björn Annby-Andersson, Faraj Bakhshinezhad, Debankur Bhattacharyya, Guilherme De Sousa, Christopher Jarzynski, Peter Samuelsson, and Patrick P. Potts
Phys. Rev. Lett. 129, 050401 (2022)

III **Maxwell's demon across the quantum-to-classical transition**

Björn Annby-Andersson, Debankur Bhattacharyya, Pharnam Bakhshinezhad, Daniel Holst, Guilherme De Sousa, Christopher Jarzynski, Peter Samuelsson, and Patrick P. Potts
(manuscript in preparation)

IV **Steady-state entanglement production in a quantum thermal machine with continuous feedback control**
Giovanni Francesco Diotallevi, **Björn Annby-Andersson**, Peter Samuelsson, Armin Tavakoli and Pharnam Bakhshinezhad
(submitted to New J. Phys.)

V **Maximal steady-state entanglement in autonomous quantum thermal machines**

Shishir Khandelwal, **Björn Annby-Andersson**, Giovanni Francesco Diotallevi, Andreas Wacker, and Armin Tavakoli
(submitted to Phys. Rev. Lett.)

VI **Probe thermometry with continuous measurements**

Julia Boeyens, **Björn Annby-Andersson**, Pharnam Bakhshinezhad, Géraldine Haack, Martí Perarnau-Llobet, Stefan Nimmrichter, Patrick P. Potts and Mohammad Mehboudi
New J. Phys. 25 123009 (2023)

Publications not included in this thesis:

Continuous feedback protocols for cooling and trapping a quantum harmonic oscillator
Guilherme De Sousa, Pharnam Bakhshinezhad, **Björn Annby-Andersson**, Peter Samuelsson, Patrick P. Potts, and Christopher Jarzynski
(manuscript in preparation)

Acknowledgements

First, I would like to thank my supervisor, Peter, for giving me the opportunity to become a PhD student in his group. I am especially thankful for all the guidance, support, freedom and encouragement during these years. You have given me the opportunity to supervise a number of bachelor and master students – this has been very rewarding. I am also very grateful for your enormous generosity with travel funds. Over the years, I went on several exciting and stimulating trips to other research groups and conferences. Overall, I have learned and developed a lot under your supervision.

I would also like to thank my assistant supervisor, Patrick, for introducing me to many fun problems, and for giving me the chance to interact with his visitors and colleagues. My and Pharnam's visit to Basel was great! Thanks for always being positive, letting me explore various concepts in my own pace, and for providing constructive feedback. This has been very valuable for my development as a PhD student.

To all the members of Peter's group, both during my time as a master student as well as a PhD student, thanks! It was great getting to know you. We had many nice discussions during the group meetings. Especially, I want to thank Pharnam for all our discussions. They were really helpful. And thanks for hosting me in Vienna!

I want to express my gratitude to the whole Division of Mathematical Physics for all the fun lunch breaks and fikas. Thanks, Armin, for giving me the opportunity to collaborate outside my research group. Over the years, I shared office with many friendly colleagues – Asimina, Alex, Martin, Mattias, Philipp, Jennifer, and Akshat – thanks for all the discussions and fun moments! And sorry if I forgot someone! Especially, I want to thank Jennifer for all the fruitful discussions. I want to thank Tomas for the nice course and conference about gender in science. And most importantly, Katarina – thanks for all the help with administrative tasks, and for all the nice chit-chats in the lunch room.

My research visit to University of Maryland was one of the highlights of my PhD program. I met several nice persons there. Thank you, Chris, for hosting me! Thanks Debankur, Guilherme, Greeshma, Long Him, Josh, Roi and Wade for the nice time we spent together! In particular, I want to thank Debankur for all the nice work we did together, and for showing me around.

I would like to thank Peter, Patrick and Johan Rathsman for providing useful comments when proofreading my thesis. Also, I want to thank Elias for helping me improve the popular summary.

Thanks Patrik, Elias, Ellen, Asimina, Katerina and Orion for all the support and fun moments outside of work. Finally, I want to thank mamma, pappa, Malin, Allan and Cleo for all the support and encouragement.

Populärvetenskaplig sammanfattning på svenska

Denna uppsats sammanställer sex forskningsstudier som undersöker teorin för återkoppling och termodynamik i små system. Den mest centrala studien resulterade i en ekvation som kan beskriva återkoppling i kvantmekaniska system. Många av de övriga studierna utgår från den här ekvationen. Exempelvis studerades en implementation av Maxwells demon i en dubbelkvantprick. Dessutom studerades hur återkoppling kan användas för att stärka sammanflätningen i en mikroskopisk värmemaskin.

Orden 'små system' syftar på strukturer med storlekar i intervallet 1-100 nanometer. Sådana system kan tillverkas på olika sätt. Ett sätt är att begränsa rörelsen hos elektroner i halvledarmaterial till mycket små områden. Sådana områden kallas kvantprickar. Ofta beskrivs de som artificiella atomer eftersom de delar många egenskaper med vanliga atomer. Genom att koppla två närliggande kvantprickar bildas en dubbelkvantprick – en artificiell molekyl. Detta system spelar en stor roll i uppsatsen, eftersom kvantprickar kan kontrolleras och mätas med hög noggrannhet. De är också tillräckligt små för att urskilja kvantmekaniska effekter. Dubbelkvantprickar är därför utmärkta för att studera kvantfysik.

Kvantmekaniska effekter är beteenden som är unika för kvantfysiken och kan inte beskrivas av den klassiska fysiken. En stor skillnad mellan kvantfysik och klassisk fysik är hur partiklar, så som elektroner, atomer eller molekyler, antas bete sig. I den klassika fysiken ses partiklar som små, solida sfärer eller sammansättningar därav. I kvantfysiken kan partiklar även ha vågegenskaper, och det är dessa som ger upphov till kvanteffekter. Vanligtvis upplever vi att kvanteffekter strider mot hur vi uppfattar världen omkring oss. Ett exempel på detta är en elektron som i en dubbelkvantprick kan befinna sig i båda prickarna samtidigt. I den verklighet som vi upplever har objekt alltid har en välbestämd plats – de existerar aldrig på två platser samtidigt. Man kan undra varför vi inte observerar vågegenskaper i vår vardag. Anledningen kallas dekoherens – en process där vågegenskaper störs ut. När en partikel interagerar med sin omgivning (andra partiklar) förloras dess vågegenskaper. Ju större ett objekt är, desto snabbare förloras de. Därför är det enklast att observera kvanteffekter i små system som är välisolerade från sin omgivning.

Ett typexempel på en kvanteffekt är sammanflätning (entanglement på engelska). Det finns både fundamentala och praktiska anledningar för att intressera sig för sammanflätning. Från ett fundamentalt perspektiv är sammanflätning en speciell typ av korrelation som är unik för kvantfysiken. Om vi har två sammanflätade partiklar, och mäter på den ena, kommer en liknande mätning på den andra ge ett utfall som är perfekt korrelerat med utfallet från den första mätningen. Sådana korrelationer kan även existera mellan sammanflätade partiklar som har separerats långt från varandra. Det finns ingen motsvarande korrelation inom den klassiska fysiken. Från ett praktiskt perspektiv är sammanflätning intressant eftersom det kan utnyttjas i olika sammanhang. Detta är den grundläggande idén inom kvantteknologin,

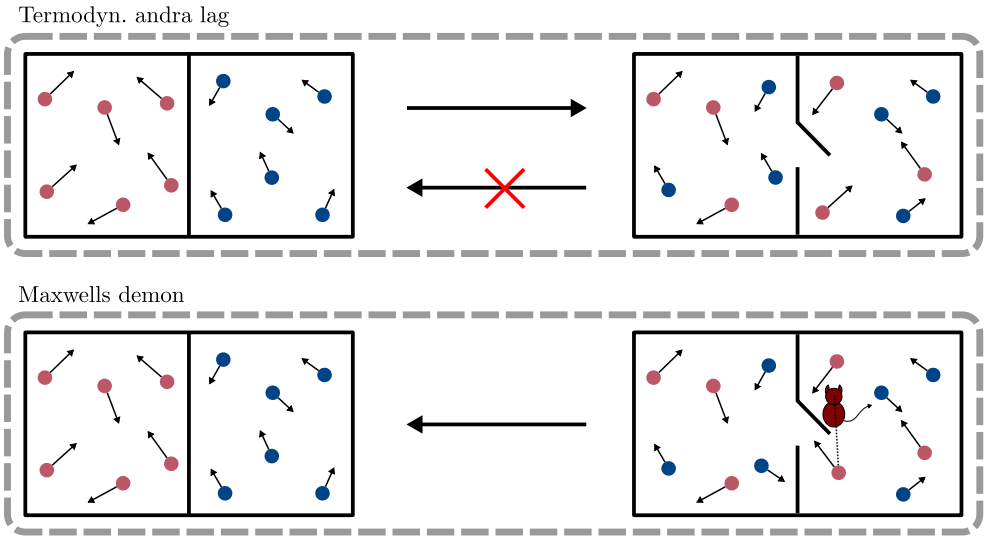

Figur 1: Illustration av termodynamikens andra lag och Maxwells demon.

där sammanflätning används för att utveckla teknologier som kan utföra vissa uppgifter mer effektivt än vad dagens teknologi klarar av. Ett bra exempel är kvantdatorn. För att sådana teknologier ska bli verklighet måste vi förstå hur sammanflätning kan skapas, kontrolleras och stabiliseras.

Just kontroll och stabilisering är centrala koncept för återkopplade reglersystem. Idén med återkoppling är att mäta ett system för att sedan använda den erhållna informationen i syfte att styra systemet. Denna kontrollstrategi har spelat en stor roll för utvecklingen av vårt samhälle, både inom medicin och teknologi. Ett bra exempel är pacemakern, som hjälper hjärtat att slå om det avviker från dess normala rytm. Eftersom små system, t. ex. kvantprickar, kan mätas och kontrolleras med hög noggrannhet förväntas återkoppling spela en stor roll för utvecklingen av kvantteknologier. Det finns dock en rad utmaningar innan sådana teknologier kan bli en kommersiell verklighet. Till exempel, när ett kvantsystem mäts störs dess vågegenskaper. För att bevara vågegenskaperna måste man interagera svagt med systemet. Under de senaste 30–40 åren har metoder för att göra sådana mätningar utvecklats. Flera experiment har demonstrerat hur återkoppling kan användas för att manipulera och stabilisera kvanteffekter. Detta är viktiga steg för utvecklingen av kvantteknologier.

Återkoppling kan också vara intressant i andra sammanhang. Ett bra exempel är Maxwells demon – ett tanke-experiment formulerat av James Clerk Maxwell. Till en början var Maxwells idé att utforska giltigheten hos termodynamikens andra lag. Den andra lagen säger att entropin (oordningen) hos ett system antingen ökar eller är oförändrad. Den övre delen av figur 1 illustrerar den andra lagen. Tänk dig en låda med två gaser, en varm och en kall, som är separerade av en vägg. Om en dörr i väggen öppnas flödar värme från varmt till kallt tills gaserna är blandade och nått en mellanliggande temperatur. Entropin, eller oordningen, ökar. Detta betyder att den omvända processen inte kan ske spontant. Maxwell utmanade

detta i sitt tanke-experiment (se nedre delen av figuren). Om en varelse (demonen) kan se de individuella gaspartiklarna skulle den kunna öppna dörren varje gång en snabb (varm) partikel närmade sig dörren från höger. På samma sätt kan demonen öppna dörren när en långsam (kall) partikel närmar sig från vänster. På så sätt kan varelsen separera gasen i en varm och en kall del, utan att manipulera gaspartiklarna. Entropin måste därför minska i lådan. Betyder detta att processen bryter mot andra lagen? Svaret är nej. Det visar sig att varelsens insamling och processering av information ökar dess entropi. Ökningen av entropi i varelsen är större än minskningen i lådan, vilket medför att den totala entropin ökar. I enlighet med den andra lagen. Maxwells tanke-experiment belyser att det finns ett samband mellan information och termodynamik. Detta är särskilt intressant i små system, t. ex. kvantprickar, där det går att manipulera och mäta enskilda partiklar. Under de senaste 15 åren har Maxwells demon gått från tanke-experiment till verklighet i en mängd olika system, t. ex. i DNA-molekyler och i kvantprickar.

Resultaten i den här avhandlingen bidrar till förståelsen av små system. Speciellt i relation till återkoppling, termodynamik och sammanflätning. Återkopplingsekvationen som härleddes i uppsatsens mest centrala studie är ett komplementerande teoretiskt verktyg för att förstå återkoppling i kvantmekaniska system. Med hjälp av ekvationen går det att göra kvalitativa förutsägningar som tidigare verktyg inte klarade av. Uppsatsens studier av Maxwells demon bidrar med en teoretisk överblick av hur information kan användas för att manipulera elektroner i dubbelkvantprickar. Studierna av sammanflätning i värmemaskiner breddar vår förståelse av hur sammanflätning kan skapas, kontrolleras och stabiliseras. I sin helhet bidrar studierna i uppsatsen till fundamental förståelse av den mikroskopiska världen. Ökad förståelse leder förhoppningsvis till nya verktyg och teknologier som kan förbättra vårt samhälle och vår hälsa.

Chapter 1

Introduction

The technological and scientific advancements over the last 30-40 years have paved the way for fabrication of physical systems with sizes of 1-100 nm. At these length scales, fluctuations and quantum effects, such as tunneling and superposition, become prominent elements of the world. Small systems thus enable the exploration of these effects, and tremendous efforts have been invested in this direction. On the one hand, fundamental aspects are of great interest, with questions such as "How can thermodynamic concepts, such as heat, work, and entropy, be defined in microscopic systems?", "How can microscopic systems be controlled and modeled?", or "What are the energetics of a quantum measurement?". These questions are central in the fields of stochastic [1–10] and quantum [11–14] thermodynamics, as well as in the field of quantum feedback control [15–17]. On the other hand, it is interesting to explore how microscopic properties can be harnessed. This is central for quantum technologies [18], in which quantum features are utilized to outperform classical technologies. Prime examples are quantum cryptography and quantum computers [19]. The realization of quantum technologies partially relies on a good understanding of quantum feedback control and the thermodynamics of small systems. In this thesis, we make contributions to both of these fields, with a strong focus on feedback control.

The interest in thermodynamics in microscopic systems originates from the discoveries of out-of-equilibrium relations during the 1990s [2]. From these emerged the field of stochastic thermodynamics, extending conventional thermodynamics and statistical mechanics from close-to-equilibrium macroscopic systems to microscopic systems operating far from equilibrium. Typically, these systems, e.g., DNA molecules, colloidal particles, and nano-sized electronic circuits, are well-described by classical models. At the heart of the field lies fluctuation theorems, generalizing the second law of thermodynamics for microscopic systems far from equilibrium. Another interesting discovery is the thermodynamic uncertainty relations (TURs) [20], establishing trade-offs between precision and dissipation.

TURs are particularly interesting when studying nanosized thermal machines, where temperature gradients are used to perform useful tasks, such as producing work or cooling.

During the past 15 years, the increased ability to control and measure small systems has stimulated the development of information thermodynamics [21]. This field extends stochastic thermodynamics by including the thermodynamics of acquiring and processing information. This is famously illustrated by Maxwell's demon [22–24], where information is used to rectify heat flows, seemingly violating the second law of thermodynamics. However, by accounting for information in the thermodynamic book-keeping, a violation is not observed. The demon has been realized in a wide range of systems, both in the classical [25–30] as well as the quantum regime [31–34]. This progress has propelled the theoretical development of information thermodynamics, including many generalizations of fluctuation theorems and TURs for feedback-controlled stochastic systems, see, e.g., Refs. [35–37].

Quantum thermodynamics expands these ideas one step further, aiming at defining concepts such as work, heat and entropy in the quantum realm. For instance, fluctuation theorems [7] and TURs [38] have been generalized to quantum systems. The concept of thermal machines can be transferred to the quantum domain as well. In addition to performing "standard" tasks, such as cooling, producing work and keeping time [13], quantum thermal machines can perform tasks that are inherently quantum, like generating entanglement [39]. Therefore, they are interesting platforms for investigating fundamental aspects of quantum physics. Furthermore, the last few years have witnessed an increased interest in exploring the thermodynamics of measurements and feedback control, with various interesting developments. This includes the thermodynamics of quantum measurements [40], as well as the extension of fluctuation theorems [41] and TURs [42] to feedback-controlled quantum systems.

While feedback control is of fundamental interest in thermodynamics, it extends beyond Maxwell's demon. The idea of feedback control is to measure a physical system and use the acquired information to drive the system towards a desired state [43]. During the development of modern society, this control strategy has been of great importance, with inventions such as the pacemaker and ABS breaks. Feedback control can be carried over to the quantum realm, with the aim of controlling quantum dynamics [15–17]. This introduces a number of challenges. For instance, quantum measurements induce dephasing, and it is, therefore, important to minimize backaction, to preserve quantum coherence. Additionally, it is essential to develop accurate control techniques that can steer a system towards a target state, preferably with long coherence times. Already numerous steps have been taken in this direction, including deterministic entanglement generation [44], atomic clocks [45], quantum state stabilization [46–48], and reversing quantum jumps [49].

Semiconductor quantum dots [50] are promising platforms for exploring feedback control and thermodynamics in the microscopic domain [51]. Therefore, quantum dot systems are

central for this thesis. A quantum dot can be thought of as an artificial atom, which can host a single or a few electrons. Often quantum dots are interacting with adjacent electron reservoirs, exchanging energy and particles. They are thus natural testbeds for experiments in thermodynamics. Additionally, quantum dots can be accurately controlled and measured in real time [52–54]. This makes them suitable for feedback experiments. Separating two quantum dots with a tunnel barrier forms a double quantum dot. This platform features quantum effects, such as tunneling and superpositions of charge states. These effects are commonly suppressed by dephasing. However, the large tunability of tunnel barriers in these systems offers the possibility to find a regime where the coherent dynamics is faster than the dephasing. It is thus possible to maintain the quantum features of the system. The double quantum dot thus provides fertile ground for exploring fundamental aspects of quantum physics.

This thesis is a compilation of the six research papers included at the end of this document. These papers explore feedback control and continuous measurements in small systems. An exception is Paper V, which addresses entanglement generation in thermal machines. While some papers consider systems in unspecified platforms, most of them focus on implementations in quantum dots. This includes studies of Maxwell's demon as well as temperature estimation. The main text of this document introduces the background theory required for understanding and reproducing the results of the papers. Note that a substantial part of the main text is adapted from the licentiate thesis by Björn Annby-Andersson [55][1]. The main text covers four topics; stochastic processes and parameter estimation (Chapter 2), open quantum systems (Chapter 3), continuous measurements and feedback control (Chapter 4), and the thermodynamics of small systems (Chapter 5).

[1]The PhD thesis of Debankur Bhattacharyya (University of Maryland, College Park, Maryland, USA), supervised by Christopher Jarzynski, treats similar topics as in this thesis. He will defend his thesis at the end of the spring semester 2024.

Chapter 2

Stochastic processes and parameter estimation

The dynamics of physical systems are commonly described by differential equations. Two important examples are Maxwell's equations and the Schrödinger equation. These descriptions are deterministic, such that if we (with precision) know the initial conditions of a system, we can with certainty predict its future. This is no longer the case when exposing a system to randomly fluctuating forces. The dynamics becomes stochastic and it is difficult to predict its exact future.

A prime example of this is Brownian motion, where the spatial motion of a pollen grain becomes random when suspended in a liquid. The thermal motion of the liquid molecules kicks the pollen grain in random directions, making it impossible to predict its spatial trajectory. Another example is noise in electronic circuits. Here we discuss two sources of such noise, Johnson-Nyquist (thermal) noise [56, 57] and shot noise [58]. At finite temperature, the velocities of electrons in any conductor are thermally distributed. At any instance in time, there is thus a thermally fluctuating current in the conductor, even in the absence of an external voltage source. The magnitude of these fluctuations scales with the square root of the temperature of the conductor. The fluctuations can thus be reduced by cooling. This is known as Johnson-Nyquist noise. Shot noise, on the other hand, is due to the intrinsic properties of a conductor. For instance, consider a solid state device with a tunnel barrier. With a train of electrons approaching the barrier, only a fraction tunnel through it – the others are reflected. The arrival times of tunneling electrons are random, leading to a fluctuating tunnel current with an average determined by the height and width of the barrier. Another random process, central to this thesis, is measurements. The stochasticity of measurements can arise because of various reasons. Here we discuss two. In quantum mechanics, measurements are postulated to be inherently random. For instance, by mea-

suring the position of a quantum particle, the observer obtains a random outcome and the wavefunction collapses on the measured position. Another example, also relevant for classical systems, is the presence of Johnson-Nyquist noise in electronic measurement devices, providing random outcomes.

To model stochastic processes, it is common to employ stochastic differential equations (SDEs). In the physical sciences, SDEs are commonly written as Langevin equations – first order differential equations describing both the deterministic and stochastic contributions to the dynamics of a system. The stochastic contribution is commonly driven by white noise. Later in this chapter, we will see that white noise is an idealization, and that the Langevin equation, therefore, must be handled with care. With too naive mathematical manipulations, one reaches erroneous results. To resolve this issue, one can introduce the concept of Itô calculus, and rewrite the Langevin equation in Itô form. This provides a sound framework for calculations. The Langevin (and Itô) equation typically describes the dynamics of some random system variable. An alternative formulation of the situation is provided by the probability distribution of the random variable. The dynamics of such a distribution is governed by a Fokker-Planck equation – typically formulated as a second order partial differential equation. We note that every Langevin (or Itô) equation has a corresponding Fokker-Planck equation. That is, we can always describe the stochastic dynamics from two points of view – via the stochastic variable or its probability distribution.

The second topic of this chapter is parameter estimation, where the central aim is to use a sequence of measurement outcomes to estimate the value(s) of some unknown parameter(s) of a physical system. Typically, the measurement contains a random component, and the sequence of outcomes thus resembles a stochastic process. The theory of stochastic processes is, therefore, useful when studying parameter estimation. In the literature, one can find various approaches for estimating parameters. Here, we introduce two; the classical (frequentist) and the Bayesian approaches. In particular, we are interested in the Bayesian approach, where the unknown parameter is treated as a random variable – this is central for Paper VI. To provide a broader perspective, we also discuss the classical approach, where the unknown parameter is assumed to be deterministic.

We begin this chapter by briefly discussing stochastic processes in Sec. 2.1. We introduce the concepts of stochastic trajectories, trajectory averages, correlation functions, and Markovian processes. Section 2.2 introduces Langevin, Itô, and Fokker-Planck equations on a general level. We also provide two important examples of stochastic processes, Brownian motion (Wiener process) and the Ornstein-Uhlenbeck process. In Sec. 2.3, we motivate why it is necessary to introduce Itô calculus. Section 2.4 outlines the basics of Bayesian parameter estimation, building on the framework introduced in Sec. 2.1.

2.1 Stochastic processes

Above we introduced a few examples of stochastic processes in physical systems – it could, e.g., be the position of a particle, the current in an electronic circuit, or the outcome of a measurement. In this chapter, we typically denote the value of a random process at time t by a capital letter $X(t)$. The process can be continuous or discrete in time. Any observation of $X(t)$ over time results in a trajectory $\boldsymbol{X} = \{x_0, x_1, \ldots, x_{n-1}\}$, where $x_j = X(t_j)$ is the value of the process at time $t_0 \leq t_j \leq t_{n-1}$, with t_0 and t_{n-1} being the initial and final times of the trajectory, respectively. By observing a very large number of trajectories, we can determine the probability $P[\boldsymbol{X}] = P[x_0, \ldots, x_{n-1}]$ of following a specific trajectory $\boldsymbol{X}$. Integrating $P[\boldsymbol{X}]$ over all possible values except x_j, we get

$$P[x_j] = \int dx_0 \cdots dx_{j-1} dx_{j+1} \cdots dx_{n-1} P[x_0, \ldots, x_{n-1}], \tag{2.1}$$

where $P[x_j]$ is the probability distribution of observing x_j at time t_j. Note that we will use the notations $P[x_j] = P[X(t_j)] = p_{t_j}(x)$ interchangeably. With Bayes' theorem, the probability of observing trajectory $\boldsymbol{X}$ can be written as

$$P[x_0, \ldots, x_{n-1}] = \left[\prod_{j=1}^{n-1} P[x_{n-j} | x_0, x_1, \ldots, x_{n-j-1}] \right] P[x_0], \tag{2.2}$$

where $P[x_{n-j}|x_0, x_1, \ldots, x_{n-j-1}]$ is the transition probability to observe x_{n-j} given that the random process followed trajectory $x_0, x_1, \ldots, x_{n-j-1}$ up till time t_{n-j-1}. With the trajectory probability, we may calculate trajectory averages for functions $f[\boldsymbol{X}]$. The function could, for instance, be the work performed on a system along a trajectory $\boldsymbol{X}$ – this will be the case in Chapter 5, where we define work, heat and entropy along stochastic trajectories of microscopic systems. A trajectory average can be computed with a path integral according to

$$\langle f[\boldsymbol{X}] \rangle = \int \mathfrak{D}[\boldsymbol{X}] f[\boldsymbol{X}] P[\boldsymbol{X}], \tag{2.3}$$

where $\mathfrak{D}[\boldsymbol{X}] = dx_0 \cdots dx_{n-1}$. For functions $f[X(t_j)]$, depending only on the value of $X(t_j)$ at any arbitrary time $t_0 \leq t_j \leq t_{n-1}$, we get the trajectory average

$$\langle f[X(t_j)] \rangle = \int dx_j f[x_j] P[x_j] = \int d[X(t_j)] f[X(t_j)] P[X(t_j)], \tag{2.4}$$

where the two notations to the left and right of the second equal sign will be used interchangeably. We will use this in several parts of the thesis. Trajectory averages are, e.g., important when computing correlation functions, such as

$$\mathcal{C}_X(t, t') = \langle X(t) X(t') \rangle - \langle X(t) \rangle \langle X(t') \rangle. \tag{2.5}$$

Compared to the average $\langle X(t)\rangle$ and the variance $\langle X^2(t)\rangle - \langle X(t)\rangle^2$, the correlation function $\mathcal{C}_X(t,t')$ provides additional information about the dynamics of a stochastic process. In particular, it measures how the value of the process at time t, $X(t)$, influences the value $X(t')$ at a later time $t' > t$. Typically, we are interested in the stationary state of the correlation function, where it only depends on the difference in time $\tau = t' - t$, i.e., when $\mathcal{C}_X(t,t') = \mathcal{C}_X(\tau)$. It is useful to define the power spectrum of the stationary correlator $\mathcal{C}_X(\tau)$ as

$$S_X(\omega) = \int_{-\infty}^{\infty} d\tau e^{i\omega\tau}\mathcal{C}_X(\tau), \tag{2.6}$$

which is the Fourier transform of the correlation function. This provides a spectrum of the underlying frequencies present in the noise of the stochastic process. An important example is delta correlated noise, with stationary correlation function $\mathcal{C}_X(\tau) = \delta(\tau)$, where $\delta(\cdot)$ is the Dirac delta function. Its power spectrum reads $S_X(\omega) = 1$. That is, the spectrum is flat, and contains an equal weight of all frequencies. This is important when, for example, studying Johnson-Nyquist noise [59]. The concept of correlation functions and power spectra will be especially useful in Chapter 3, where we discuss Full counting statistics.

Up to this point, the theory is completely general, and we have not made any strong assumptions, except introducing the concept of having a stationary state. However, it is often required to make assumptions in order to derive analytical results. A common assumption, that is relevant for this thesis, is the one of Markovian dynamics. This means that the transition probabilities only are conditioned on the previous value of the process, rather than the entire trajectory of the process, i.e., $P[x_j|x_0,\ldots,x_{j-1}] = P[x_j|x_{j-1}]$. This is the definition of Markov processes. The trajectory probability for a Markov process [Eq. (2.2)] can be written as

$$P[x_0,\ldots,x_{n-1}] = \left[\prod_{j=1}^{n-1} P[x_{n-j}|x_{n-j-1}]\right] P[x_0]. \tag{2.7}$$

This will be important in Chapter 5 when we derive fluctuation theorems. The probability of observing three consecutive events x_{j-2}, x_{j-1}, and x_j in any Markov process can be written as $P[x_{j-2},x_{j-1},x_j] = P[x_j|x_{j-1}]P[x_{j-1}|x_{j-2}]P[x_{j-2}]$. With Bayes' theorem, we find the Chapman-Kolmogorov equation [59]

$$P[x_j|x_{j-2}] = \int dx_{j-1} P[x_j|x_{j-1}]P[x_{j-1}|x_{j-2}], \tag{2.8}$$

stating that if the transition probabilities $P[x_j|x_{j-1}]$ and $P[x_{j-1}|x_{j-2}]$ are known, we can always find the transition probability $P[x_j|x_{j-2}]$. This will be an important reference when discussing Markovian dynamics of quantum systems in Chapter 3.

2.2 Langevin, Itô, and Fokker-Planck equations

In the previous section, we studied trajectory probabilities of stochastic processes. Now we change focus to stochastic differential equations, and study the dynamics of the random process $X(t)$. In the physical sciences, it is common to write the equation of motion of $X(t)$ as a Langevin equation [59]

$$\dot{X}(t) = \alpha[X(t)] + \beta[X(t)]\xi(t), \tag{2.9}$$

where the dot above $X(t)$ denotes the time derivative, α and β are real functions, and $\xi(t)$ is a time-continuous, rapidly varying random process (noise term) with mean $\langle \xi(t) \rangle = 0$. Here $\langle \cdot \rangle$ denotes a trajectory average as defined in Eq. (2.3). We may assume that the mean is zero as any non-zero mean can be baked into the function α. The first term on the rhs of the Langevin equation describes the deterministic dynamics of the process, and is commonly referred to as a drift term as it describes the overall direction in which $X(t)$ is moving. The second term describes how randomly fluctuating forces influence the dynamics of $X(t)$, and adds noise on top of the deterministic behavior. The noise term is assumed to be stationary, such that its correlation function $\langle \xi(t)\xi(t+\tau) \rangle$ is invariant under translations in t, and thus only depend on the distance τ between two points in time. We require that the correlation function is normalized according to

$$\int_{-\infty}^{\infty} d\tau \langle \xi(t)\xi(t+\tau) \rangle = 1. \tag{2.10}$$

In this way, we assure that $\langle \xi(t)\xi(t+\tau) \rangle$ decays to zero for large τ, such that the present state of $\xi(t)$ is uncorrelated with itself in the distant past. In fact, we will concentrate on Markovian processes, where the characteristic correlation time is so short that for any $\epsilon > 0$, we have

$$\int_{-\epsilon}^{\epsilon} d\tau \langle \xi(t)\xi(t+\tau) \rangle = 1. \tag{2.11}$$

This implies that the noise term is delta correlated, with $\langle \xi(t)\xi(s) \rangle = \delta(t-s)$. The power spectrum [see Eq. (2.6)] is thus flat (as discussed above), and we refer to $\xi(t)$ as a white noise process, as it similarly to white light contains the same weight of all frequencies. In particular, we note that the variance of $\xi(t)$ diverges, $\mathrm{Var}[\xi(t)] = \delta(0)$. This is unphysical, and, therefore, somewhat problematic, but the noise term still has physical meaning. For example, it can serve as a good approximation, or be used to derive other stochastic processes. Because of this, white noise should be considered as an idealization, or a limiting case of a random process that is physical. For instance, the singularity of the variance may be derived from another process $\eta(t)$ with correlation function $\langle \eta(t)\eta(t+\tau) \rangle = \tau_c^{-1} e^{-|\tau|/\tau_c}$, where τ_c is a finite characteristic correlation time. When τ_c is small, formally when $\tau_c \to 0$, we get a delta correlation in accordance with the Markov assumption above. That is, if the characteristic correlation time is very small, we approximate the process as delta correlated.

It should be noted that this approximation can lead to peculiar results, as indicated with the diverging variance above. Therefore, Langevin equations should be treated with care. In general, one must introduce Itô calculus and rewrite the Langevin equation in Itô form, as will be motivated in Sec. 2.3.

The Itô form of the Langevin equation (2.9) is given by

$$dX(t) = a[X(t)]dt + b[X(t)]dW(t), \tag{2.12}$$

where $dX(t) = X(t+dt) - X(t)$ is an infinitesimal increment of the stochastic process, with dt being an infinitesimal timestep, while a and b are real functions related to α and β via

$$\begin{cases} a(x) &= \alpha(x) + \frac{1}{2}\beta(x)\beta'(x), \\ b(x) &= \beta(x), \end{cases} \tag{2.13}$$

where the prime denotes differentiation with respect to x, and $dW(t)$ is a Wiener increment. The Wiener increment stems from the Wiener process (see Sec. 2.2.1), and is a Gaussian random variable with mean $\langle dW(t)\rangle = 0$ and variance $\mathrm{Var}[dW(t)] = dt$. We also note that $dW(t)$ and $dW(t')$, for $t \neq t'$, are independent. This implies that $X(t)$ and $dW(t)$ are independent as well, such that $\langle f[X(t)]dW(t)\rangle = 0$ for any function f. This is rigorously proven in Appendix A. The most important, and also most remarkable[1], property of the Wiener increment is that $[dW(t)]^2 = dt$. This property is the main result of (Itô) stochastic calculus, and is often referred to as the Itô rule. In Sec. 2.3, we motivate the origin of this rule and why it is necessary when manipulating SDEs. An important consequence of the Itô rule arises when studying functions $f[X(t)]$. The infinitesimal increment of the function is given by

$$df(X) = \left[a(X)f'(X) + \frac{1}{2}b^2(X)f''(X)\right]dt + b(X)f'(X)dW, \tag{2.14}$$

where we omitted the time arguments for brevity. To obtain this equation, we expanded $f(X + dX)$ around X to first order in dt. To carry out this expansion, it is important to note that the Itô rule implies that $dW(t)$ scales as $\sqrt{dt}$, which means that $f(X)$ must be expanded to second order in $dW(t)$ to obtain the correct expansion to first order in dt.

It is worth pointing out that the noise term of Eq. (2.12) not necessarily must be Gaussian. If it is non-Gaussian, other rules of stochastic calculus apply [15, 60]. One example is the point process, where $dW(t)$ is replaced by a stochastic variable $dN(t) = 0, 1$. The point process will be important in Chapter 3.4 when we discuss unravelings of quantum master equations. Therefore, we introduce it in detail in that chapter, and focus our discussion on Gaussian noise here, as it is the main process we will look at in this thesis.

[1] That is, the square of the Wiener increment, a random variable, is not a random variable, but is deterministic.

The Itô equation provides a useful tool for simulating trajectories of $X(t)$ and for calculating the statistics of the process. However, solving it analytically is, in general, hard, but there are a few cases where it is possible [60]. The solution of an Itô equation specifies the probability distribution of $X(t)$. One can also think of individual trajectories of $X(t)$ as solutions to the Itô equation. As the increment $dW(t)$ can be chosen in an infinite number of ways, the Itô equation has infinitely many solutions – if all of them were known, we could construct the probability distribution $p_t(x) = P[X(t) = x]$ at all times t. In practice, this is a daunting task as a very large number of trajectories would be required to correctly construct the tails of the distribution. Luckily, the distribution can be found by alternative ways. In fact, every Itô (or Langevin) equation has a corresponding Fokker-Planck equation – a partial differential equation determining the dynamics of $p_t(x)$. In the remaining paragraphs of this section, we outline how the Itô equation (2.12) can be transformed into a Fokker-Planck equation for $p_t(x)$.

We begin by noting that the distribution is given by

$$p_t(x) = \langle \delta[X(t) - x] \rangle = \int d[X(t)] \delta[X(t) - x] P[X(t)], \tag{2.15}$$

where $\langle \cdot \rangle$ again denotes the trajectory average defined in Eq. (2.3). From Eq. (2.14), we find the increment

$$\begin{aligned} d\delta[X(t) - x] = \Big\{ a[X(t)] \delta'[X(t) - x] + \frac{1}{2} b^2[X(t)] \delta''[X(t) - x] \Big\} dt \\ + b[X(t)] \delta'[X(t) - x] dW(t), \end{aligned} \tag{2.16}$$

where primes denote derivatives with respect to $X(t)$. By taking the average $\langle \cdot \rangle$ over this equation, we get

$$dp_t(x) = -\partial_x [a(x) p_t(x)] dt + \frac{1}{2} \partial_x^2 [b^2(x) p_t(x)] dt, \tag{2.17}$$

where we used that $\langle b[X(t)] \delta'[X(t) - x] dW(t) \rangle = 0$ as $X(t)$ and $dW(t)$ are independent – see Appendix A. Since this equation is linear in dt, we find the standard form of the Fokker-Planck equation

$$\partial_t p_t(x) = -\partial_x [a(x) p_t(x)] + \frac{1}{2} \partial_x^2 [b^2(x) p_t(x)]. \tag{2.18}$$

The drift term $a(x)$ determines the deterministic evolution of the stochastic process, i.e., how the center of $p_t(x)$ evolves over time. The diffusion term $b^2(x)$ determines the magnitude of the noise in the process, in other words the width of $p_t(x)$.

The three descriptions above – Langevin, Itô, and Fokker-Planck equations – are equivalent, and can be used to describe the same process. We now briefly study two common processes in terms of these three descriptions.

2.2.1 Brownian motion (Wiener process)

Brownian motion can be defined via the Langevin or Itô equations

$$\dot{X}(t) = \sigma\xi(t) \qquad \text{and} \qquad dX(t) = \sigma dW(t), \tag{2.19}$$

where $\sigma > 0$ is referred to as the diffusion constant. In the case of a particle subjected to thermal fluctuations, σ is proportional to the temperature of its environment. If $\sigma = 1$, we refer to the process as a Wiener process, even though its qualitatively identical to Brownian motion. The Itô equation may be solved by integration,

$$X(t) = \sigma \int_{t_0}^{t} dW(t) = \sigma \lim_{N\to\infty} \sum_{j=0}^{N-1} \delta W(t_0 + j\delta t), \tag{2.20}$$

where we in the last equality discretized time into N segments of length $\delta t = (t - t_0)/N$, and introduced the finite Wiener increment $\delta W(t)$, which is a Gaussian random variable with mean 0 and variance δt. The integral object in this equation is referred to as a (Itô) stochastic integral [59, 60]. In this thesis, we will not need this type of mathematical tools, and will thus not dig deeper into it than this. Instead, we use the sum representation in Eq. (2.20), together with the central limit theorem, to conclude that $X(t)$ is a Gaussian random variable with mean $\langle X(t)\rangle = 0$ and variance $\mathrm{Var}[X(t)] = \sigma^2(t - t_0)$.

Equivalently, one can define Brownian motion via the Fokker-Planck equation

$$\begin{cases} \partial_t p_t(x) &= \frac{\sigma^2}{2}\partial_x^2 p_t(x), \\ p_{t_0}(x) &= \delta(x), \end{cases} \tag{2.21}$$

where the second line defines the intial condition. The solution to this initial value problem reads [59]

$$p_t(x) = \frac{e^{-x^2/2\sigma^2(t-t_0)}}{\sqrt{2\pi\sigma^2(t - t_0)}}. \tag{2.22}$$

That is, $X(t)$ is a Gaussian random variable centered at $x = 0$ with variance $\sigma^2(t-t_0)$, just as above. With the initial value used here, the process describes the position of a Brownian particle moving in one dimension, starting at the origin at t_0. As random, unbiased noise is the only force acting on the particle, it stays at the origin on average. The variance of the position grows linearly with time as the particle always has the possibility of moving far from the origin if it is exposed to the random force for a long time. In Fig. 2.1(a), we illustrate a typical trajectory of Brownian motion in one dimension.

As mentioned above, if $\sigma = 1$, we refer to this process as a Wiener process, and denote it by $W(t)$. A special property of this process is that all increments $\Delta W(t) = W(t + \Delta t) - W(t)$ are independent of each other, and of $W(t)$ for any $\Delta t > 0$. Note that the Wiener increment is Gaussian as well, with $\langle \Delta W(t)\rangle = 0$ and $\mathrm{Var}[\Delta W(t)] = \Delta t$ [59].

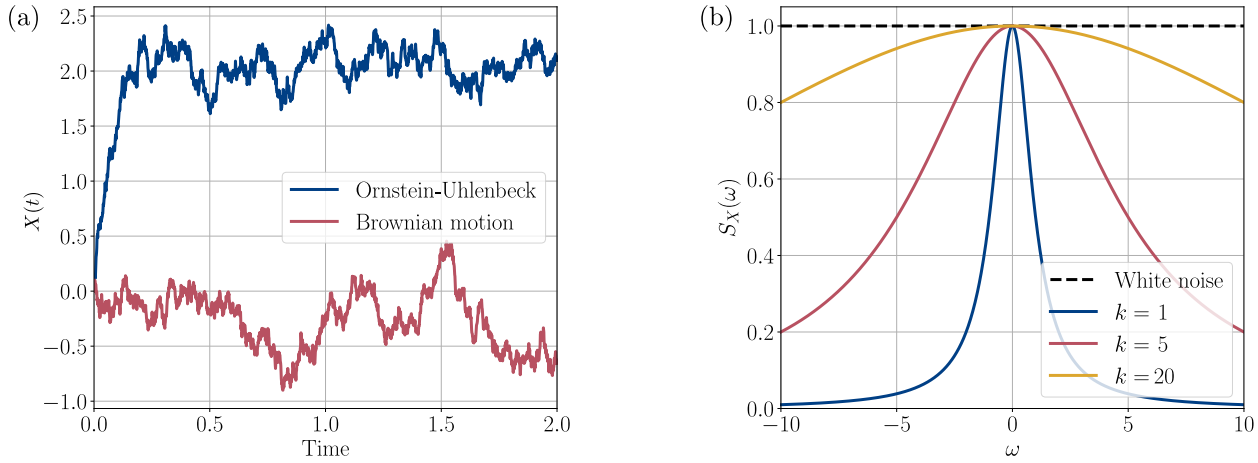

Figure 2.1: (a) Typical trajectories of Brownian motion and the Ornstein-Uhlenbeck process. The Brownian motion stays, on average, around 0, while the Onstein-Uhlenbeck process drifts towards an equilibrium position. To simulate these trajectories, we used the Itô equations (2.19) and (2.23), together with the following parameters, $x_0 = 0$, $\sigma = 30$, $k = 15 \cdot 10^{-3}$, $m = 2$, and $dt = 10^{-3}$. (b) Comparison of the power spectra of a white noise process (black, dashed line) and the Ornstein-Uhlenbeck process [see Eq. (2.28)] for a few choices of k (solid lines). Note that Eq. (2.28) tends to the white noise spectrum as k is increased. Here we use $\sigma = k$, such that the maximum of $S_X(\omega)$ is invariant of different choices of k.

2.2.2 The Ornstein-Uhlenbeck process

The Ornstein-Uhlenbeck process is a generalization of Brownian motion with an additional drift term that drives the process towards a specific position. Its Langevin and Itô equations are given by

$$\dot{X}(t) = k[m - X(t)] + \sigma\xi(t) \qquad \text{and} \qquad dX(t) = k[m - X(t)]dt + \sigma dW(t). \quad (2.23)$$

Here $k, \sigma > 0$ are constants, with units of inverse time, and m determines the position which the system is driven towards [m has the same unit as $X(t)$]. In practice, the Ornstein-Uhlenbeck process describes the position of a Brownian particle with overdamped dynamics in a harmonic potential, where the friction term proportional to $\dot{X}(t)$ dominates over the acceleration term proportional to $\ddot{X}(t)$, such that the latter can be neglected from the equation of motion. The Ornstein-Uhlenbeck process thus describes a noisy relaxation towards an equilibrium position. As we will see in Chapter 4, it can be used to model measurement signals. In fact, the Ornstein-Uhlenbeck process has applications in a wide range of situations, for instance, in financial mathematics, where it is used to model interest rates [61].

The Itô equation in Eq. (2.23) can be solved analytically, see, e.g., Ref. [60], but to avoid clutter, we present only the solution of the corresponding Fokker-Planck equation. The solutions are equivalent anyway. The Fokker-Planck equation is given by

$$\begin{cases} \partial_t p_t(x) &= k\partial_x[(x - m)p_t(x)] + \frac{\sigma^2}{2}\partial_x^2 p_t(x), \\ p_0(x) &= \delta(x - x_0), \end{cases} \quad (2.24)$$

where the initial distribution is centered at some arbitrary value x_0. The solution reads

$$p_t(x) = \sqrt{\frac{k}{\pi\sigma^2(1-e^{-2kt})}} e^{-\frac{k}{\sigma^2(1-e^{-2kt})}\left[x-m(1-e^{-kt})-x_0e^{-kt}\right]^2}. \tag{2.25}$$

The Ornstein-Uhlenbeck process is thus a Gaussian random variable with mean $\langle X(t)\rangle = m(1-e^{-kt}) + x_0e^{-kt}$ and variance $\mathrm{Var}[X(t)] = \sigma^2(1-e^{-2kt})/2k$. In the stationary limit, we obtain

$$p_{\mathrm{ss}}(x) = \lim_{t\to\infty} p_t(x) = \sqrt{\frac{k}{\pi\sigma^2}} e^{-\frac{k}{\sigma^2}(x-m)^2}. \tag{2.26}$$

The Ornstein-Uhlenbeck process thus reaches a stationary distribution – this was not the case with Brownian motion. In fact, the Ornstein-Uhlenbeck process is the only single-variable stochastic process which is Gaussian, Markovian, and has a stationary distribution [59]. We also see that Eqs. (2.25) and (2.26) provide a nice illustration of the noisy relaxation mentioned above. At $t = 0$, the process starts at the initial position x_0 and makes a random walk towards the equilibrium position $x = m$. The timescale of the relaxation is determined by $1/k$. The variance is 0 at time $t = 0$ (we know exactly where the particle is), and grows towards $\sigma^2/2k$ at a rate given by $2k$. We illustrate a sample trajectory of the Ornstein-Uhlenbeck process in Fig. 2.1(a).

The stationary correlation function of the Ornstein-Uhlenbeck process is given by [59]

$$\mathcal{C}_X(\tau) = \frac{\sigma^2}{2k} e^{-k|\tau|}. \tag{2.27}$$

That is, the correlation between two points in time separated by τ decays exponentially on a timescale $1/k$, as expected for a Markovian process. Its power spectrum [see Eq. (2.6)] reads

$$S_X(\omega) = \frac{\sigma^2}{k^2+\omega^2}. \tag{2.28}$$

The spectrum thus has a Lorentzian shape with width $2k$ (full width at half maximum). In Fig. 2.1(b), we compare Eq. (2.28) to the spectrum of white noise for different choices of k, where we use $\sigma = k$ such that the maximum of $S_X(\omega)$ remains invariant under changes of k. We observe that the width of the spectrum increases with k, and in the limit $k \to \infty$, we recover the white noise spectrum. This can also be seen from the correlation function, $\mathcal{C}_X(\tau) \to \delta(\tau)$ as $k \to \infty$ for $\sigma = k$.

2.3 Motivation for stochastic calculus

In this section, we provide a motivation for why stochastic calculus and the Itô equation are necessary for obtaining sensible results. In fact, the Langevin equation, or rather the

white noise term $\xi(t)$ in Eq. (2.9), is not rigorously defined – a too naive mathematical treatment leads to the wrong results. We begin by motivating this, and then show how we can go from the Langevin equation to the Itô equation. Note that the idea of this section is to motivate why stochastic calculus is needed, rather than providing rigorous derivations. We closely follow the discussions in Refs. [15] and [59].

We begin by assuming that $X(t)$ and $\xi(t)$ are statistically independent, and that $\dot{X} = dX/dt$. The latter assumption corresponds to what we would expect from conventional calculus. We now show that these two assumptions cannot be true simultaneously, and that one of them needs to be relaxed. To this end, it is illuminating to calculate the infinitesimal increment $dX(t) = X(t+dt) - X(t)$. The Langevin equation (2.9) provides the following result,

$$dX(t) = \alpha[X(t)]dt + \beta[X(t)]\xi(t)dt. \qquad \text{(wrong)} \tag{2.29}$$

We indicate already here that this result is wrong, and should not be used for calculations – we only work with it in this paragraph to highlight the subtleties of the Langevin equation. It yields the average increment $\langle dX(t)\rangle = \langle \alpha[X(t)]\rangle dt$, which is independent of the noise term, as expected from the assumptions. For the variance of the increment, we get $\mathrm{Var}[dX(t)] = \langle [dX(t)]^2\rangle = 0$, where we used that all nonlinear terms in dt vanish. This suggests that the increments are deterministic, and that the noise term does not induce any noise to the process – quite contrary to what to expect from a stochastic process. We understand that our two assumptions cannot be true simultaneously. Here we will relax the second assumption. That is, the fluxion $\dot{X}$ will not be interpreted as dX/dt, but we still assume independence between $X(t)$ and $\xi(t)$. Note that we are not required to make this relaxation – one can still assume that $\dot{X} = dX/dt$ holds, but must then relax the other assumption. Equation (2.9) is then referred to as a Stratonovich equation, and requires computational tools that are not discussed here [15].

To further motivate why we relaxed this assumption, we will, in this paragraph, assume that $\dot{X} = dX/dt$ holds, and show that we run into other problems than the one above. Under this assumption, the solution to Eq. (2.9) would read

$$X(t) - X(t_0) = \int_{t_0}^{t} dt' \alpha[X(t')] + \int_{t_0}^{t} dt' \beta[X(t')]\xi(t'). \tag{2.30}$$

For this to hold, the function

$$W(t) = \int_{t_0}^{t} dt' \xi(t') \tag{2.31}$$

must exist. From the central limit theorem, $W(t)$ can be shown to be a Gaussian random variable with mean 0 and variance $t - t_0$. In fact, $W(t)$ is a Wiener process [59]. Because of the fractal structure of $W(t)$, see Fig. 2.2, it is impossible to linearize it as $h \to 0$ in

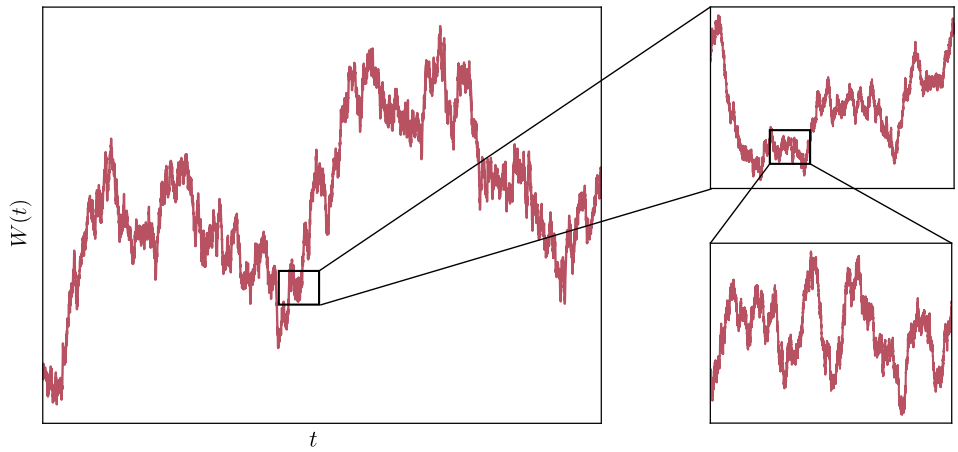

Figure 2.2: Illustration of the fractal structure of a Wiener process $W(t)$. When zooming in, the Wiener process never becomes linear. Therefore, it has no derivative.

$[W(t+h)-W(t)]/h$. Therefore, the derivative $\dot{W}(t)$, and thereby also $\xi(t)$, does not exist in a rigorous mathematical sense [59]. This provides further support why $\dot{X} \neq dX/dt$. Despite being nonexistent in a mathematical sense, we will continue to use $\xi(t)$ in our discussion as it is commonly used in the physical sciences.

From the discussion in the preceding paragraphs, we understand that analyzing and solving the stochastic differential equation (2.9) raise several warning bells, indicating that the equation must be treated with care. As conventional calculus does not apply as we are used to, one way to proceed is to introduce Itô calculus, and rewrite Eq. (2.9) in Itô form. Itô calculus provides computational rules that allow us to calculate and manipulate the increment dX in a mathematically and physically sensible way.

To introduce Itô calculus, we begin by studying the Wiener process in Eq. (2.31), and note that for $t > s$

$$W(t) - W(s) = \int_s^t dt' \xi(t'), \tag{2.32}$$

implying that any Wiener increment $\Delta W(t) = W(t + \Delta t) - W(t)$ is independent of $W(t)$, as discussed above. We also note that $\Delta W(t)$ is Gaussian with $\langle \Delta W(t) \rangle = 0$ and $\text{Var}[\Delta W(t)] = \langle \Delta W^2(t) \rangle = \Delta t$, as we expect for the Wiener process, see discussion above. This gives us the infinitesimal increment $dW(t) = \xi(t)dt$, suggesting that $\xi(t)$ is the derivative $dW(t)/dt$. As noted above, mathematically this derivative does not exist, but is still used here (and in the physical sciences) because of the convenient notation. The increment should, as we stated above, satisfy $[dW(t)]^2 = dt$.

To understand why, we make use of a small Wiener increment $\delta W(t) = W(t+\delta t) - W(t)$ and study it over a time period $\Delta t = t - t_0$. By discretizing Δt into N intervals, $\delta t =$

$\Delta t/N$. We now define a quantity

$$\chi = \sum_{j=0}^{N-1} [\delta W(t_j)]^2, \tag{2.33}$$

where $t_j = t_0 + j\delta t$. The mean and variance of χ are given by

$$\begin{cases} \langle \chi \rangle & = \Delta t, \\ \langle \chi^2 \rangle - \langle \chi \rangle^2 & = \frac{\Delta t}{N/2}. \end{cases} \tag{2.34}$$

In the continuous limit, $N \to \infty$, the variance vanishes and χ becomes deterministic – more specifically, $\chi \to \Delta t$. In this limit, we may interpret the sum in Eq. (2.33) as an integral, and we get

$$\Delta t = \int_t^{t+\Delta t} dt = \int_t^{t+\Delta t} dW^2, \tag{2.35}$$

where we omitted the time argument for brevity. This implies the Itô rule $dW^2 = dt$. When we analyzed Eq. (2.9) above, we thought that $dW = \xi(t)dt$ was scaling as dt. The Itô rule teaches us that dW actually scales as $\sqrt{dt}$, and partly explains why our analysis of Eq. (2.9) went wrong. At this point, it is tempting to replace $\xi(t)dt$ with dW in Eq. (2.29), but a little more care is needed to find the correct form for the infinitesimal increment $dX(t)$.

To find the increment $dX(t)$ corresponding to Eq. (2.9), we Taylor expand $X(t + dt)$ as

$$X(t + dt) = e^{dt\partial_s} X(s)\Big|_{s=t}, \tag{2.36}$$

where we write the expansion as an exponential function for brevity. In fact, all terms in the expansion are not needed, only the ones scaling as dt. To calculate the derivatives $\partial_s^n X(s)$ ($n > 1$), we assume that

$$\partial_s X(s)\Big|_{s=t} = \Big(\alpha[X(s)] + \beta[X(s)]\xi(t)\Big)\Big|_{s=t}. \tag{2.37}$$

This assumption is based on the fact that $\xi(t)$ in reality must have a small, but finite correlation time τ_c over which it remains constant. That is, during an infinitesimal time increment $dt \ll \tau_c$, $\xi(t)$ is constant, and is not affected by time derivatives of Eq. (2.37). Using this, as well as the first and second order terms in the Taylor expansion (2.36), alternatively to first order in dt, i.e., second order in $dW(t) = \xi(t)dt$ due to the Itô rule, we get the correct increment (the Itô equation)

$$dX(t) = a[X(t)]dt + b[X(t)]dW(t), \tag{2.38}$$

where the coefficients $a[X(t)] = \alpha[X(t)] + \frac{1}{2}\beta[X(t)]\beta'[X(t)]$ and $b[X(t)] = \beta[X(t)]$ show the relation to Eq. (2.9). The prime in $a[X(t)]$ denotes the derivative with respect to $X(t)$. We can now calculate the variance of the increment – it is given by

$$\langle (dX)^2 \rangle = \langle b^2(X) \rangle dt, \tag{2.39}$$

where we used that $\langle dX \rangle = \langle a(X) \rangle dt$, and that $X(t)$ and $dW(t)$ are independent. That is, the variance of the increment is nonzero, indicating that the noise term induces noise in the process, as desired. This motivates why Itô calculus is required to obtain reasonable results, and why the increment in Eq. (2.29) should be avoided.

2.4 Bayesian parameter estimation

In this section, we discuss parameter estimation. We introduce both the classical (frequentist) and Bayesian philosophies. Especially the latter is important for Paper VI. However, it is interesting to introduce both philosophies to provide a broader perspective. More detailed discussions can be found in Refs. [62, 63].

The typical scenario of parameter estimation is the following. Consider a system with an unknown parameter θ (temperature, chemical potential, mass, etc.) that we want to estimate. We do this by recording n measurements of some system property, and put our observations into a vector $\boldsymbol{x} = (x_1, \ldots, x_n)$. The unknown parameter is estimated by constructing an estimator $\hat{\theta}(\boldsymbol{x})$, taking the measurement outcomes as input. The method for constructing estimators and deciding their performance depends on the philosophy that is employed.

Classical approach

In the classical approach, the parameter θ is deterministic, and has a true, but unknown, value θ_0. The measurement record $\boldsymbol{x}$ is random, and sampled from a distribution $p(\boldsymbol{x}; \theta_0)$, depending on the true value θ_0. We assume that all outcomes are independent, such that

$$p(\boldsymbol{x}; \theta_0) = \prod_{j=1}^{n} p(x_j; \theta_0), \tag{2.40}$$

where $p(x_j; \theta_0)$ is the probability distribution of observing the outcome x_j when θ_0 is the true value. An estimator $\hat{\theta}(\boldsymbol{x})$ is a random variable depending on the recorded data. The estimator is said to be consistent[2] if $\hat{\theta}(\boldsymbol{x}) \to \theta_0$ as $n \to \infty$. The average of the estimator

[2]A more rigorous definition is that the probability $P[|\hat{\theta}(\boldsymbol{x}) - \theta_0| > \varepsilon] \to 0$ as $n \to \infty$ for any $\varepsilon > 0$.

over all possible realizations of the measurement is defined via

$$\mathrm{E}[\hat{\theta}(\boldsymbol{x})] = \int \mathfrak{D}[\boldsymbol{x}]\hat{\theta}(\boldsymbol{x})p(\boldsymbol{x};\theta_0), \tag{2.41}$$

which is similar to the average in Eq. (2.3). In general, $\mathrm{E}[\hat{\theta}(\boldsymbol{x})] = \theta_0 + b$, where b is referred to as the bias. For $b = 0$, the estimator is said to be unbiased. The error of an estimator is commonly defined as the mean square error (MSE)

$$\mathrm{MSE}(\hat{\theta}) = \mathrm{E}\left[\left(\theta_0 - \hat{\theta}(\boldsymbol{x})\right)^2\right] = \mathrm{Var}[\hat{\theta}(\boldsymbol{x})] + b^2, \tag{2.42}$$

where $\mathrm{E}[\cdot]$ and $\mathrm{Var}[\cdot]$ are calculated with respect to $p(\boldsymbol{x};\theta_0)$. For unbiased estimators, the MSE coincides with the variance of the estimator, and obeys the Cramer-Rao inequality [64, 65]

$$\mathrm{Var}[\hat{\theta}(\boldsymbol{x})] \geq \frac{1}{ni(\theta_0)}, \tag{2.43}$$

where

$$i(\theta_0) = -\mathrm{E}\left[\frac{\partial^2 \ln[p(x;\theta)]}{\partial\theta^2}\Big|_{\theta=\theta_0}\right] = -\int dx \frac{\partial^2 \ln[p(x;\theta)]}{\partial\theta^2}\Big|_{\theta=\theta_0} p(x;\theta_0) \tag{2.44}$$

is the Fisher information for one observation. The Fisher information tells us how much information we obtain, on average, by doing the measurement. Note that the Fisher information is related to the curvature of $p(x;\theta)$ with respect to θ, and thus contains information on how broadly peaked $p(x;\theta)$ is around θ_0. For a broad (narrow) peak, i.e., when $i(\theta_0)$ is small (large), we obtain less (more) information. The Fisher information for the entire measurement record is given by $I(\theta_0) = ni(\theta_0) = -\mathrm{E}\{\partial^2 \ln[p(\boldsymbol{x};\theta)]/\partial\theta^2\big|_{\theta=\theta_0}\}$. The Cramer-Rao inequality provides a universal bound on how small the MSE can be for unbiased estimators. An estimator reaching the lower bound is said to be efficient. We note that by letting n become large, the lower bound becomes very small, suggesting that it is possible to estimate the unknown parameter arbitrarily close to θ_0.

A common classical approach for obtaining estimators is the maximum likelihood (ML) method. In general, the distribution $p(\boldsymbol{x};\theta)$ is known up to the unknown parameter θ. The ML estimator is defined as

$$\hat{\theta} = \arg\max_{\theta} p(\boldsymbol{x};\theta). \tag{2.45}$$

Often it is easier to find the maximum of $\ln[p(\boldsymbol{x};\theta)]$ which coincides with the maximum of $p(\boldsymbol{x};\theta)$. When n is large, the ML estimator approaches a Gaussian random variable centered at the true value θ_0, with variance $1/ni(\theta_0)$ [62]. Adding more data thus improves the estimation.

Bayesian approach

In the Bayesian approach, we assume that the unknown parameter is a random variable. Often, we have some prior knowledge about θ, and we encode this into a prior distribution $p(\theta)$. We could, for instance, know that the parameter is restricted to a certain interval $\theta_1 \leq \theta \leq \theta_2$. Such knowledge often leads to more accurate estimations – especially for small n [62]. By assuming a certain probability distribution $p(\boldsymbol{x}|\theta)$ (likelihood function) for obtaining the measurement record $\boldsymbol{x}$, given that θ is the value of the unknown parameter, we find, via Bayes' rule, the posterior distribution

$$p(\theta|\boldsymbol{x}) = \frac{p(\boldsymbol{x}|\theta)p(\theta)}{p(\boldsymbol{x})}, \tag{2.46}$$

with $p(\boldsymbol{x}) = \int d\theta p(\boldsymbol{x}|\theta)p(\theta)$. The posterior distribution tells us how likely it is for θ to take certain values, given that we observed the record $\boldsymbol{x}$. Here we assume that the observations are independent, such that $p(\boldsymbol{x}|\theta) = \prod_{j=1}^{n} p(x_j|\theta)$, where $p(x_j|\theta)$ is the probability to observe outcome x_j given θ.

To define a Bayesian estimator, we must first introduce some additional quantities. First, we define the error as $\epsilon = \theta - \hat{\theta}$, where $\hat{\theta}$ is an arbitrary Bayesian estimator, which, as we will see below, is dependent on the measurement data $\boldsymbol{x}$. In contrast to the classical approach, we do not make use of the true (but unknown) value θ_0 to define the error. Note that the error is a random variable, as θ and $\hat{\theta}$ are random variables. Second, we introduce a cost function of the error, $C(\epsilon)$. This function tells us how "costly" an error is. For instance, if $C(\epsilon) = \epsilon^2$, the cost of errors grow quadratically, penalizing large errors harder than smaller errors. Below we explore a few different cost functions. Finally, we introduce the risk function

$$\begin{aligned} R = \mathrm{E}[C(\theta - \hat{\theta})] &= \int \mathfrak{D}[\boldsymbol{x}] \int d\theta C(\theta - \hat{\theta}) p(\boldsymbol{x}, \theta) \\ &= \int \mathfrak{D}[\boldsymbol{x}] \left(\int d\theta C(\theta - \hat{\theta}) p(\theta|\boldsymbol{x}) \right) p(\boldsymbol{x}), \end{aligned} \tag{2.47}$$

where the average is taken with respect to the joint distribution $p(\boldsymbol{x}, \theta)$. In the second line, we used $p(\boldsymbol{x}, \theta) = p(\theta|\boldsymbol{x})p(\boldsymbol{x})$. An estimator is found by minimizing the risk function with respect to $\hat{\theta}$, which corresponds to

$$\hat{\theta} = \arg\min_{z} \int d\theta C(\theta - z) p(\theta|\boldsymbol{x}). \tag{2.48}$$

The choice of cost function thus decides the form of the estimator. We now list a few common cost functions and their corresponding estimators. We begin with the quadratic cost function

$$C_{\mathrm{Q}}(\epsilon) = \epsilon^2 \qquad \Rightarrow \qquad \hat{\theta}_{\mathrm{Q}} = \mathrm{E}[\theta|\boldsymbol{x}] = \int d\theta \theta p(\theta|\boldsymbol{x}), \tag{2.49}$$

where the estimator is the mean of the posterior. For the quadratic cost function, the risk function is referred to as the Bayesian mean square error (BMSE) due to its similarity to the MSE defined above. The absolute value cost function

$$C_{\mathrm{A}}(\epsilon) = |\epsilon| \qquad \Rightarrow \qquad \hat{\theta}_{\mathrm{A}} = \mathrm{median}[p(\theta|\boldsymbol{x})], \tag{2.50}$$

where the estimator is the median of the posterior. The hit-or-miss cost function

$$C_{\mathrm{HM}}(\epsilon) = \begin{cases} 0, & |\epsilon| < \delta \\ 1, & |\epsilon| > \delta \end{cases} \qquad \Rightarrow \qquad \hat{\theta}_{\mathrm{HM}} = \arg\max_{\theta} p(\theta|\boldsymbol{x}), \tag{2.51}$$

where the estimator simply is the argument that maximizes the posterior. Note that $\delta > 0$. This is often referred to as the maximum a posteriori (MAP) estimator. The notation $\hat{\theta}_{\mathrm{MAP}}$ is typically used for this estimator. Lastly, the squared relative error cost function

$$C_{\mathrm{R}}(\epsilon) = \left(\frac{\epsilon}{\theta}\right)^2 \qquad \Rightarrow \qquad \hat{\theta}_{\mathrm{R}} = \frac{\int d\theta p(\theta|\boldsymbol{x})/\theta}{\int d\theta p(\theta|\boldsymbol{x})/\theta^2}. \tag{2.52}$$

Often numerical methods are required to evaluate all of these estimators. However, a benefit of the first three is that they are straightforward to evaluate analytically for simple models. The squared relative error cost function does, in contrast to C_{Q} and C_{A}, not depend on the absolute value of the parameter θ, but results in a more complicated estimator.

To determine the performance of an estimator, one may study the error $\epsilon = \theta - \hat{\theta}$. An estimator is considered as good if the average of ϵ, with respect to $p(\boldsymbol{x}, \theta)$, is zero. Additionally, one may evaluate the variance of ϵ. An estimator is said to be consistent (in the Bayesian sense) if $\mathrm{Var}[\epsilon] \to 0$ as $n \to \infty$. Note that the average error can be written like $\mathrm{E}[\epsilon] = \int d\theta b(\theta) p(\theta)$, where we introduced the bias

$$b(\theta) = \int \mathfrak{D}[\boldsymbol{x}](\theta - \hat{\theta}) p(\boldsymbol{x}|\theta). \tag{2.53}$$

When the bias vanishes, $\mathrm{E}[\epsilon] = 0$, and we find that the variance of the error coincides with the BMSE, which is lower bounded by the Cramer-Rao-like inequality [66]

$$\mathrm{Var}[\epsilon] = \mathrm{BMSE}(\hat{\theta}) \geq \int d\theta \frac{p(\theta)}{ni(\theta)}, \tag{2.54}$$

where $i(\theta) = -\int dx \partial^2 \ln[p(\theta|x)]/\partial\theta^2 p(x|\theta)$ is the Fisher information for one single observation for an arbitrary θ.

Finally, we introduce the Bernstein-von Mises theorem [67], which links the classical and Bayesian approaches. For large n, the posterior $p(\theta|\boldsymbol{x})$ approaches a Gaussian distribution centered at the true value θ_0, with variance $1/ni(\theta_0)$, where $i(\theta_0)$ is the Fisher information for one single observation, evaluated at θ_0 (see definition in the previous paragraph). The theorem thus assures that the posterior distribution converges towards a narrow peak around θ_0 as n becomes large. We note that this is similar to the ML estimator above.

Probe thermometry

To illustrate some of the theory introduced above, we look at a simple model of probe thermometry. Imagine a heat bath with a well-defined, but unknown temperature T_0, which we aim to estimate. To this end, we let n independent, classical two-level systems, with states 0 and 1, thermalize with the heat bath. By measuring the state of every probe, we can estimate the temperature. It is assumed that the heat bath remains in thermal equilibrium during the whole process. The probability to observe outcome $x = 0, 1$ when measuring the state of any probe is given by the Boltzmann distribution

$$p_x(T) = \frac{e^{-E_x/T}}{e^{-E_0/T} + e^{-E_1/T}}, \tag{2.55}$$

with E_0 and E_1 being the energies of state 0 and 1, respectively. Note that we put $k_B = 1$ (Boltzmann constant) to avoid clutter. After measuring all probes, the outcomes are put into a vector $\boldsymbol{x} = (x_1, \ldots, x_n)$, where x_j is the outcome for probe j. Out of all entries in this vector, there will be k zeros and $n - k$ ones.

To find the ML estimator, we begin by noting that the distribution to obtain $\boldsymbol{x}$ is given by

$$p(\boldsymbol{x}; T) = p_0^k(T) p_1^{n-k}(T) = \frac{e^{[k(E_1 - E_0) - nE_1]/T}}{\left(e^{-E_0/T} + e^{-E_1/T}\right)^n}, \tag{2.56}$$

where it is assumed that all measurements are independent. When $E_1 \neq E_0$, the ML estimator is given by[3]

$$\hat{T}_{\mathrm{ML}} = \frac{E_1 - E_0}{\ln\left(\frac{k}{n-k}\right)}. \tag{2.57}$$

As $k \to n$, $\hat{T}_{\mathrm{ML}} \to 0$. That is, when only observing zeros, our best guess of the temperature is 0. As $k \to n/2$, $\hat{T}_{\mathrm{ML}} \to \infty$, illustrating that if half of the observations are zeros, our best guess of the temperature is ∞. Some caution must be taken with this estimator. If $k < n - k$, $\hat{T}_{\mathrm{ML}} < 0$, quite contrary to what we expect. Also, with $k = 0$, $\hat{T}_{\mathrm{ML}} \to 0$. This is can observed for small n. However, for large n, we get $k \geq n - k$, assuring that $\hat{T}_{\mathrm{ML}} \geq 0$.

For Bayesian estimators, we use the uniform prior distribution

$$p(T) = \begin{cases} (T_2 - T_1)^{-1}, & \text{if } \ T_1 \leq T \leq T_2, \\ 0 \qquad\qquad\quad , & \text{otherwise.} \end{cases} \tag{2.58}$$

[3]For large n, we can make an alternative derivation of this estimator. The probability of observing 0 can be well approximated with the relative frequency $p_0 \sim k/n$. Similarly, we find $p_1 \sim (n - k)/n$. Therefore, $p_0/p_1 = e^{(E_1 - E_0)/T} \sim k/(n - k)$. This results in $T \sim (E_1 - E_0)/\ln[k/(n - k)]$, just as above.

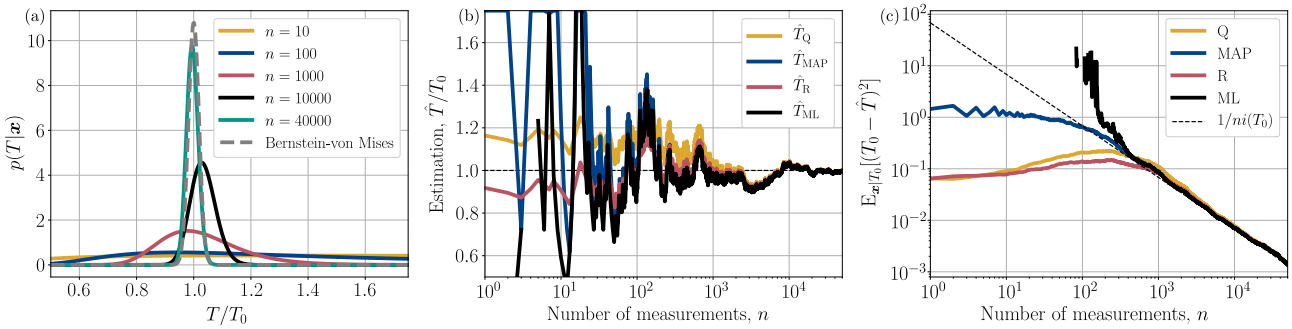

Figure 2.3: Numerical results for the probe thermometry model. (a) Posterior distribution $p(T|\boldsymbol{x})$ as a function of T for a single realization of $\boldsymbol{x}$. The distribution is plotted for various choices of n. As n increases, the posterior converges towards the Bernstein-von Mises theorem. (b) Various estimators for the same realization of $\boldsymbol{x}$ as in (a). Note that the ML estimator can diverge, as well as produce values outside of the range $[T_1, T_2]$. (c) Mean square error of all estimators in (b), averaged over 500 realizations of $\boldsymbol{x}$. The error converges to the Cramer-Rao lower bound $1/ni(T_0)$ for all estimators. Parameters: $E_0/T_0 = 0$, $E_1/T_0 = 0.5$, $T_1/T_0 = 0.5$, $T_2/T_0 = 1.75$, $n = 50000$.

The likelihood function for observing $\boldsymbol{x}$, given T, reads [it coincides with the ML method above in Eq. (2.56)]

$$p(\boldsymbol{x}|T) = p_0^k(T)p_1^{n-k}(T). \tag{2.59}$$

By using this, the posterior was calculated numerically with $p(T|\boldsymbol{x}) = p(\boldsymbol{x}|T)p(T)/p(\boldsymbol{x})$. The posterior is visualized in Fig. 2.3(a) for a specific realization of $\boldsymbol{x}$. As n is increased, the distribution goes from being flat to sharply peaked at the true value T_0. This illustrates the Bernstein-von Mises theorem. In Fig. 2.3(b), we plot the Bayesian estimators $\hat{T}_{\mathrm{Q}}$, $\hat{T}_{\mathrm{MAP}}$, and $\hat{T}_{\mathrm{R}}$, as well as the ML estimator $\hat{T}_{\mathrm{ML}}$ for the same realization of $\boldsymbol{x}$ as in (a). For small n, the estimators returns quite different outputs. Note that the ML estimator has discontinuities for small n, as it can diverge (see above). For large n, all estimators converge to T_0 as expected (Bernstein-von Mises theorem and asymptotic behavior of ML estimators). Note that the ML estimator can return numbers outside the interval $[T_1, T_2]$ as no prior knowledge was incorporated into this estimator.

To get an idea of the performance of the estimators, we plot their MSEs

$$\mathrm{E}_{\boldsymbol{x}|T_0}\left[(T_0 - \hat{T})^2\right] = \int \mathfrak{D}[\boldsymbol{x}](T_0 - \hat{T})^2 p(\boldsymbol{x}|T_0) \tag{2.60}$$

in Fig. 2.3(c), where we use the true temperature T_0. For unbiased estimators $\hat{T}$, i.e., $\int d\boldsymbol{x}\hat{T}p(\boldsymbol{x}|T_0) = T_0$, the MSE is lower bounded by the Cramer-Rao bound

$$\mathrm{E}_{\boldsymbol{x}|T_0}\left[(T_0 - \hat{T})^2\right] \geq \frac{1}{ni(T_0)}, \tag{2.61}$$

where the Fisher information for a single observation can be calculated analytically,

$$i(T) = \frac{(E_1 - E_0)^2 \operatorname{sech}^2(\frac{E_1 - E_0}{2T})}{4T^4}. \tag{2.62}$$

In Fig. 2.3(c), the MSE for all estimators approaches the lower bound for large n. The noise in each line is due to the average $\mathrm{E}_{\boldsymbol{x}|T_0}[\cdot]$ being taken over a finite number of trajectories $\boldsymbol{x}$. For the ML estimator, we observe several discontinuities for $n \lesssim 10^2$. This happens as $\hat{T}_{\mathrm{ML}}$ can diverge for small n. With the analytical expression of the Fisher information, we find that the optimal gap that maximizes $i(T)$ is given by $E_1 - E_0 \approx 2.4T$. For this gap, the MSE goes to zero the fastest as n grows.

Chapter 3

Open quantum systems

The textbook description of basic quantum mechanics is based on closed systems that are completely isolated from their environment and described by pure states. Such a description can teach us a great deal about the foundations of quantum physics, but it is inevitable that quantum systems never are isolated in reality. They always interact with their environment by exchanging energy and/or particles, and are thereby open.

A typical example of this is the light-matter interaction between an atom (system) and an electromagnetic field (environment) [68, 69]. Another relevant example, especially important for this thesis, is solid state quantum dots (system) [50] defined in semiconductor materials (environment), where the quantum dots may exchange electrons and phonons with its environment. A complete description of the physics in these examples requires a full theoretical treatment of both the system and the environment. For instance, to understand all processes in the example of light-matter interactions, we must quantize the electromagnetic field, and keep track of all possible photon states of the field. Similarly, for semiconductor quantum dots, one needs to include all possible electronic (or phonon) states in the theoretical description. As there are an infinite number of such states, it is, in general, a formidable task to theoretically model such a problem. To this end, it is necessary to develop a manageable theory for open quantum systems [19, 70, 71].

The joint unit of system and environment can be treated as a closed system, and by tracing out the environment, we obtain a description of the system alone. By performing such a trace operation, we lose information about the correlations between the system and the environment, and introduce uncertainty about which state the system is in. The state of an open quantum system is thus, typically, mixed. Often, it is interesting to study the dynamics of these systems. By assuming a weak coupling between the system and the environment, the dynamics follow a Markovian master equation – the Lindblad equation.

This equation effectively describes how the environment influences the system, without having to keep track of the environmental degrees of freedom. The Lindblad equation is an important tool for modeling open quantum systems and is used in Papers II-V.

In this chapter, we discuss the basic theoretical tools required to describe open quantum systems. We begin by reviewing the dynamics of pure states in closed systems in Sec. 3.1. This acts as a reference for the remaining sections. Section 3.2 introduces mixed states and the density operator. The latter is a valuable tool in the theory of open quantum systems. In particular, we motivate the origin of mixed states. Section 3.3 is devoted to the dynamical description of open systems. Most importantly, we introduce the Lindblad master equation. In Sec. 3.4, we unravel the Lindblad equation, and show that open systems also can be described by stochastic master equations, resolving individual exchanges of energy/particles with the environment. Section 3.5 discusses decoherence – a process induced by the environment of an open system, degrading its quantum coherence. The effect of decoherence is thus to push a quantum system to a classical representation that does not contain coherence. In particular, we derive a model for the quantum-to-classical transition induced by decoherence. We do this for a double quantum dot system, but note that the model can be straightforwardly extended to other systems as well. Before concluding this chapter, we introduce full counting statistics in Sec. 3.6 – a tool for gaining full statistical knowledge of particle transport in nanoscale systems described by Markovian master equations. This was a useful tool for Papers I-III.

3.1 Pure states

The state of a quantum system is said to be pure if it can be described by one single, normalized state vector $|\psi(t)\rangle$, for which $\langle\psi(t)|\psi(t)\rangle = 1$. For a closed system, the time evolution of this state is described by the Schrödinger equation

$$\partial_t |\psi(t)\rangle = -i\hat{H}(t) |\psi(t)\rangle , \tag{3.1}$$

where $\hat{H}(t)$ is the (possibly time dependent) Hamiltonian of the system. The time dependence may stem from the interaction with an external driving field, such as in the semiclassical description light-matter interactions. Note that we have absorbed the factor of $\hbar^{-1}$ into the Hamiltonian in Eq. (3.1) such that all energy units are given in inverse units of time (alternatively known as the convention $\hbar = 1$). The solution to the Schrödinger equation is given by

$$|\psi(t)\rangle = \hat{U}(t, t_0) |\psi(t_0)\rangle , \tag{3.2}$$

where $|\psi(t_0)\rangle$ is the initial state vector of the system at time t_0, with $\langle\psi(t_0)|\psi(t_0)\rangle = 1$, and $\hat{U}(t, t_0)$ is the time evolution operator given by

$$\hat{U}(t, t_0) = \mathcal{T} e^{-i\int_{t_0}^{t} ds \hat{H}(s)}, \tag{3.3}$$

where $\mathcal{T}$ is the time ordering operator. The time evolution operator is unitary, i.e., $\hat{U}(t,t_0)\hat{U}^\dagger(t,t_0) = \hat{U}^\dagger(t,t_0)\hat{U}(t,t_0) = \mathbb{1}$, such that the normalization of the state vector is preserved; $\langle\psi(t)|\psi(t)\rangle = \langle\psi(t_0)|\hat{U}^\dagger(t,t_0)\hat{U}(t,t_0)|\psi(t_0)\rangle = \langle\psi(t_0)|\psi(t_0)\rangle = 1$. With the state vector, we may calculate all moments of any observable $\hat{A}$ at time t as $\langle\hat{A}^k\rangle = \langle\psi(t)|\hat{A}^k|\psi(t)\rangle$.

3.2 Mixed states

The preceding discussion was concerned with pure states of closed quantum systems. We now proceed with mixed states which cannot be described by a single state vector. Suppose that we are dealing with a quantum system (closed or open), where we are uncertain about the exact system state. This uncertainty can be expressed by a probability distribution p_j, normalized with $\sum_j p_j = 1$, specifying the probability that the system is in some state $|\psi_j\rangle$. The possible system states $|\psi_j\rangle$ are not necessarily mutually orthogonal. Under these conditions, the system state is said to be mixed, and is represented by the density operator[1]

$$\hat{\rho} = \sum_j p_j \, |\psi_j\rangle\langle\psi_j| \, . \tag{3.4}$$

The density operator is positive (and thereby Hermitian, $\hat{\rho}^\dagger = \hat{\rho}$), i.e., $\langle\Phi|\hat{\rho}|\Phi\rangle \geq 0$ for any state vector $|\Phi\rangle$, and has trace $\mathrm{tr}\{\hat{\rho}\} = 1$. The latter property follows from the normalization of the distribution p_j, stating that the system must be in one of the states $|\psi_j\rangle$. Note that if $p_{j=k} = 1$ for some $j = k$, and 0 for all $j \neq k$, the state is pure and has density operator $\hat{\rho} = |\psi_k\rangle\langle\psi_k|$. If this is the case, the system is equally well described by the state vector $|\psi_k\rangle$. Regardless of being pure or mixed, the density operator can always be written as a matrix in any orthonormal basis $\{|n\rangle\}_n$, where the diagonal elements $\rho_{nn} = \langle n|\hat{\rho}|n\rangle$ are referred to as populations and give us the probability to be in state $|n\rangle$, while the off-diagonal elements $\rho_{nm} = \langle n|\hat{\rho}|m\rangle$ are referred to as coherences and originate from superpositions of basis states. We note that if all coherences vanish, there exist no superpositions of basis states. We will return to this point when discussing decoherence and measurements in Sec. 3.5 and Chapter 4, respectively. Before continuing, we note that all moments of an observable $\hat{A}$ can be calculated with the density matrix as $\langle\hat{A}^k\rangle = \mathrm{tr}\{\hat{A}^k\hat{\rho}\}$.

As mentioned above, the density matrix must be used when we are uncertain about the exact state of a system. Such uncertainty can arise in various situations – here we discuss two cases. First, imagine that we are preparing a state vector for an experiment. Due to imprecision in the lab equipment, it is not possible to know with certainty which state the

[1]Note that the density operator is not uniquely generated by the set $\{p_j, \, |\psi_j\rangle\}$. By unitary transformations, this set can be transformed into other sets $\{q_k, \, |\varphi_k\rangle\}$ that generate the same density operator [19].

system is in. If this is the case, the system state is mixed, and needs to be described by a density matrix.

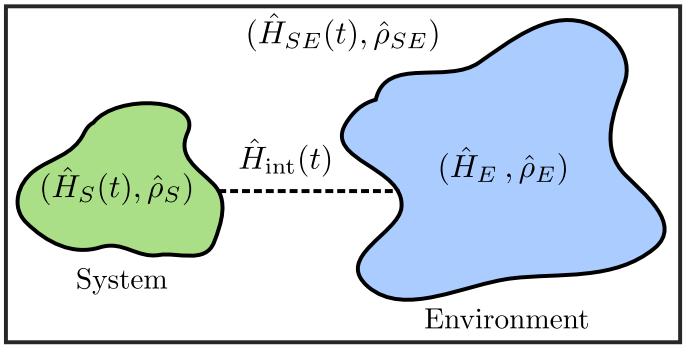

Figure 3.1: Illustration of an open quantum system that interacts with its environment. The system, referred to as S in the text, has a bare Hamiltonian $\hat{H}_S(t)$ and density operator $\hat{\rho}_S$. The environment (E) has a bare Hamiltonian $\hat{H}_E$ and density operator $\hat{\rho}_E$. The system and the environment interact by exchanging energy and particles – this is described by the interaction Hamiltonian $\hat{H}_{\rm int}(t)$. By the rectangular box we highlight that the combined unit of system and environment constitutes a closed system which is described by the Hamiltonian $\hat{H}_{SE}(t)$ and density operator $\hat{\rho}_{SE}$.

As a second case, we consider an open quantum system S coupled to an environment E, as visualized in Fig. 3.1. We assume that the state of the combined unit $S + E$ is pure. Therefore, it be written as

$$|\psi\rangle = \sum_{jk} c_{jk} \, |s_j\rangle \otimes \, |e_k\rangle \,, \qquad\qquad \sum_{jk} |c_{jk}|^2 = 1, \tag{3.5}$$

where $|s_j\rangle \otimes \, |e_k\rangle$ are orthonormal basis vectors for the composite state space of $S + E$, while $|s_j\rangle$ and $|e_j\rangle$ are orthonormal basis vectors for S and E, respectively, and $c_{jk} = (\, \langle s_j| \otimes \, \langle e_k|) \, |\psi\rangle$ are complex coefficients for which $|c_{jk}|^2$ is the probability to obtain outcome ξ_{jk} when measuring the observable $\hat{A} = \sum_{jk} \xi_{jk} \, |s_j\rangle\langle s_j| \otimes \, |e_k\rangle\langle e_k|$. The corresponding density operator of $S + E$ is given by $\hat{\rho}_{SE} = |\psi\rangle\langle\psi|$. To find a description of S alone, we trace $\hat{\rho}_{SE}$ over the environment, and find the system density matrix

$$\hat{\rho}_S = {\rm tr}_E\{\hat{\rho}_{SE}\} = \sum_k \langle e_k|\psi\rangle \, \langle\psi|e_k\rangle = \sum_k \, |\tilde{\psi}_k\rangle\langle\tilde{\psi}_k| \,, \tag{3.6}$$

where ${\rm tr}_E\{\cdot\}$ denotes the partial trace over the environment (here computed in the basis $|e_k\rangle$), and $|\tilde{\psi}_k\rangle = \sum_j c_{jk} \, |s_j\rangle$ is a vector in the state space of S. Note that $|\tilde{\psi}_k\rangle$ is not normalized as

$$\langle\tilde{\psi}_k|\tilde{\psi}_k\rangle = \sum_j |c_{jk}|^2 < 1. \tag{3.7}$$

We therefore introduce $|\tilde{\psi}_k\rangle = \sqrt{p}_k \, |\psi_k\rangle$, for which $\langle\psi_k|\psi_k\rangle = 1$, where $p_k = \langle\tilde{\psi}_k|\tilde{\psi}_k\rangle$ is interpreted as the probability to be in state $|\psi_k\rangle$. It follows that

$$\hat{\rho}_S = \sum_k p_k \, |\psi_k\rangle\langle\psi_k| \,, \tag{3.8}$$

which coincides with the definition in Eq. (3.4). We see that by applying the partial trace in Eq. (3.6), we lose all information encoded in the correlations between S and E, and thus introduce uncertainty about the state of S. Therefore, open systems are prime examples where we, in general, need the density matrix to describe the state of the system.

3.3 Dynamics

For a closed system described by a density matrix, as in Eq. (3.4), each state $|\psi_j\rangle$ evolves in time according to the Schrödinger equation (3.1). This implies that the density matrix can be translated in time according to $\hat{\rho}(t) = \hat{U}(t, t_0)\hat{\rho}(t_0)\hat{U}^\dagger(t, t_0)$, where $\hat{\rho}(t_0)$ is the density matrix at time t_0, and $\hat{U}(t, t_0)$ is the time evolution operator in Eq. (3.3). Differentiating with respect to time, we find the von Neumann equation

$$\partial_t \hat{\rho}(t) = -i[\hat{H}(t), \hat{\rho}(t)]. \tag{3.9}$$

This equation determines the dynamics of $\hat{\rho}(t)$ for closed systems, and can be regarded as the Schrödinger equation for mixed states. Due to the unitary time evolution, the eigenvalues of $\hat{\rho}(t)$ and the probabilities p_j are stationary over time.

We now proceed with open quantum systems. As introduced above, an open system interacts with its environment – see Fig. 3.1. By environment, we typically refer to one or several thermal reservoirs, but it could also be a smaller system, such as a qubit. Due to the possibly large dimension of the environment, it is difficult, or impossible, to carry out calculations with the composite density operator $\hat{\rho}_{SE}$ of $S + E$. For instance, for a bath with infinitely many energy modes, the von Neumann equation (3.9) of $\hat{\rho}_{SE}$ would result in an infinitely large hierarchy of coupled differential equations, which, in general, does not have an exact analytical solution. Instead, we aim to work with the reduced density operator $\hat{\rho}_S = \mathrm{tr}_E\{\hat{\rho}_{SE}\}$ of S.

For the combined unit $S + E$, the total Hamiltonian reads

$$\hat{H}_{SE}(t) = \hat{H}_S(t) + \hat{H}_E + \hat{H}_{\mathrm{int}}(t), \tag{3.10}$$

where $\hat{H}_S(t)$ and $\hat{H}_E$ are the bare Hamiltonians of S and E, respectively, and $\hat{H}_{\mathrm{int}}(t)$ describes the interaction between S and E. The total density operator $\hat{\rho}_{SE}$ can be translated in time with the unitary operator (3.3). If $\hat{\rho}_{SE}(t_0)$ is the initial state of $S + E$, and $\hat{\rho}_S(t_0)$ is the initial state of S, the state of S at a later time t is given by

$$\hat{\rho}_S(t) = \mathrm{tr}_E\{\hat{U}(t, t_0)\hat{\rho}_{SE}(t_0)\hat{U}^\dagger(t, t_0)\} \equiv \mathcal{K}_{(t,t_0)}\hat{\rho}_S(t_0), \tag{3.11}$$

where $\mathcal{K}_{(t,t_0)}$ is referred to as a dynamical map, and is always dependent on the unitary $\hat{U}(t, t_0)$ and the initial state of the environment, i.e., $\hat{\rho}_E(t_0) = \mathrm{tr}_S\{\hat{\rho}_{SE}(t_0)\}$. As

$\hat{\rho}_{SE}(t_0)$ might contain correlations between S and E, $\mathcal{K}_{(t,t_0)}$ is generally dependent on the initial state of S as well. This is unsatisfactory as the map $\mathcal{K}_{(t,t_0)}$ depends on the state it acts on – we would like to have a map that is universal and can take any input state $\hat{\rho}_S(t_0)$ as its argument. In fact, by choosing an uncorrelated initial state $\hat{\rho}_{SE}(t_0) = \hat{\rho}_S(t_0) \otimes \hat{\rho}_E(t_0)$, we find a universal dynamical map (UDM)

$$\hat{\rho}_S(t) = \mathrm{tr}_E\{\hat{U}(t,t_0)[\hat{\rho}_S(t_0) \otimes \hat{\rho}_E(t_0)]\hat{U}^\dagger(t,t_0)\} \equiv \mathcal{E}_{(t,t_0)}\hat{\rho}_S(t_0), \tag{3.12}$$

where $\mathcal{E}_{(t,t_0)}$ only depends on $\hat{U}(t,t_0)$ and the initial state $\hat{\rho}_E(t_0)$ of the environment. This map is independent on the initial state of S, and can, therefore, take any state $\hat{\rho}_S(t_0)$ as its argument for a fixed $\hat{\rho}_E(t_0)$. As $\hat{\rho}_E(t_0)$ is a positive operator, it can be written in its spectral representation $\hat{\rho}_E(t_0) = \sum_j \lambda_j \, |e_j\rangle\langle e_j|$, with eigenvalues λ_j, for which $0 \leq \lambda_j \leq 1$ and $\sum_j \lambda_j = 1$, and eigenstates $|e_j\rangle$. By computing the partial trace in Eq. (3.12) in this eigenbasis, the UDM can be written as [19, 70, 71]

$$\mathcal{E}_{(t,t_0)}\hat{\rho}_S = \sum_{kj} \hat{E}_{kj}(t,t_0)\hat{\rho}_S\hat{E}_{kj}^\dagger(t,t_0), \tag{3.13}$$

with Kraus operators $\hat{E}_{kj}(t,t_0) = \sqrt{\lambda_j}\,\langle e_k|\hat{U}(t,t_0)|e_j\rangle$, satisfying the completeness relation $\sum_{kj} \hat{E}_{kj}^\dagger(t,t_0)\hat{E}_{kj}(t,t_0) = \mathbb{1}$. The completeness relation ensures that $\mathcal{E}_{(t,t_0)}$ preserves the trace of $\hat{\rho}_S$. We further note that $\mathcal{E}_{(t,t_0)}$ is linear and completely positive. Complete positivity ensures that any map $\mathcal{E}_{(t,t_0)} \otimes \mathbb{1}_D$, with $\mathbb{1}_D$ being the D-dimensional identity operator, acting on the composite system of S and any external D-dimensional system is also a positive map. Finally, a remark: In general, the initial state of $S + E$ contains correlations between the subsystems and cannot be written as a product state as in Eq. (3.12). However, when experimentally preparing the initial state of S, it is common that all correlations between S and E are destroyed, such that $\hat{\rho}_{SE}(t_0) = \hat{\rho}_S(t_0) \otimes \hat{\rho}_E(t_0)$ is no serious restriction.

In general, it is desirable to find a Markovian equation of motion for $\hat{\rho}_S$, rather than translating the state in time with $\mathcal{E}_{(t,t_0)}$. To this end, we begin by noting that we typically have the indivisibility condition $\mathcal{E}_{(t,t_0)} \neq \mathcal{E}_{(t,\tau)}\mathcal{E}_{(\tau,t_0)}$ for $t_0 < \tau < t$. The maps $\mathcal{E}_{(t,t_0)}$ and $\mathcal{E}_{(\tau,t_0)}$ are UDMs, but $\mathcal{E}_{(t,\tau)}$ is not a UDM as $\hat{\rho}_{SE}(\tau)$, the joint state of $S + E$ at time τ, can contain correlations between S and E. Therefore, $\mathcal{E}_{(t,\tau)}$ depends on the input state $\hat{\rho}_S(\tau) = \mathrm{tr}_E\{\hat{\rho}_{SE}(\tau)\}$. However, when the correlations between S and E are weak, and have a negligible effect on the dynamics of S, we get the divisibility condition $\mathcal{E}_{(t,t_0)} = \mathcal{E}_{(t,\tau)}\mathcal{E}_{(\tau,t_0)}$, where all maps $\mathcal{E}_{(t,t_0)}$, $\mathcal{E}_{(t,\tau)}$, and $\mathcal{E}_{(\tau,t_0)}$ are UDMs – compare to the Chapman-Kolmogorov equation (2.8) for classical stochastic systems. The divisibility condition is typically justified when the coupling between S and E is weak. We can thus use the divisibility condition to write down a Markovian master equation [71]

$$\partial_t\hat{\rho}_S(t) = \lim_{\epsilon\to 0}\frac{\hat{\rho}_S(t+\epsilon) - \hat{\rho}_S(t)}{\epsilon} = \lim_{\epsilon\to 0}\frac{\mathcal{E}_{(t+\epsilon,t)} - \mathbb{1}}{\epsilon}\mathcal{E}_{(t,t_0)}\hat{\rho}_S(t_0) = \mathcal{L}(t)\hat{\rho}_S(t), \tag{3.14}$$

where we introduced the Liouville superoperator $\mathcal{L}(t) = \lim_{\epsilon\to 0}[\mathcal{E}_{(t+\epsilon,t)} - \mathbb{1}]/\epsilon$. Such a Markovian master equation can always be written on Lindblad (or GKLS) form (named after the persons that first derived it: Gorini, Kossakowski, Lindblad and Sudarshan) [70–73] as

$$\begin{aligned}\partial_t\hat{\rho}_S(t) = \mathcal{L}(t)\hat{\rho}_S(t) = -i[\hat{H}(t), \hat{\rho}_S(t)] \\ + \sum_k \gamma_k(t)\left[\hat{L}_k(t)\hat{\rho}_S(t)\hat{L}_k^\dagger(t) - \frac{1}{2}\{\hat{L}_k^\dagger(t)\hat{L}_k(t), \hat{\rho}_S(t)\}\right],\end{aligned} \tag{3.15}$$

where $\hat{H}(t)$ is an Hermitian operator, the coefficients $\gamma_k(t) \geq 0$, and $\hat{L}_k(t)$ are referred to as Lindblad operators. Typically, $\hat{H}(t)$ does not exactly coincide with the bare Hamiltonian $\hat{H}_S(t)$ of S, but also contain terms originating from the coupling between S and E [70, 71]. If the extra terms are negligible, the first term of the Lindblad equation (3.15) corresponds to the von Neumann equation (3.9), and describes the dynamics of S in the absence of E. The combinations of operators under the sum in the Lindblad equation are commonly written on the compact superoperator form $\mathcal{D}[\hat{L}_k(t)]\hat{\rho} = \hat{L}_k(t)\hat{\rho}\hat{L}_k^\dagger(t) - \frac{1}{2}\{\hat{L}_k^\dagger(t)\hat{L}_k(t), \hat{\rho}\}$, and describes how the environment affects the system. Often, the Lindblad operators are ladder operators of the system, describing how the system gets excited or de-excited by interacting with the environment. In general, this interaction can be considered as incoherent, and does not involve the off-diagonals of the density matrix. The coefficients $\gamma_k(t)$ are transition rates and can be expressed in terms of the properties of the environment and the coupling between S and E. Below we study an explicit example; the double quantum dot.

The Liouville superoperator, or Liouvillian, $\mathcal{L}(t)$ is said to be a generator of the UDM $\mathcal{E}_{(t,t_0)}$, and we can write

$$\mathcal{E}_{(t,t_0)} = \mathcal{T}e^{\int_{t_0}^{t} ds\mathcal{L}(s)}, \tag{3.16}$$

where $\mathcal{T}$ is the time ordering operator. If $\mathcal{L}(t)$ is time independent, $\mathcal{E}_{(t,t_0)} = \exp\{\mathcal{L}(t - t_0)\}$ only depends on the time difference $\tau = t - t_0$, such that $\mathcal{E}_{(t,t_0)} = \mathcal{E}_\tau$. This UDM satisfies the semigroup property $\mathcal{E}_t\mathcal{E}_\tau = \mathcal{E}_{t+\tau}$ [71]. Starting from this property, we may show the converse, i.e., that the semigroup property leads to a time independent Liouvillian $\mathcal{L}$ [71], where all time dependence in the Lindblad equation (3.15) can be removed. For such a time independent Liouvillian, we are typically interested in the stationary state of the dynamics when $t \to \infty$ [a time dependent $\mathcal{L}(t)$ does not necessarily have a stationary state]. To motivate why we focus only on the stationary state, we note that for quantum heat engines or feedback-controlled devices, it is desirable that the system reaches a target state that is stable over time. That is, we want to find the state $\hat{\rho}_{\text{ss}}$ that satisfies $\mathcal{L}\hat{\rho}_{\text{ss}} = 0$. The total solution to the Lindblad equation can be written in the general form

$$\hat{\rho}_S(t) = \sum_j c_j e^{\lambda_j(t-t_0)}\hat{\sigma}_j, \tag{3.17}$$

where c_j are coefficients determined by the initial condition $\hat{\rho}_S(t_0)$, and λ_j are the eigenvalues of $\mathcal{L}$ with corresponding (linearly independent) eigenstates $\hat{\sigma}_j$. To have a stationary state, there must be one eigenvalue $\lambda_0 = 0$ with $c_0\hat{\sigma}_0 = \hat{\rho}_{\rm ss}$. The other eigenvalues have a negative real part such that only the $j = 0$ term survives in the long time limit.

The double quantum dot

An important open quantum system in this thesis is the double quantum dot (DQD). Here we briefly introduce the absolute basics of nanowire quantum dots, and show how the dynamics of a DQD can be described by a Lindblad master equation.

Quantum dots (QDs) are manmade structures where electrons are spatially confined in all three dimensions. For such confinement, the electrons can, according to quantum mechanics, only have certain discrete energies. Therefore, QDs are often referred to as artificial atoms. By putting two QDs in series, we form a DQD. Figure 3.2(a) depicts one way of manufacturing DQDs, using a semiconductor nanowire where layers of different materials, or crystal structures, form QDs. Note that the manufacturing can be done in alternative ways as well, see, for instance, Ref. [50]. Figure 3.2(b) illustrates the effective potential experienced by electrons traversing the nanowire. The layering of materials creates tunnel barriers, forming QDs in between them. Here we consider the case where electrons can only have the discrete energies ϵ_L and ϵ_R, for the left and right dot, respectively. These energies can often be externally controlled by using electrode gates. The middle barrier couples the left and right dots via the tunnel strength g. Electrons can also tunnel between the QDs and the metallic strips via the left and right barriers. This occurs with rates Γ_L and Γ_R. Electrons in the metallic strips are distributed according to the Fermi-Dirac distribution

$$n_{\rm F}^{(\alpha)}(\epsilon) = \frac{1}{e^{(\epsilon-\mu_\alpha)/k_BT_\alpha}+1}, \qquad \alpha = L, R, \tag{3.18}$$

where k_B is the Boltzmann constant, ϵ is energy, and T_α and μ_α are the temperature and chemical potential of strip α. With these features, the DQD becomes a basic unit for studying electron transport, including quantum effects such as tunneling and coherence. In addition, DQDs can be accurately controlled and measured [53], and are thus promising platforms for studying quantum feedback control.

Often, these systems can be tuned to a regime with large inter- and intradot Coulomb repulsion, such that only one electron can reside in the DQD at any time. Under these conditions, the DQD Hamiltonian reads

$$\hat{H}_{\rm DQD} = \epsilon_L \left|L\right\rangle\!\left\langle L\right| + \epsilon_R \left|R\right\rangle\!\left\langle R\right| + g\left(\left|L\right\rangle\!\left\langle R\right| + \left|R\right\rangle\!\left\langle L\right|\right), \tag{3.19}$$

where $|L\rangle$ ($|R\rangle$) represents the state when one electron resides in the left (right) dot, while the right (left) is empty. Both dots can also be empty, we denote this state by $|0\rangle$. The first

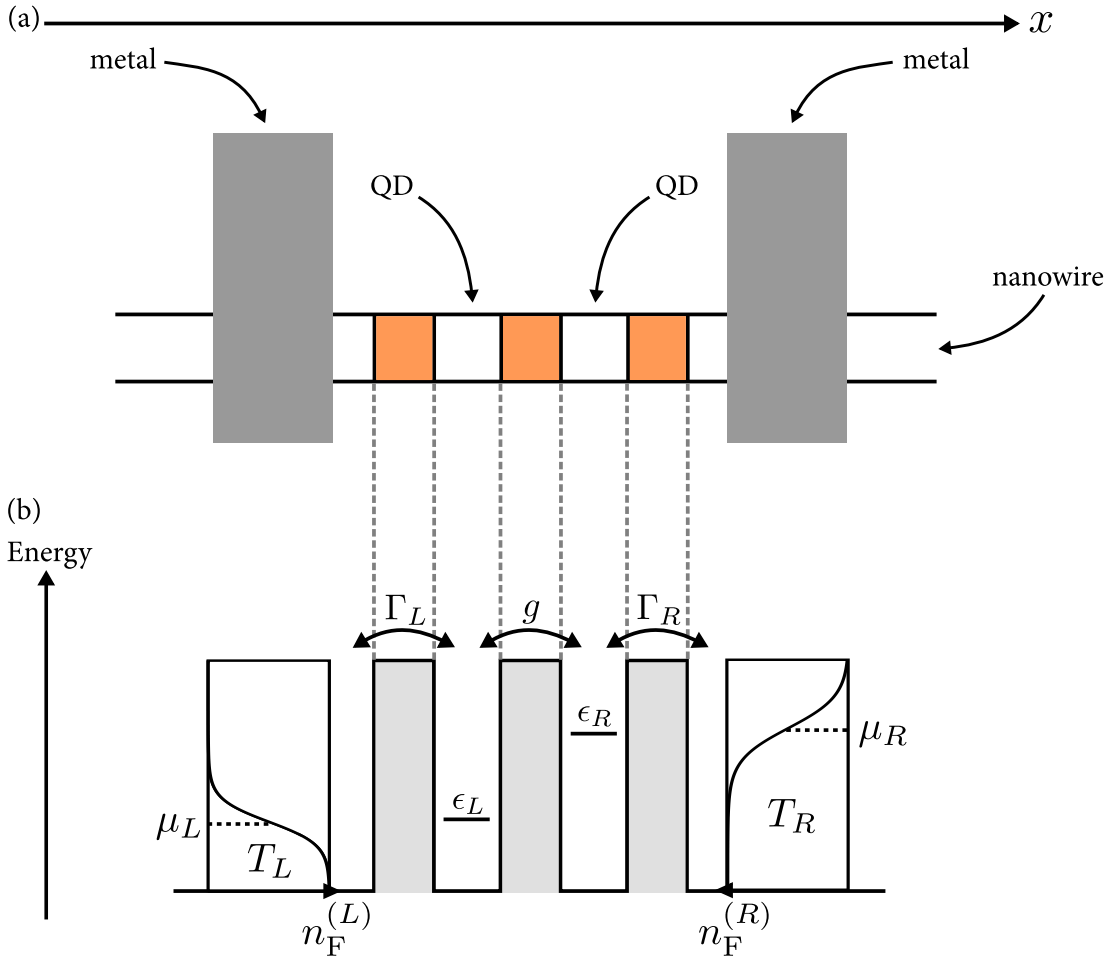

Figure 3.2: (a) Qualitative sketch of a nanowire double quantum dot. The white and orange regions in the wire correspond to different materials or crystal structures. Typically, a wire has a diameter of roughly 10-100 nm and extends a few micrometers along the x-axis. The quantum dots (QD) are defined in the white regions squeezed in between the orange regions. Electrons in the QDs are confined in all three spatial dimensions. The two strips of metal lying on top of the wire act as electron reservoirs, providing and absorbing electrons from the double quantum dot. (b) Sketch of the of the effective potential landscape experienced by electrons in the nanowire. The orange regions correspond to tunnel barriers. In the quantum dots (in between the barriers), electrons can have discrete energies ϵ_L and ϵ_R, respectively. Electrons can tunnel between the dots with tunnel strength g. Electrons can additionally tunnel between the dots and the metal strips with rates Γ_L and Γ_R. Electrons in the metal strips are distributed according to the Fermi-Dirac distribution $n_{\mathrm{F}}^{(\alpha)}$, where T_α and μ_α are the temperatures and chemical potentials of strip $\alpha = L, R$. The Fermi-Dirac distributions are sketched in the boxes to the left and right of the leftmost and rightmost tunnel barriers.

terms of the Hamiltonian correspond to the energy of the left and right dot, respectively, while the third term describes coherent interdot tunneling. For a small interdot Coulomb repulsion, both dots can be occupied simultaneously. If this is the case, the Hamiltonian must be modified with an additional term $U\,|LR\rangle\langle LR|$, where $|LR\rangle$ represents the state when both dots are occupied, and U is the repulsion energy between the electrons. This is used in Paper IV and V, but here we solely concentrate on the case where $U \to \infty$ and $|LR\rangle$ can be ignored.

The DQD is an open quantum system, where the metallic strips correspond to the envi-

ronment in the description above. The dynamics of the DQD can thus be written as a Lindblad equation. Depending on the hierarchy of timescales in the system, the Lindblad equation can be written in local or global form. The local equation is obtained when the coupling g is small, such that electrons mostly are localized in either the left or right dot. In the global equation, g is large, such that electrons become delocalized over both dots. Here we only concentrate on the local model[2]. The local Lindblad master equation of the DQD reads[3]

$$\begin{aligned}\partial_t\hat{\rho}(t) = &-i[\hat{H}_{\rm DQD},\hat{\rho}(t)]\\ &+\sum_{\alpha=L,R}\left(\Gamma_\alpha n_{\rm F}^{(\alpha)}(\bar{\epsilon})\mathcal{D}[\hat{\sigma}_\alpha^\dagger]+\Gamma_\alpha[1-n_{\rm F}^{(\alpha)}(\bar{\epsilon})]\mathcal{D}[\hat{\sigma}_\alpha]\right)\hat{\rho}(t),\end{aligned} \tag{3.20}$$

where $\bar{\epsilon}=(\epsilon_L+\epsilon_R)/2$ and $\hat{\sigma}_\alpha=|0\rangle\langle\alpha|$. This equation is valid when

$$\max\{k_BT_\alpha,|\bar{\epsilon}-\mu_\alpha|\}\gg\Gamma_\alpha,\sqrt{\Delta^2+g^2}, \tag{3.21}$$

where $\Delta=(\epsilon_L-\epsilon_R)/2$. The master equation is derived in Appendix D. Note that the Fermi-Dirac distributions are evaluated at $\bar{\epsilon}$, rather than at the local dot energies ϵ_α, which are commonly used in the literature. Actually, Eq. (3.20) only gives reasonable results as long as Δ is small. If this is the case, we can replace $\bar{\epsilon}\to\epsilon_\alpha$ without problems. For large Δ, the system can undergo interdot transitions that are thermodynamically questionable. In Chapter 5, we continue this discussion when we study thermodynamics. The stationary solution of the master equation, evaluated in the $\{|0\rangle,|L\rangle,|R\rangle\}$-basis, reads

$$\begin{aligned}\rho_{00}&=\left\{4g^2(\kappa_L+\kappa_R)^2+\kappa_L\kappa_R[16\Delta^2+(\kappa_L+\kappa_R)^2]\right\}/\mathcal{N},\\ \rho_{LL}&=\left\{4g^2(\gamma_L+\gamma_R)(\kappa_L+\kappa_R)+\gamma_L\kappa_R[16\Delta^2+(\kappa_L+\kappa_R)^2]\right\}/\mathcal{N},\\ \rho_{RR}&=\left\{4g^2(\gamma_L+\gamma_R)(\kappa_L+\kappa_R)+\gamma_R\kappa_L[16\Delta^2+(\kappa_L+\kappa_R)^2]\right\}/\mathcal{N},\\ \rho_{LR}&=\left\{2g\left[4\Delta+i(\kappa_L+\kappa_R)\right](\gamma_L\kappa_R-\gamma_R\kappa_L)\right\}/\mathcal{N},\end{aligned} \tag{3.22}$$

where $\rho_{ab}=\langle a|\hat{\rho}_{\rm ss}|b\rangle$, with $a,b=0,L,R$, $\gamma_\alpha=\Gamma_\alpha n_F^{(\alpha)}(\bar{\epsilon})$, $\kappa_\alpha=\Gamma_\alpha[1-n_F^{(\alpha)}(\bar{\epsilon})]$ and $\mathcal{N}=4g^2(\kappa_L+\kappa_R)[2(\gamma_L+\gamma_R)+\kappa_L+\kappa_R]+[16\Delta^2+(\kappa_L+\kappa_R)^2](\gamma_L\kappa_R+\gamma_R\kappa_L+\kappa_L\kappa_R)$. Note that the remaining matrix elements of $\hat{\rho}_{\rm ss}$ are zero as they are decoupled from the elements in Eq. (3.22).

3.4 Unraveling quantum jumps

Many experiments exhibit stochastic evolution rather than the smooth, deterministic evolution of Eqs. (3.9) and (3.15). Good examples of this are electrons jumping in and out of

[2]A discussion on local and global models can, for instance, be found in Refs. [74, 75].

[3]We have dropped the subscript 'S' on the density matrix for ease of notation, cf. Eq. (3.15). However, the density matrix describes the reduced state of the DQD, and does not include the environment (metallic strips).

quantum dots and photo-detection. Jumps, or detections, are observed at random times that cannot be deterministically predicted. To recover the randomness of the dynamics in a theoretic description, one can unravel the deterministic dynamics. The unraveling can be seen as a quantum trajectory [76] resolving all stochastic events. In such a description, the state of a system evolves according to a stochastic master equation and is conditioned on the entire history of the quantum trajectory. As an example, consider a two-level atom monitored by a photo-detector. If we observe a photon, we know that the atom must be in the ground state just after the detection. That is, the state becomes conditioned on the observation. Unravelings become interesting when trying to understand the dynamics of an experiment, or system, on the level of single quantum trajectories. Typically, this is common when studying feedback control or systems subjected to measurements. We note that the deterministic description is recovered when averaging over all possible realizations of quantum trajectories.

In this section, we unravel the Lindblad equation (3.15), and derive a stochastic master equation that resolves jumps (such as in quantum dots or photo-detection). Our derivation closely follows Refs. [15, 77]. The results of this section are relevant for Chapter 4 as well as Papers I, II, and III.

For simplicity, we consider an open quantum system with a time-independent[4] Hamiltonian $\hat{H}$, such that the system density matrix at time $t + dt$ is given by

$$\begin{aligned}\hat{\rho}(t+dt) &= e^{\mathcal{L}dt}\hat{\rho}(t) \approx (\mathbb{1} + dt\mathcal{L})\,\hat{\rho}(t) \\ &= \hat{\rho}(t) - idt\left(\hat{H}_{\text{eff}}\hat{\rho}(t) - \hat{\rho}(t)\hat{H}_{\text{eff}}^{\dagger}\right) + dt\sum_{k=1}^{N}\hat{L}_k\hat{\rho}(t)\hat{L}_k^{\dagger},\end{aligned} \tag{3.23}$$

where $\hat{\rho}(t)$ is the density matrix at time t, and we defined the effictive non-Hermitian Hamiltonian

$$\hat{H}_{\text{eff}} = \hat{H} - \frac{i}{2}\sum_{k=1}^{K}\hat{L}_k^{\dagger}\hat{L}_k. \tag{3.24}$$

To write the evolution in this form, we used the Lindblad equation (3.15) with K Lindblad operators $\hat{L}_k$, and expanded the exponential to first order in the infinitesimal timestep dt. As $e^{\mathcal{L}dt}$ is a UDM, we can write [see Eq. (3.13)]

$$\hat{\rho}(t+dt) = \sum_{k=0}^{K}\hat{E}_k\hat{\rho}(t)\hat{E}_k^{\dagger}, \tag{3.25}$$

with the Kraus operators

$$\begin{aligned}\hat{E}_0 &= \mathbb{1} - idt\hat{H}_{\text{eff}}, \\ \hat{E}_k &= \sqrt{dt}\hat{L}_k, \quad k = 1, \ldots, K.\end{aligned} \tag{3.26}$$

[4]For a time-dependent Hamiltonian, the end results are the same, but the derivation requires time ordering.

This choice ensures that $\sum_{k=0}^{K} \hat{E}_k^\dagger \hat{E}_k = \mathbb{1}$ to first order in dt. The operators $\hat{E}_{k\neq 0}$ can be interpreted as jump operators, and we say that $\hat{E}_{k\neq 0}$ describes a jump in channel k. As an example, for the DQD, $\hat{\sigma}_\alpha^\dagger$ describes an electron jumping into dot α from bath α. The operator $\hat{E}_0$ corresponds to the dynamics when no jump occurs. We note that $\hat{E}_0$ describes non-unitary evolution, reflecting that our knowledge about the system is updated even though no jump occurs.

When observing a jump in channel $k = 1, \ldots, K$, our state of knowledge updates according to the map

$$\hat{\rho}(t) \to \frac{\hat{E}_k \hat{\rho}(t) \hat{E}_k^\dagger}{p_k(t)}, \tag{3.27}$$

where the normalization

$$p_k(t) = \mathrm{tr}\left\{\hat{E}_k^\dagger \hat{E}_k \hat{\rho}(t)\right\} = dt\, \mathrm{tr}\left\{\hat{L}_k^\dagger \hat{L}_k \hat{\rho}(t)\right\} \tag{3.28}$$

is the probability of observing a jump in channel k. As $p_k(t) \propto dt$, it is not very likely to observe a jump during the timestep dt. In fact, the probability to not observe a jump, $p_0(t) = 1 - dt \sum_{k=1}^{K} \mathrm{tr}\{\hat{L}_k^\dagger \hat{L}_k \hat{\rho}(t)\}$, tells us that nothing happens most of the time. During timesteps of no jump, the state evolves as

$$\hat{\rho}(t) \to \frac{\hat{E}_0 \hat{\rho}(t) \hat{E}_0^\dagger}{1 - dt \sum_{k=1}^{K} p_k(t)}. \tag{3.29}$$

As the state is normalized with the probability $p_k(t)$, $k = 0, 1, \ldots, K$, in both Eqs. (3.27) and (3.29), the updated density matrix will be conditioned on the jump that occurred (compare with Bayes' rule). Thus, if the state is evolved over a time interval $[t_0, t]$, the density matrix will be conditioned on the full history of jumps in that interval. Therefore, we introduce the notation $\hat{\rho}_c(t)$, indicating that the state is conditioned on all previous jumps. Conditioned states are revisited in Chapter 4, where we discuss quantum measurements.

Our goal is to find a stochastic master equation resolving the quantum jumps. To this end, we introduce random variables $dN_k(t) = 0, 1$, $k = 1, \ldots, K$, which tell us whether a jump occurred (1) or not (0) in channel k. The probability of a jump occuring in channel k is given by $p_k^{(c)}(t) = dt\, \mathrm{tr}\{\hat{L}_k^\dagger \hat{L}_k \hat{\rho}_c(t)\}$, as above. Note that we added a superscript "(c)" to indicate that this probability is conditioned on all previous jumps. By $dN_0(t) = 1 - \sum_{k=1}^{K} dN_k(t)$, we describe a stochastic variable for the no jump event. The probability of having $dN_0(t) = 1$ is, as above, given by $p_0^{(c)}(t) = 1 - \sum_{k=1}^{K} p_k^{(c)}(t)$. We note that the following relations hold,

$$\begin{aligned} dN_l(t) dN_k(t) &= dN_k(t) \delta_{lk}, \\ dt\, dN_j(t) &= 0, \quad j = 1, \ldots, K. \end{aligned} \tag{3.30}$$

The first of these relations tells us that only one channel can host a jump at a time, and defines point processes [60]. In fact, this relation is the equivalent of the Itô rule for point processes (see Chapter 2). The second relation can be motivated by noting that $\mathrm{E}[dtdN_j(t)] \propto dt^2 = 0$, where $\mathrm{E}[\cdot]$ denotes an ensemble average over all possible trajectories of jumps. In Appendix E, we introduce a way of calculating such averages. We can now write the update of the density matrix in the compact form

$$\hat{\rho}_c(t+dt) = \sum_{k=0}^{K} dN_k(t) \frac{\hat{E}_k \hat{\rho}_c(t) \hat{E}_k^\dagger}{p_k^{(c)}(t)}. \tag{3.31}$$

By using Eq. (3.30) and the expansion $1/(1-adt) \approx 1+adt$ to first order in dt, Eq. (3.31) can be written as a stochastic master equation

$$\begin{aligned} d\hat{\rho}_c(t) = -idt[\hat{H}, \hat{\rho}_c(t)] + \sum_{k=1}^{K} dN_k(t) \left(\frac{\hat{L}_k \hat{\rho}_c(t) \hat{L}_k^\dagger}{\mathrm{tr}\left\{ \hat{L}_k^\dagger \hat{L}_k \hat{\rho}_c(t) \right\}} - \hat{\rho}_c(t) \right) \\ + dt \sum_{k=1}^{K} \left(\hat{\rho}_c(t)\, \mathrm{tr}\left\{ \hat{L}_k^\dagger \hat{L}_k \hat{\rho}_c(t) \right\} - \frac{1}{2} \left\{ \hat{L}_k^\dagger \hat{L}_k, \hat{\rho}_c(t) \right\} \right), \end{aligned} \tag{3.32}$$

where $d\hat{\rho}_c(t) = \hat{\rho}_c(t+dt) - \hat{\rho}_c(t)$. We call this an unraveling of the Lindblad equation (3.15). The unraveling can be seen as a fine-grained description of the dynamics, resolving all jumps that occur. Therefore, the dynamical description is stochastic. Note that this equation is nonlinear in $\hat{\rho}_c(t)$ because of the second term in the first row, and the first term in the second row. The nonlinearlity arises as we normalize the state after each timestep dt [see Eq. (3.31)]. The Lindblad equation can be seen as an ensemble averaged description of the stochastic dynamics, and is obtained by taking the average $\mathrm{E}[\cdot]$ of Eq. (3.32) (see Appendix E). Note that the Lindblad equation can be unraveled in many various ways, see Chapter 4 for other unravelings.

As stated above, a natural example is the DQD. By chosing $\hat{L}_1 = \sqrt{\gamma_L}\hat{\sigma}_L^\dagger$, $\hat{L}_2 = \sqrt{\kappa_L}\hat{\sigma}_L$, $\hat{L}_3 = \sqrt{\gamma_R}\hat{\sigma}_R^\dagger$, and $\hat{L}_4 = \sqrt{\kappa_R}\hat{\sigma}_R$, the jumps correspond to electron exchanges with the baths. Unravelings are also useful when studying photo-detection. For a two-level atom with states $|0\rangle$ and $|1\rangle$, the choice $\hat{L} = \sqrt{\kappa}\,|0\rangle\langle 1|$ corresponds to a click in the detector, with κ being the rate of spontaneous emission, see Ref. [15] for more details.

Typically, Eq. (3.32) is difficult to solve analytically and one has to resort to numerical methods. In each timestep dt, we must draw a random number from the distribution $\{p_k^{(c)}(t)\}_{k=0}^K$ to decide whether a jump occurs in any of the channels. This is followed by updating the state according to Eq. (3.31) or (3.32). However, if the Hilbert space is large, it can become difficult to store the trajectory of the density matrix on a normal computer. For a Hilbert space of dimension M, it takes $\sim M^2$ real numbers to store the density matrix at

each instant of time. This can be circumvented for pure initial states, where one can work with the stochastic evolution of state vectors $|\psi(t)\rangle$, which require $\sim M$ real numbers to store. In quantum dots, one can always manipulate the system to achieve a pure initial state. The state vector evolves according to the stochastic Schrödinger equation [15]

$$|\psi(t+dt)\rangle = \sum_{k=1}^{K} dN_k(t) \frac{\hat{L}_k |\psi(t)\rangle}{\sqrt{\langle \hat{L}_k^\dagger \hat{L}_k \rangle(t)}} + \left[1 - \sum_{k=1}^{K} dN_k(t)\right] \left[\mathbb{1} - dt \left(i\hat{H} + \frac{1}{2} \sum_{k=1}^{K} \left\{ \hat{L}_k^\dagger \hat{L}_k - \langle \hat{L}_k^\dagger \hat{L}_k \rangle(t) \right\} \right)\right] |\psi(t)\rangle \,, \tag{3.33}$$

where $\langle \hat{L}_k^\dagger \hat{L}_k \rangle(t) = \langle \psi(t) | \hat{L}_k^\dagger \hat{L}_k | \psi(t) \rangle$. The conditional density matrix is recovered via $\hat{\rho}_c(t) = |\psi(t)\rangle\langle\psi(t)|$, and the unconditioned density matrix via $\hat{\rho}(t) = \mathrm{E}[|\psi(t)\rangle\langle\psi(t)|]$. For a very large dimension M, it can also be useful to study the ensemble averaged evolution of certain system observables [15, 78], see, for instance, Ref. [79].

3.5 Decoherence

In contrast to classical physics, quantum mechanics allows particles to be delocalized. A good example illustrating this is the DQD, where an electron can be in superpositions of $|L\rangle$ and $|R\rangle$, thus being delocalized over the whole system. However, delocalized states are very fragile, and quickly decay into localized states due to interactions with the environment. One can think of the interactions as measurements, gradually collapsing delocalized wavefunctions. This process is called decoherence, or dephasing [70, 80, 81]. Often this process is fast, making it one of the main challenges in the development of quantum technologies, where delocalized effects, such as entanglement, are exploited to perform various tasks. While being detrimental for quantum technologies, decoherence is interesting from a fundamental point of view. For instance, when a quantum particle is dephased in the position basis, it gets a localized wavefunction, and a well-defined position – just as in classical physics. Decoherence is thus the key process behind the quantum-to-classical transition, from which the classical world emerges[5].

In this section, we begin by introducing a simple model to understand how decoherence can emerge through environmental interactions. Then we explore the quantum-to-classical transition in the DQD, and derive a classical rate equation from the Lindblad equation (3.20). The discussion of this section is important for later chapters and Paper III.

[5]The quantum-to-classical transition has, e.g., been observed in diffraction experiments [82]. By sending fullerene molecules through a grating, one observes a diffraction pattern, demonstrating the (delocalized) wave nature of the molecules. When increasing the ambient gas pressure, the diffraction pattern gradually disappears, demonstrating the quantum-to-classical transition.

Simple model with fluctuating levels

Here we consider a two-level atom with states $|0\rangle$ and $|1\rangle$. We assume that the atom is immersed in a gas, where it scatters against gas molecules. During scattering events, the potential of the atom gets perturbed, giving rise to random fluctuations in the level splitting between the ground and excited states. The Hamiltonian of the atom reads

$$\hat{H}(t) = \left[\frac{\Delta}{2} + X(t)\right]\hat{\sigma}_z, \tag{3.34}$$

where Δ is the unperturbed level splitting, $X(t)$ is a random variable capturing the effect of the scattering events, and $\hat{\sigma}_z$ is the Pauli-Z operator. The random variable has the following properties,

$$\langle X(t)\rangle = 0, \qquad \text{and} \qquad \langle X(t)X(t')\rangle = \frac{\sigma^2}{2}\delta(t-t'). \tag{3.35}$$

The first property tells us that there is no preferred perturbation direction on average. The second property tells us that scattering events at different times are uncorrelated. Note that both σ^2 and $\delta(t-t')$ must have the unit of inverse time. As $[\hat{H}(t), \hat{H}(t')] = 0$, the atom evolves according to the unitary evolution

$$\hat{U}(t) = e^{-i\left[\frac{\Delta t}{2} + Y(t)\right]\hat{\sigma}_z}, \tag{3.36}$$

where

$$Y(t) = \int_0^t ds X(s) \tag{3.37}$$

is the accumulated phase shift due all scattering events in the time interval $[0, t]$. The accumulated phase shift is a Gaussian random variable with zero mean and variance $\sigma^2 t$ (follows from the central limit theorem). For an infinitesimal timestep dt, we can write $Y(dt) = \sigma dW$, where dW is a Wiener increment (see Chapter 2). The process $Y(t)$ can thus be decomposed as $Y(t) = \sigma \int_0^t dW(s)$, which effectively is a sum of many Wiener increments. An infinitesimal evolution of the atom is described by

$$\hat{U}(dt) = e^{-i\left[\frac{\Delta dt}{2} + \sigma dW\right]\hat{\sigma}_z}. \tag{3.38}$$

If $\hat{\rho}_c(t)$ is the density matrix of the atom at time t, conditioned on that the random phase followed the trajectory $\{dW(\tau), 0 \leq \tau < t\}$, the state at time $t + dt$ is given by

$$\hat{\rho}_c(t+dt) = \hat{U}(dt)\hat{\rho}_c(t)\hat{U}^\dagger(dt). \tag{3.39}$$

By expanding the unitary operators to first order in dt, i.e., to second order in dW (according to the Itô rule from Chapter 2), the evolution can be written as a stochastic master equation,

$$d\hat{\rho}_c(t) = -i\left[\frac{\Delta dt}{2} + \sigma dW(t)\right][\hat{\sigma}_z, \hat{\rho}_c(t)] + \sigma^2 dt \mathcal{D}[\hat{\sigma}_z]\hat{\rho}_c(t). \tag{3.40}$$

To obtain an equation that is independent on the history of the underlying noise process, we average over all possible trajectories $\{dW(\tau), 0 \leq \tau < t\}$. We denote this average as $\mathrm{E}[\cdot]$, and find $\mathrm{E}[\hat{\rho}_c(t)] = \hat{\rho}(t)$ (unconditioned density matrix), and $\mathrm{E}[dW(t)\hat{\rho}_c(t)] = 0$, as the scattering event at time t is independent of the state of the atom. Averaged over all possible realizations, the two-level atom evolves according to the master equation

$$\partial_t \hat{\rho}(t) = -i\frac{\Delta}{2}[\hat{\sigma}_z, \hat{\rho}(t)] + \sigma^2 \mathcal{D}[\hat{\sigma}_z]\hat{\rho}(t). \tag{3.41}$$

The first term describes how the unperturbed atom evolves in time, while the second term describes the decoherence effect induced by scattering. If the density matrix initially is given by $\hat{\rho}(0) = \rho_{00}\left|0\right\rangle\!\left\langle 0\right| + \rho_{11}\left|1\right\rangle\!\left\langle 1\right| + \rho_{01}\left|0\right\rangle\!\left\langle 1\right| + \rho_{10}\left|1\right\rangle\!\left\langle 0\right|$, the master equation tells us that the state at time t reads

$$\hat{\rho}(t) = \rho_{00}\left|0\right\rangle\!\left\langle 0\right| + \rho_{11}\left|1\right\rangle\!\left\langle 1\right| + e^{-2\sigma^2 t}\left(\rho_{01}e^{-i\Delta t}\left|0\right\rangle\!\left\langle 1\right| + \rho_{10}e^{i\Delta t}\left|1\right\rangle\!\left\langle 0\right|\right). \tag{3.42}$$

The effect of the decoherence is thus to exponentially dampen the coherence of the atom, at a rate proportional to σ^2. At long times,

$$\lim_{t\to\infty} \hat{\rho}(t) = \rho_{00}\left|0\right\rangle\!\left\langle 0\right| + \rho_{11}\left|1\right\rangle\!\left\langle 1\right|, \tag{3.43}$$

which is a classical mixture. That is, the atom is either in the ground or excited state, but never in a superposition of the two. This kind of exponential decay of coherences is general for all quantum systems subjected to decoherence. More sophisticated decoherence models can be found in Refs. [70, 80].

Quantum-to-classical transition in the DQD

Decoherence is the process through which the classical world emerges. A good system to explore the quantum-to-classical transition is the DQD, which is simple to model and offers quantum effects such as electron tunneling and superpositions of electron states. Additionally, DQDs are subjected to decoherence induced by the electronic leads, as well as electron and phonon scattering in the materials which the system is defined in. If the decoherence effects are strong, the coherence is heavily suppressed (as we saw in the previous subsection). Because of this, DQDs are often well-described by classical rate equations [52, 83]. Here we derive such a rate equation for the DQD, starting from the full quantum master equation (3.20). A similar derivation was done in Ref. [84].

To begin, we write Eq. (3.20) as

$$\partial_t \hat{\rho}_t = \left(\mathcal{L}_0 + \mathcal{C} + \Gamma_\varphi \mathcal{D}[\hat{A}]\right)\hat{\rho}_t, \tag{3.44}$$

where $\mathcal{L}_0\hat{\rho} = -i[\epsilon_L \left|L\right\rangle\!\left\langle L\right| + \epsilon_R \left|R\right\rangle\!\left\langle R\right|, \hat{\rho}] + \sum_\alpha \left(\gamma_\alpha \mathcal{D}[\hat{\sigma}_\alpha^\dagger]\hat{\rho} + \kappa_\alpha \mathcal{D}[\hat{\sigma}_\alpha]\hat{\rho}\right)$, and $\mathcal{C}\hat{\rho} = -ig[\left|L\right\rangle\!\left\langle R\right| + \left|R\right\rangle\!\left\langle L\right|, \hat{\rho}]$. Note that we have added an additional term $\Gamma_\varphi \mathcal{D}[\hat{A}]$ representing environmental dephasing occurring at the rate Γ_φ, with $\hat{A} = \left|R\right\rangle\!\left\langle R\right| - \left|L\right\rangle\!\left\langle L\right|$.

We now introduce the Nakajima-Zwanzig superoperators [85, 86]

$$\mathcal{P}\hat{\rho} = \sum_{\alpha=0,L,R} \rho_{\alpha\alpha} \left|\alpha\right\rangle\!\left\langle\alpha\right|, \qquad \text{and} \qquad \mathcal{Q} = 1 - \mathcal{P}, \tag{3.45}$$

which singles out the diagonal ($\mathcal{P}$) and off-diagonal ($\mathcal{Q}$) elements of $\hat{\rho}$ in the basis $\{\left|0\right\rangle, \left|L\right\rangle, \left|R\right\rangle\}$. As before, $\rho_{\alpha\alpha} = \langle\alpha|\hat{\rho}|\alpha\rangle$. Note that $\mathcal{P}^2 = \mathcal{P}$ and $\mathcal{Q}^2 = \mathcal{Q}$. By explicit evaluation, we find that $[\mathcal{L}_0, \mathcal{P}] = [\mathcal{L}_0, \mathcal{Q}] = [\mathcal{D}[\hat{A}], \mathcal{Q}] = \mathcal{P}\mathcal{D}[\hat{A}] = \mathcal{D}[\hat{A}]\mathcal{P} = \mathcal{P}\mathcal{C}\mathcal{P} = \mathcal{Q}\mathcal{C}\mathcal{Q} = 0$. With these relations, Eq. (3.44) can be split into two coupled differential equations,

$$\partial_t \mathcal{P}\hat{\rho}_t = \mathcal{L}_0 \mathcal{P}\hat{\rho}_t + \mathcal{P}\mathcal{C}\mathcal{Q}\hat{\rho}_t, \tag{3.46a}$$

$$\partial_t \mathcal{Q}\hat{\rho}_t = \left(\mathcal{L}_0 + \Gamma_\varphi \mathcal{D}[\hat{A}]\right) \mathcal{Q}\hat{\rho}_t + \mathcal{Q}\mathcal{C}\mathcal{P}\hat{\rho}_t. \tag{3.46b}$$

The solution to Eq. (3.46b) reads

$$\mathcal{Q}\hat{\rho}_t = e^{\left(\mathcal{L}_0 + \Gamma_\varphi \mathcal{D}[\hat{A}]\right)\mathcal{Q}(t-t_0)} \mathcal{Q}\hat{\rho}_{t_0} + \int_{t_0}^{t} ds e^{\left(\mathcal{L}_0 + \Gamma_\varphi \mathcal{D}[\hat{A}]\right)\mathcal{Q}(t-s)} \mathcal{Q}\mathcal{C}\mathcal{P}\hat{\rho}_s. \tag{3.47}$$

We note that $\mathcal{L}_0 + \Gamma_\varphi \mathcal{D}[\hat{A}]$ has negative eigenvalues in Q-space, such that the first term decays exponentially, and can be ignored at long times (we are most often interested in the stationary state). Alternatively, we may assume that $\mathcal{Q}\hat{\rho}_{t_0} = 0$. For the integral, we make the substitution $\tau = t - s$. Additionally, we assume that the exponential decays to zero on a timescale during which $\mathcal{P}\hat{\rho}_t$ remains constant. The density matrix may thus be moved outside the integral, and we replace $\mathcal{P}\hat{\rho}_s \to \mathcal{P}\hat{\rho}_t$. Also note that the upper integration limit can be extended to ∞ under these assumptions. Finally, we find

$$\mathcal{Q}\hat{\rho}_t = -\left\{\left(\mathcal{L}_0 + \Gamma_\varphi \mathcal{D}[\hat{A}]\right) \mathcal{Q}\right\}^{-1} \mathcal{Q}\mathcal{C}\mathcal{P}\hat{\rho}_t, \tag{3.48}$$

where we introduced the Drazin inverse [87, 88]

$$\left\{\left(\mathcal{L}_0 + \Gamma_\varphi \mathcal{D}[\hat{A}]\right) \mathcal{Q}\right\}^{-1} = -\int_0^\infty d\tau e^{\left(\mathcal{L}_0 + \Gamma_\varphi \mathcal{D}[\hat{A}]\right)\mathcal{Q}\tau}. \tag{3.49}$$

By explicit calculation, one can show that $-\left\{\left(\mathcal{L}_0 + \Gamma_\varphi \mathcal{D}[\hat{A}]\right) \mathcal{Q}\right\}^{-1} \mathcal{Q}\mathcal{C} = \xi\Big(\mathcal{D}[\left|L\right\rangle\!\left\langle R\right| + \left|R\right\rangle\!\left\langle L\right|]\Big)$, with the classical interdot tunneling rate

$$\xi = \frac{4g^2\left(\kappa_L + \kappa_R + 4\Gamma_\varphi\right)}{\left(\kappa_L + \kappa_R + 4\Gamma_\varphi\right)^2 + 16\Delta^2}. \tag{3.50}$$

We note that this rate is suppressed when the external dephasing Γ_φ is large. In this limit, interdot tunneling is heavily slowed down, which we expect for strong dephasing, as electrons in the DQD get localized on either the left or right dot. As $\Gamma_\varphi \to \infty$, the coherence vanishes and $\xi \to 0$, reflecting that tunneling is a quantum process which requires coherence. However, for finite Γ_φ, we expect that tunneling is well-modeled by classical jumps occuring at rate ξ. We also note that ξ has a Lorentzian profile in the splitting Δ, resulting from the lifetime broadening of the individual levels. As stated earlier, we expect the equations to hold only for small Δ (see also Chapter 5).

By plugging Eq. (3.48) into Eq. (3.46a), we find the classical equation of motion

$$\partial_t \mathcal{P}\hat{\rho}_t = \mathcal{L}_0 \mathcal{P}\hat{\rho}_t + \xi\Big(\mathcal{D}[|L\rangle\langle R|] + \mathcal{D}[|R\rangle\langle L|]\Big)\mathcal{P}\hat{\rho}_t, \tag{3.51}$$

for the populations of the DQD. We may rewrite $\mathcal{P}\hat{\rho}_t$ as a vector $\boldsymbol{P}_t = [\rho_{00}(t), \rho_{LL}(t), \rho_{RR}(t)]^T$, and formulate this master equation as a classical rate equation,

$$\partial_t \boldsymbol{P}_t = \begin{pmatrix} -\gamma_L - \gamma_R & \kappa_L & \kappa_R \\ \gamma_L & -\kappa_L - \xi & \xi \\ \gamma_R & \xi & -\kappa_R - \xi \end{pmatrix} \boldsymbol{P}_t. \tag{3.52}$$

The approximations and assumptions leading to this equation are justified as long as $\Gamma_\varphi \gg \Gamma_L, \Gamma_R, \xi$, where $\Gamma_{L(R)}$ is the tunnel coupling between the DQD and the left (right) reservoir.

3.6 Full counting statistics

The central idea of full counting statistics is to gain full knowledge about particle transport in nanoscale systems. The probability distribution $P_t(n)$ of having n transferred particles during a time interval t can reveal intrinsic properties of these systems. For instance, in electronic circuits on the microscopic scale, the role of current fluctuations becomes essential for understanding a large variety of microscopic concepts [58]. Motivated by this, we introduce full counting statistics with electronic transport [89] in mind, focusing especially on how $P_t(n)$ can be obtained for systems described by Markovian master equations [90, 91]. We note that this way of counting can be extended to any type of particles – for instance, photons [92] and phonons [93].

We begin by studying the setup depicted in Fig. 3.3(a), where an open system S exchanges particles with one or several reservoirs. Our main objective is to measure the statistics of exchanged particles between S and the reservoir labeled by R during an arbitrary interaction time t. Such particle counting is, since roughly 20 years ago, possible to conduct in electronic systems, where single electron transitions can be detected [52, 54, 94–98]. As

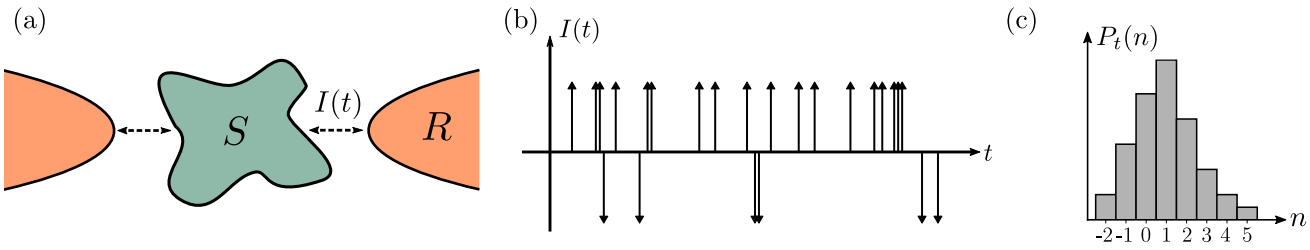

Figure 3.3: (a) A standard setup for nanoscale experiments. A system (S) is coupled to one or several environments. We are interested in investigating the intrinsic properties of S by measuring the particle exchange between S and the environment labeled by R. This exchange can be measured via the particle current $I(t)$, as marked in the figure. (b) A schematic sketch of how the current $I(t)$ changes over time. The current is a series of δ-peaks centered at the times at which the jumps occur. The positive (negative) peaks correspond to jumps from S to R (R to S). (c) The probability distribution $P_t(n)$ of the number of particles n exchanged between S and R after time t. By relating $n(t)$ and $I(t)$ as in Eq. (3.53), we may find the moments and cumulants of $P_t(n)$ directly from the current correlations.

long as the response rate of the detector is much larger than the electron transition rate, one can accurately infer the transport statistics. When the electron transition rate is similar to, or larger than the detector response rate, it is no longer possible to resolve all electron transitions, and the recorded data would give inaccurate transport statistics. Instead, one could measure the current $I(t)$ (here interpreted as a particle current rather than an electronic current) to infer something about the transport statistics[6]. In Fig. 3.3(b), we have sketched a time trace of the current between S and R, which is a series of δ-peaks due to the discrete nature of particle jumps. In Appendix G we provide more details on discrete jump currents and how a diffusive current can emerge from this picture. Note that the results of Sec. 3.6.1 hold for discrete jumps – a similar treatment for diffusion currents can be found in Ref. [77]. The number of particles exchanged with R after time t is obtained via

$$n(t) = \int_0^t d\tau I(\tau). \tag{3.53}$$

Here we use the convention that $I(t) > 0$ when the current flows from S towards R, such that $n(t) > 0$ when particles enter R. Since $I(t)$ and $n(t)$ are random processes, it is difficult to draw general conclusions about the transport statistics from single trajectories of these quantities. Instead, by repeating the experiment a large number of times N, and keeping track of $n(t)$ for each run, we can find the number of times K_n where we observe n exchanged particles after time t. The relative frequency of observing n particles is given by K_n/N, and in the limit of large N, we get

$$\lim_{N\to\infty} \frac{K_n}{N} = P_t(n), \tag{3.54}$$

[6]In this thesis, we interpret $I(t)$ as a classical current. This allows for straightforward manipulations when calculating higher order statistics as in Eq. (3.55). In a full quantum treatment, the current is introduced as an operator $\hat{I}(t)$. This raises some subtleties, such as time ordering. For instance, Eq. (3.55) does not, in general, hold when the current is an operator. For a full quantum treatment, see, for example, Refs. [89, 99, 100].

the probability of observing n exchanged particles after time t. Figure 3.3(c) illustrates a typical distribution function $P_t(n)$.

We can also use the current to find the moments of $P_t(n)$. By taking an average $\langle\cdot\rangle$ over many experimental realizations [similar to Eq. (2.3)], we get

$$\langle n^k(t)\rangle = \int_0^t d\tau_1 \cdots \int_0^t d\tau_k \langle I(\tau_1)\cdots I(\tau_k)\rangle, \tag{3.55}$$

where we used Eq. (3.53). For $k = 1$, we get the average $\langle n(t)\rangle$. For long times t, the average current $\langle I(t)\rangle$ reaches a stationary state, and becomes independent on time. In that case, the average current can be moved outside the integral, and we get $\langle n(t)\rangle = \langle I\rangle_{\rm ss} t$. The stationary current can thus be written on the intuitive form

$$\langle I\rangle_{\rm ss} = \lim_{t\to\infty} \frac{\langle n(t)\rangle}{t}. \tag{3.56}$$

We can further calculate the variance of $P_t(n)$ using the current,

$$\begin{aligned}\langle\langle n^2(t)\rangle\rangle &= \langle n^2(t)\rangle - \langle n(t)\rangle^2 \\ &= \int_0^t d\tau_1 \int_0^t d\tau_2 \left[\langle I(\tau_2)I(\tau_1)\rangle - \langle I(\tau_2)\rangle\langle I(\tau_1)\rangle\right].\end{aligned} \tag{3.57}$$

From this, we find the second order current cumulant

$$\langle\langle I^2(t)\rangle\rangle = \partial_t \langle\langle n^2(t)\rangle\rangle = 2\int_0^t d\tau \left[\langle I(\tau)I(t)\rangle - \langle I(\tau)\rangle\langle I(t)\rangle\right]. \tag{3.58}$$

From these expressions, we can define a current correlator $\mathcal{C}_I(t,t') = \langle I(t)I(t')\rangle - \langle I(t)\rangle\langle I(t')\rangle$. We are interested in the stationary state of the current correlator, where it is translationally invariant in time and only depends on the difference $t - t'$, i.e., $\mathcal{C}_I(t,t') = \mathcal{C}_I(t-t')$. We further assume that the system is Markovian, meaning that the correlator quickly decays to zero on some correlation time τ_c. Finally, we assume that the correlator is symmetric under the exchange $t \leftrightarrow t'$, such that all points separated by $t - t'$ are correlated identically. When the measurement time t greatly exceeds the correlation time τ_c, the variance of $P_t(n)$ becomes linear in time,

$$\langle\langle n^2(t)\rangle\rangle = t\int_{-\infty}^{\infty} d\tau \left[\langle I(\tau)I(0)\rangle - \langle I(\tau)\rangle\langle I(0)\rangle\right]. \tag{3.59}$$

This implies the stationary second current cumulant

$$\langle\langle I^2\rangle\rangle_{\rm ss} = \lim_{t\to\infty} \frac{\langle\langle n^2(t)\rangle\rangle}{t} = \int_{-\infty}^{\infty} d\tau \left[\langle I(\tau)I(0)\rangle - \langle I(\tau)\rangle\langle I(0)\rangle\right]. \tag{3.60}$$

With the noise spectrum of the stationary current correlator [see Eq. (2.6)]

$$S_I(\omega) = \int_{-\infty}^{\infty} d\tau e^{i\omega\tau} \mathcal{C}_I(\tau), \tag{3.61}$$

we find that the zero frequency noise $S_I(0)$ coincides with Eq. (3.60). Therefore, we understand that the variance of n, in the long time limit, is given by

$$\langle\langle n^2(t) \rangle\rangle = S_I(0)t. \tag{3.62}$$

The variance thus grows linearly with time at a rate determined by the zero frequency noise of the current correlator. This linear increase reflects that different trajectories of $n(t)$ will be less similar the longer we measure. The uncertainty in the number of exchanged particles should therefore grow with time. This is similar to the variance of Brownian motion in Chapter 2.

3.6.1 Full counting statistics in Markovian master equations

In the previous section, we described how the moments of the distribution $P_t(n)$ can be calculated by measuring particle currents. Here we discuss how $P_t(n)$, and its moments and cumulants, may be calculated from a Markovian master equation.

Our starting point is the Markovian master equation

$$\partial_t \hat{\rho}_t = \mathcal{L}\hat{\rho}_t, \tag{3.63}$$

where the Liouville superoperator $\mathcal{L}$ is assumed to be in Lindblad form [see Eq. (3.15)]. This superoperator can be decomposed as $\mathcal{L} = \mathcal{L}_0 + \mathcal{J}_+ + \mathcal{J}_-$, where $\mathcal{L}_0$ describes all dynamics that leaves the number of exchanged particles with R unchanged, and the jump superoperators $\mathcal{J}_\pm$ describe how one particle is added $(+)$ or removed $(-)$ from R [see Fig. 3.3(a)]. We are interested in the n-resolved density matrix $\hat{\rho}_t(n)$, representing the system state when n particles have been exchanged with R. In particular, we note that $P_t(n) = \mathrm{tr}\{\hat{\rho}_t(n)\}$ is the probability distribution of our interest, and that $\hat{\rho}_t = \sum_n \hat{\rho}_t(n)$. By taking the Laplace transform of the master equation (3.63), we can show (Appendix B) that the number resolved density matrix evolves according to

$$\partial_t \hat{\rho}_t(n) = \mathcal{L}_0 \hat{\rho}_t(n) + \mathcal{J}_+ \hat{\rho}_t(n-1) + \mathcal{J}_- \hat{\rho}_t(n+1), \tag{3.64}$$

providing an infinitely large system of coupled differential equations. Typically, the initial condition is given by $\hat{\rho}_{t_0}(n) = \delta_{n,0}\hat{\rho}_{t_0}$, such that zero particles have been exchanged initially. To solve this set of equations, we introduce the counting field χ via the discrete Fourier transform

$$\hat{\rho}_t(\chi) = \sum_n \hat{\rho}_t(n) e^{in\chi}. \tag{3.65}$$

Note that the system state is recovered for zero counting field, $\hat{\rho}_t = \hat{\rho}_t(\chi = 0)$. Fourier transforming Eq. (3.64) results in

$$\partial_t \hat{\rho}_t(\chi) = \mathcal{L}(\chi)\hat{\rho}_t(\chi), \tag{3.66}$$

where the counting field dependent Liouvillian reads $\mathcal{L}(\chi) = \mathcal{L}_0 + e^{i\chi}\mathcal{J}_+ + e^{-i\chi}\mathcal{J}_-$, and the initial condition is given by $\hat{\rho}_{t_0}(\chi) = \hat{\rho}_{t_0}$. This master equation has the formal solution $\hat{\rho}_t(\chi) = e^{\mathcal{L}(\chi)t}\hat{\rho}_{t_0}$.

Since $P_t(n) = \mathrm{tr}\{\hat{\rho}_t(n)\}$, we can define a moment generating function

$$M_t(\chi) = \mathrm{tr}\{\hat{\rho}_t(\chi)\} = \sum_n P_t(n)e^{in\chi}, \tag{3.67}$$

such that the moments of $P_t(n)$ can be calculated as

$$\langle n^k(t)\rangle = (-i)^k \partial_\chi^k M_t(\chi)\big|_{\chi=0}. \tag{3.68}$$

In a strict mathematical sense, $M_t(\chi)$ is the characteristic function of $P_t(n)$, but as the characteristic function exists for all distributions, it is more beneficial to work with compared to the conventional moment generating function, which does not exist for all distributions [101]. Note that the first moment conveniently can be calculated as $\langle n\rangle = -it\,\mathrm{tr}\{\mathcal{L}'(\chi)|_{\chi=0}\hat{\rho}_t\}$, where the prime denotes the derivative with respect to χ. One can further define a cumulant generating function

$$C_t(\chi) = \ln[M_t(\chi)], \tag{3.69}$$

which provides the cumulants of $P_t(n)$ via

$$\langle\langle n^k(t)\rangle\rangle = (-i)^k \partial_\chi^k C_t(\chi)\big|_{\chi=0}. \tag{3.70}$$

As the moment and cumulant generating functions are related, one can write the cumulants in terms of the moments. In particular, $\langle\langle n(t)\rangle\rangle = \langle n(t)\rangle$ is the mean of $P_t(n)$, and $\langle\langle n^2(t)\rangle\rangle = \langle n^2(t)\rangle - \langle n(t)\rangle^2$ is the variance of $P_t(n)$. In fact, the second and third cumulants exactly correspond to the second and third central moments of $P_t(n)$. We also note that the third and fourth cumulants are related to the skewness and kurtosis of $P_t(n)$. The current cumulants are found by differentiating with respect to time,

$$\langle\langle I^k(t)\rangle\rangle = \partial_t\langle\langle n^k(t)\rangle\rangle. \tag{3.71}$$

With the definitions of the moment and cumulant generating functions, we can calculate the probability distribution according to

$$P_t(n) = \frac{1}{2\pi}\int_{-\pi}^{\pi} d\chi e^{C_t(\chi)-in\chi}. \tag{3.72}$$

In general, this must be calculated numerically, even if we know the cumulant generating function. However, the saddle point approximation [102–104] is useful for finding analytical expressions in the long time limit.

In many cases, we can find an approximate expression for the cumulant generating function in the long time limit. The solution of Eq. (3.66) can be written as

$$\hat{\rho}_t(\chi) = \sum_{j=0}^{N-1} c_j e^{\lambda_j(\chi)t} \hat{\sigma}_j(\chi), \tag{3.73}$$

where the coefficients c_j are determined by the initial condition $\hat{\rho}_0$ (we use $t_0 = 0$), $\lambda_j(\chi)$ are the eigenvalues of $\mathcal{L}(\chi)$ with corresponding eigenstates $\hat{\sigma}_j(\chi)$, and N is the dimension of $\mathcal{L}(\chi)$. We are interested in systems with a unique steady state. For such systems, there exists one single eigenvalue for which $\lambda_0(0) = 0$ (here labeled with $j = 0$), and where all other eigenvalues $\lambda_j(0) \neq 0$. Since the system tends to a stationary state, all eigenvalues with $j \neq 0$ must have negative real parts, such that all terms except $j = 0$ are vanishingly small when t is large [see discussion below Eq. (3.17)]. For finite χ, we assume that all eigenvalues have negative real parts, with the real part of $\lambda_0(\chi)$ being the largest, such that we, for large t, find

$$\hat{\rho}_t(\chi) \approx c_0 e^{\lambda_0(\chi)t} \hat{\sigma}_0(\chi). \tag{3.74}$$

The moment generating function now reads $\mathrm{tr}\{\hat{\rho}_t(\chi)\} \approx \mathrm{tr}\{\hat{\sigma}_0(\chi)\} c_0 e^{\lambda_0(\chi)t}$, and we may approximate the cumulant generating function as

$$C_t(\chi) \approx \lambda_0(\chi) t, \tag{3.75}$$

up to a correction term $\ln[c_0 \,\mathrm{tr}\{\hat{\sigma}_0(\chi)\}]$ which has been neglected. In the long time limit, it is justified to neglect this term as it is small compared to $\lambda_0(\chi)t$. Consequently, the number cumulants will have an error determined by the χ-derivatives of $\ln[c_0 \,\mathrm{tr}\{\hat{\sigma}_0(\chi)\}]$. However, in the current cumulants, this error will not be present as we take a time derivative in Eq. (3.71). We note that the approximate form in Eq. (3.75) reproduces the linear-in-time behavior of the number cumulants in Eq. (3.62). We emphasize that this formalism can be generalized to multiple counting fields, keeping track of the counting statistics in multiple reservoirs simultaneously. In such a generalization, it is possible to calculate correlations between different particle transitions.

Chapter 4

Continuous measurements and feedback control

Measurements and feedback control are the central themes of this thesis. In this chapter, we introduce the basic theory of these concepts. In particular, we discuss the necessary theory for understanding and reproducing the results of Paper II. Papers III, IV and VI later build on these results.

Section 4.1 begins with a short review of von Neumann (projective) measurements, commonly discussed in basic courses on quantum mechanics. Since this is a special class of measurements, we also introduce generalized quantum measurements, providing a general framework describing any type of measurement. Section 4.2 is devoted to time-continuous measurements, where a continuous flow of information is recorded. We begin by introducing a Gaussian measurement operator suitable to describe such measurements. We use this operator to derive both deterministic and stochastic equations of motion for a continuously measured quantum system. At the end of the section, we extend the theory to include a realistic detector model. Section 4.3 discusses quantum feedback control, where a measurement is used to control the dynamics of a system. In particular, we discuss two special scenarios where it is possible to derive Markovian master equations for feedback-controlled systems.

4.1 Quantum measurements

Fundamental to measurements in quantum mechanics is the concept of *von Neumann measurements* – or projective measurements. This type of measurement describes how the

state of a quantum system is collapsed (projected) onto one of the eigenstates of the measured observable after performing a measurement. More precisely, any observable $\hat{A}$ has a diagonal representation in some orthonormal basis $\{|a\rangle\}_{a=1}^{N}$, i.e., it can be written as $\hat{A} = \sum_{a=1}^{N} \xi_a |a\rangle\langle a|$, where $\{\xi_a\}_{a=1}^{N}$ are the (non-degenerate) eigenvalues of $\hat{A}$. In general, the eigenvalues can be degenerate. If that is the case, the system is projected onto a superposition of the corresponding eigenstates. In Paper IV, we exploit this to perform a backaction-free measurement – we return to this below. However, for most of our purposes, the eigenvalues will be non-degenerate, and we thus focus our discussion on that case. Note that we assume that there is a finite number N of eigenvalues, as this always will be the case in this thesis. Consider that we carry out a measurement on an arbitrary quantum system, whose state, when written in the eigenbasis of $\hat{A}$, is given by $|\psi\rangle = \sum_{a=1}^{N} c_a |a\rangle$, with complex coefficients c_a satisfying $\sum_{a=1}^{N} |c_a|^2 = 1$. Upon measuring, we obtain one of the eigenvalues $\xi_{a'}$ with probability $|c_{a'}|^2$, and the state collapses to $|a'\rangle$. That is, the system is, with certainty, in this state after the measurement. In terms of the density operator formalism introduced in Chapter 3, we note that the pre-measurement state is given by some density operator $\hat{\rho}$ (pure or mixed) but the post-measurement state will with probability $|c_{a'}|^2$ be in the pure state $\hat{\rho}' = |a'\rangle\langle a'|$.

A von Neumann measurement does not fully describe a realistic procedure for quantum measurements. In reality, an experimenter rarely interacts directly with the system of interest, but rather measures on a probe that interacts with the system. In addition, the von Neumann measurement does not add any classical noise to the measurement outcome. This must be regarded as unrealistic as a measurement device typically adds noise to the recorded signal. The idea of the system-probe model is to build up correlations between the system and the probe, and then perform a von Neumann measurement on the probe, such that we can infer something about the system without collapsing its state. As a first example of this, consider a nanowire quantum dot for which we want to measure the charge state, i.e., if there is an electron or not in the dot. In general, this is done by placing a probe in the vicinity of the dot – typically the probe is another quantum dot or a quantum point contact – and measure the electrical current through the probe. If the system-probe interaction is sensitive enough, the current will jump between discrete values when an electron jumps on or off the dot, see for instance Refs. [94] and [54]. As a second example, consider an atom interacting with an electromagnetic field. Here the field acts as the probe, and by measuring the field, for instance with a photo-detector, we can infer something about the state of the atom.

To find a mathematical description for the system-probe measurement, we consider the following model. Assume that the system and probe initially are uncorrelated, and that their joint state is given by $\hat{\rho}_{\text{tot}} = |0\rangle\langle 0| \otimes \hat{\rho}$, where the probe is prepared in some state $|0\rangle$ belonging to an orthonormal set $\{|m\rangle\}_m$ of probe states, and the system is prepared in an arbitrary state $\hat{\rho}$. By letting the system and probe interact under some unitary transforma-

tion $\hat{U}$, their states will become correlated. Now we make a von Neumann measurement on the probe, projecting it onto one of the states $|m\rangle$. After this procedure, the joint state is proportional to

$$\hat{\rho}'_{\text{tot}} \sim (|m\rangle\langle m| \otimes \mathbb{1})\, \hat{U}\, (|0\rangle\langle 0| \otimes \hat{\rho})\, \hat{U}^\dagger\, (|m\rangle\langle m| \otimes \mathbb{1}) = |m\rangle\langle m| \otimes \hat{K}_m \hat{\rho} \hat{K}_m^\dagger, \quad (4.1)$$

where we after the equal sign introduced operators $\hat{K}_m = \langle m|\hat{U}|0\rangle$ acting on the system state. Note that the mathematical procedure above resembles how the UDMs were introduced in Eq. (3.12). In fact, any operation on an open quantum system may be written like this [19].

We can now define a generalized quantum measurement as follows. Consider a system with state $\hat{\rho}$ on which we perform a measurement described by a set of measurement operators $\{\hat{K}_m\}_m$ (see definition previous paragraph), satisfying the completeness relation $\sum_m \hat{K}_m^\dagger \hat{K}_m = \mathbb{1}$. When observing outcome m, the state transforms as

$$\hat{\rho}' = \frac{\hat{K}_m \hat{\rho} \hat{K}_m^\dagger}{p_m}, \quad (4.2)$$

where $p_m = \text{tr}\{\hat{K}_m^\dagger \hat{K}_m \hat{\rho}\}$ is the probability of observing outcome m. We emphasize here that Eq. (4.2) is obtained by tracing out the probe in Eq. (4.1), i.e., $\hat{\rho}' \sim \text{tr}_P\{\hat{\rho}'_{\text{tot}}\}$, and normalizing with p_m. The completeness relation $\sum_m \hat{K}_m^\dagger \hat{K}_m = \mathbb{1}$ ensures probability conservation for p_m, but also follows directly from the definition of $\hat{K}_m$. Sometimes, this type of measurement is referred to as a POVM (positive operator-valued measure) measurement [15, 16, 19], but in this thesis, we refer to it as a generalized quantum measurement. We stress here that the measurement operators $\hat{K}_m$ are completely general, and do not necessarily represent projective measurements. Below, in Sec. 4.2, we will discuss the special case of Gaussian measurements. However, by considering projective measurement operators $\hat{K}_m = |m\rangle\langle m|$ (where $|m\rangle$ now represents basis states of the system), Eq. (4.2) boils down to the von Neumann measurement discussed above.

It is important to note that $\hat{\rho}'$ in Eq. (4.2) is conditioned on the measurement outcome m. That is, it describes our state of knowledge of the system given that we observed m in the measurement. Interestingly, this transformation is nonlinear in $\hat{\rho}$. This is in contrast to the von Neumann equation (3.9) and the Lindblad equation (3.15) which are linear. This means that quantum measurements induce a nonlinear change in the system state. We will return to this in Sec. 4.2. However, a linear description is obtained by multiplying Eq. (4.2) by p_m, but at the cost of introducing the un-normalized joint system-outcome state $\hat{\rho}(m) = \hat{\rho}' p_m = \hat{K}_m \hat{\rho} \hat{K}_m^\dagger$. By summing this state over all outcomes m results in the post-measurement state $\tilde{\rho} = \sum_m \hat{K}_m \hat{\rho} \hat{K}_m^\dagger$. This operation corresponds to averaging the conditioned state $\hat{\rho}'$ [Eq. (4.2)] over all outcomes. This is sometimes referred to as a non-selective measurement [70], reflecting that the outcome effectively is ignored when

averaging over all possible outcomes. As an example, let us consider a two-level system with density operator $\hat{\rho} = p_0 |0\rangle\langle 0| + \alpha(|0\rangle\langle 1| + |1\rangle\langle 0|) + p_1 |1\rangle\langle 1|$, where p_0 and p_1 are the probabilities to be in state $|0\rangle$ or $|1\rangle$, respectively, and α represents the coherence (here taken as real for simplicity). By performing a projective measurement, with measurement operators $\hat{K}_0 = |0\rangle\langle 0|$ and $\hat{K}_1 = |1\rangle\langle 1|$, the post-measurement state, averaged over all possible outcomes (0 or 1), is given by $\tilde{\rho} = p_0 |0\rangle\langle 0| + p_1 |1\rangle\langle 1|$. That is, after the measurement, the system will be in a statistical mixture of $|0\rangle$ and $|1\rangle$. This illustrates that the measurement destroys all coherence, but we do not know the exact state of the system, as we ignored the outcome.

Finally, we point out that quantum measurements induce a stochastic change to a system state. To understand this, consider many copies of the same system on which we perform identical measurements. The state transformation in Eq. (4.2) depends on the outcome m that was observed, and since each outcome occurs with probability p_m, the measurement operator applied on a specific copy is random. Therefore, the post-measurement state will not be the same for all copies. This implies that for a continuous measurement, the conditioned state $\hat{\rho}'$ evolves according to a stochastic master equation. This is further discussed in Sec. 4.2.

4.2 Continuous measurements

In many situations, it is common to perform a time-continuous measurement, rather than making one single measurement, and to use a measurement apparatus that outputs continuous outcomes, rather than discrete ones. Even though one measures a discrete observable, like a photon number operator, the measurement device adds noise to the signal, such that a continuous outcome space is more appropriate than a discrete one. The type of measurement, discrete or continuous in time, that is most suitable is determined by the type of system and experiment one is studying. For instance, in electronic systems, such as semiconductor quantum dots [52, 54, 105], it is possible to measure the charge occupation continuously, which suggests that a time-continuous measurement is most suitable. As another example, the state of superconducting qubits can also be monitored continuously [48]. On the other hand, when distinguishing spin states in semiconductor quantum dots, one is restricted to time-discrete measurements [106]. This is also the case when performing quantum state tomography in rare earth ion qubits [107]. However, many control procedures require continuous monitoring, such as certain schemes for quantum error correction [108], stabilizing Rabi oscillations [48], reversing quantum jumps [49], or implementing an electronic Szilard engine [27]. Therefore, we dedicate this section to time-continuous measurements with continuous outcomes. We begin by replacing the discrete outcomes m from the previous section by continuous outcomes z and introduce a Gaussian measurement operator that is useful for mathematical modeling. The theory presented above for

discrete outcomes still applies, but sums over m are typically replaced by integrals over z. In the second part of this section, we discuss how time-continuous measurements can be modeled, and how the quantum Zeno effect emerges from this description.

To describe a general measurement with a continuous outcome, we use the following Gaussian measurement operator [16, 78, 109]

$$\hat{K}(z) = \left(\frac{2\bar{\lambda}}{\pi}\right)^{1/4} e^{-\bar{\lambda}\left(z-\hat{A}\right)^2}, \tag{4.3}$$

where $\hat{A}$ is the measured observable (note that $\hat{A}^\dagger = \hat{A}$), and $\bar{\lambda}$ parameterizes the strength of the measurement. In the limit $\bar{\lambda} \to \infty$, Eq. (4.3) describes a projective von Neumann measurement, where all initial quantum coherence is destroyed, and where the post-measurement state is projected onto one of the eigenstates of $\hat{A}$. In the opposite limit, when $\bar{\lambda} \to 0$, Eq. (4.3) describes a weak, non-intrusive measurement, preserving all quantum coherence. The Gaussian operator thus provides the possibility of describing measurements with a wide range of possible interaction strengths, and allows us to investigate how the strength affects the measured system. Additionally, Eq. (4.3) implies that the measurement noise is Gaussian (see discussion below). This is commonly the case due to many independent random fluctuations in the electronic circuits of the measurement device. We also note (this will be shown below) that Eq. (4.3) is suitable for analytical manipulations, as it simplifies many calculations, while still providing general results.

To illustrate the strong and weak measurement limits, we study a simple two-level system with states $|0\rangle$ and $|1\rangle$. In the $\{|0\rangle, |1\rangle\}$-basis, the system density operator reads $\hat{\rho} = p\,|0\rangle\langle 0| + \alpha(|0\rangle\langle 1| + |1\rangle\langle 0|) + (1-p)\,|1\rangle\langle 1|$, where p and $1-p$ are the probabilities of occupying $|0\rangle$ and $|1\rangle$, respectively, and α represents the coherence (here assumed to be real for simplicity, but without loss of generality). When measuring $\hat{A} = |1\rangle\langle 1| - |0\rangle\langle 0|$, i.e., whether $|0\rangle$ or $|1\rangle$ is occupied, the state transformation is, according to Eq. (4.2), proportional to

$$\begin{aligned}\hat{K}(z)\hat{\rho}\hat{K}^\dagger(z) = \sqrt{\frac{2\bar{\lambda}}{\pi}}\Big[&pe^{-2\bar{\lambda}(z+1)^2}\,|0\rangle\langle 0| \\ &+ \alpha e^{-2\bar{\lambda}(z^2+1)}\left(|0\rangle\langle 1| + |1\rangle\langle 0|\right) + (1-p)e^{-2\bar{\lambda}(z-1)^2}\,|1\rangle\langle 1|\Big].\end{aligned} \tag{4.4}$$

For simplicity, we neglect the normalizing factor $p(z) = \mathrm{tr}\{\hat{K}^\dagger(z)\hat{K}(z)\hat{\rho}\}$. The measurement adds Gaussian weights, centered at -1,0, and 1, to the respective elements of $\hat{\rho}$, and the off-diagonal elements are suppressed by a factor $e^{-2\bar{\lambda}}$. The weights of the respective elements are sketched in Fig. 4.1. For a weak measurement, a considerable amount of the coherence is preserved when the outcome lies in the range $-1 < z < 1$. In the infinitely weak limit, $\bar{\lambda} \to 0$, the Gaussian weights become uniform distributions over all z, and the coherence is preserved. As $\bar{\lambda}$ is increased, the coherence is exponentially suppressed,

and vanishes for strong measurements, where only the $|0\rangle\langle 0|$ or $|1\rangle\langle 1|$ matrix elements are nonzero. Treating this rigorously by taking $\bar{\lambda} \to \infty$, the diagonal Gaussian weights become Dirac delta functions $\delta(z \pm 1)$ centered at ± 1, while the off-diagonal weights vanish, corresponding to a projective measurement.

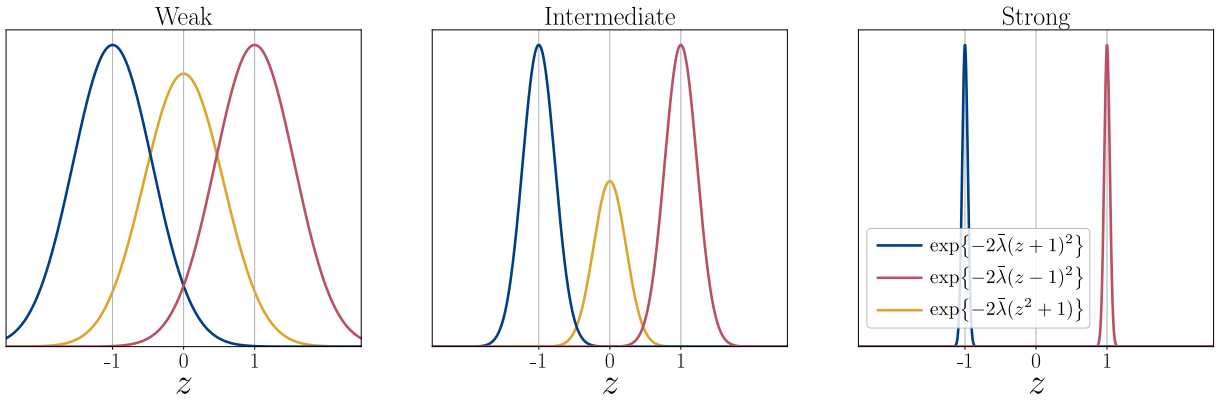

Figure 4.1: Qualitative sketch of how the Gaussian weights in Eq. (4.4) behave when going from a weak to a strong measurement (from left to right with increasing $\bar{\lambda}$). Note that for weak measurements, a substantial part of the coherence is preserved for a larger range of outcomes than in the strong measurement case. This is due to the factor $\exp\{-2\bar{\lambda}\}$ on the off-diagonal elements in Eq. (4.4).

For the two-level system, the probability distribution of outcomes z is given by

$$p(z) = \mathrm{tr}\{\hat{K}^\dagger(z)\hat{K}(z)\hat{\rho}\} = \sqrt{\frac{2\bar{\lambda}}{\pi}}\left[pe^{-2\bar{\lambda}(z+1)^2} + (1-p)e^{-2\bar{\lambda}(z-1)^2}\right]. \tag{4.5}$$

In the strong measurement limit, $\bar{\lambda} \to \infty$, the Gaussian weights become Dirac delta functions $\delta(z \pm 1)$, indicating that the only possible outcomes are ± 1. That is, for a projective measurement, there is no uncertainty in the measurement – we know, for sure, the post-measurement state. In the weak limit, $\bar{\lambda} \to 0$, the Gaussian weights become uniform distributions over all z. Therefore, the measurement can yield any value for the outcome z, but we do not know much about the state of the system – our uncertainty is maximized. To summarize, the strength of the measurement is a trade-off – a weak measurement preserves quantum coherence, but gives large measurement uncertainty, while a strong measurement destroys all quantum coherence, but gives low measurement uncertainty.

Equation (4.5) is a mixed distribution, and can be interpreted, or constructed, as follows (this is useful for simulations). Consider a random variable $x = -1, 1$ for the system state, following a two-point distribution with $P(x = -1) = p$ and $P(x = 1) = 1 - p$ being the probabilities of occupying $|0\rangle$ and $|1\rangle$, respectively. Given that we know the system state x, the random variable $z|x$ represents the measurement outcome conditioned on the system state. This variable has a Gaussian distribution with mean value x and variance $1/4\bar{\lambda}$. By applying the total law of probability, we obtain the unconditioned distribution (4.5) for z via

$$p(z) = \sum_{k=-1,1} f(z|x=k)P(x=k), \tag{4.6}$$

where $f(z|x) = \sqrt{2\bar{\lambda}/\pi}e^{-2\bar{\lambda}(z-x)^2}$ is the probability density of $z|x$.

We now consider time-continuous measurements. These can be described by discretizing time into segments of length dt, performing one measurement per segment, and finally taking the continuous limit $dt \to 0$. The strength of the measurements becomes particularly important in this description, as each measurement acts back on the system, affecting its coherence. In fact, to preserve the coherence over finite time intervals, each measurement must be weak. Otherwise, the coherence is quickly destroyd, prohibiting coherent interactions. This is known as the quantum Zeno effect [70, 110, 111]. The Zeno effect is commonly introduced by considering repeated projective measurements of a Rabi oscillator. By continuously projecting the oscillator onto one of the eigenstates of the measured observable, coherent transitions between eigenstates cannot occur. To circumvent this, we postulate that the measurement strength in Eq. (4.3) is proportional to dt [16, 78, 109], i.e., $\bar{\lambda} = \lambda dt$, with λ being a fixed constant with units of inverse time, such that each measurement becomes infinitely weak in the continuous limit $\lambda dt \to 0$. For a continuous measurement, λ is referred to as the measurement strength.

Mathematically, this can be written as the following iterative map,

$$\hat{\rho}_c(t+dt) = e^{\mathcal{L}dt}\frac{\hat{K}(z)\hat{\rho}_c(t)\hat{K}^\dagger(z)}{p_c(z)}, \tag{4.7}$$

where $\hat{\rho}_c(t)$ is the state of the system at time t, conditioned on the full trajectory of recorded outcomes. We denote this trajectory by $\boldsymbol{z} = [z(t_0), z(t_0+dt), \ldots, z(t-dt)]$, where $z(t)$ is the outcome observed at time t. The conditional state can alternatively be written as $\hat{\rho}_c(t) = \hat{\rho}(t|\boldsymbol{z})$, which is useful for derivations. The denominator $p_c(z) = \mathrm{tr}\{\hat{K}^\dagger(z)\hat{K}(z)\hat{\rho}_c(t)\} = p_t(z|\boldsymbol{z})$ is the conditional probability of observing outcome z, given that the trajectory $\boldsymbol{z}$ was observed up to time t. The Liouville superoperator[1] $\mathcal{L}$ describes the system dynamics in between measurements, and $\hat{K}(z)$ is given by Eq. (4.3).

We can now use Eq. (4.7) to understand the general effect of a continuous measurement. To this end, we average Eq. (4.7) over all possible trajectories $\boldsymbol{z}$ and derive a master equation. It is useful to write $\hat{\rho}_c(t) = \hat{\rho}_t(\boldsymbol{z})/p_t(\boldsymbol{z})$, where $\hat{\rho}_t(\boldsymbol{z})$ is the joint system-outcome state, and $p_t(\boldsymbol{z})$ is the probability of observing trajectory $\boldsymbol{z}$. By averaging over all possible trajectories, we obtain an unconditioned state $\hat{\rho}_t = \langle\hat{\rho}_c(t)\rangle_{\boldsymbol{z}}$, where $\langle\cdot\rangle_{\boldsymbol{z}}$ denotes the average over all $\boldsymbol{z}$. As discussed in Chapter 2, this average can be evaluated as

$$\langle\hat{\rho}_c(t)\rangle_{\boldsymbol{z}} = \int \mathfrak{D}[\boldsymbol{z}]\hat{\rho}_c(t)p_t(\boldsymbol{z}) = \int \mathfrak{D}[\boldsymbol{z}]\hat{\rho}_t(\boldsymbol{z}) = \hat{\rho}_t. \tag{4.8}$$

Taking this average over Eq. (4.7), and expanding the rhs to linear order in dt, provides the following master equation,

$$\partial_t\hat{\rho}_t = \mathcal{L}\hat{\rho}_t + \lambda\mathcal{D}[\hat{A}]\hat{\rho}_t, \tag{4.9}$$

[1] In this thesis, this superoperator is written on Lindblad form (see Chapter 3).

where $\mathcal{D}[\hat{O}]\hat{\rho} = \hat{O}\hat{\rho}\hat{O}^\dagger - \{\hat{O}^\dagger\hat{O}, \hat{\rho}\}/2$ for an arbitrary operator $\hat{O}$, as introduced in Chapter 3. The first term on the rhs describes the time-evolution of the system in the absence of measurements, while the second term accounts for measurement backaction. That is, the infinitely small backaction of each measurement accumulates over time, and collectively they influence the dynamics of the system. Note that this master equation is not a consequence of using the Gaussian measurement operator (4.3), but is rather a general result that holds for all continuous quantum measurements[2] [15, 70, 111, 112].

To properly understand the effect of the backaction term in Eq. (4.9), we ignore the first term of the master equation, and write the density matrix in the eigenbasis of $\hat{A}$. For element $\rho_{aa'}(t) = \langle a|\hat{\rho}_t|a'\rangle$, we get

$$\dot{\rho}_{aa'}(t) = -\frac{\lambda}{2}(\xi_a - \xi_{a'})^2\rho_{aa'}(t). \tag{4.10}$$

The effect of the measurement is thus to exponentially dampen all coherences for non-degenerate eigenvalues ($\xi_a \neq \xi_{a'}$) at a rate proportional to the measurement strength λ. For degenerate eigenvalues ($\xi_a = \xi_{a'}$), the element $\rho_{aa'}(t)$ is not subject to backaction. In fact, if $[\hat{A}, \hat{\rho}_t] = 0$ at all times, the measurement becomes backaction-free[3]. In Paper IV, we exploit this to improve the entanglement of a quantum heat engine by using feedback control. What we learn from Eq. (4.10) is that a continuous measurement imposes dephasing. To understand the impact of the dephasing, we study two limiting cases. We begin by introducing g as the strength of the coherent interactions in the system[4]. For $g \gg \lambda$, coherent interactions can be maintained for a long time despite the presence of dephasing. For $g \ll \lambda$, the dephasing prevents coherent interactions, and the coherence quickly vanishes. That is, we observe the quantum Zeno effect.

As we saw above, Eq. (4.9) describes the dynamics of a measured system when taking an ensemble average over all possible trajectories $\boldsymbol{z}$. In fact, we can unravel Eq. (4.9), and find a stochastic master equation for the dynamics of $\hat{\rho}_c(t)$, on the level of a single trajectory $\boldsymbol{z}$. To this end, we begin by noting that

$$\langle z\rangle_c = \int z p_c(z) dz = \langle \hat{A}\rangle_c \tag{4.11}$$

is the average outcome at time t conditioned on the previously observed outcomes, where $\langle \hat{A}\rangle_c = \mathrm{tr}\{\hat{A}\hat{\rho}_c(t)\}$ is the average of the measured observable $\hat{A}$ [see Eq. (4.3)] with respect

[2]Note that the master equation slightly changes in some scenarios. For instance, by measuring photons leaking out of an optical cavity, the observable $\hat{A}$ is replaced by the annihilation operator $\hat{c}$ of the measured cavity mode. The annihilation operator is not hermitian, and the description using Eq. (4.3) does not apply. For a full treatment, see Ref. [15].

[3]This is always the case for incoherent dynamics.

[4]In this thesis, g has the unit of inverse time, as we choose $\hbar = 1$ in Chapter 3.

to $\hat{\rho}_c(t)$. This implies, for small dt, that the outcome at time t can be written as a random variable as

$$z = \langle \hat{A} \rangle_c + \frac{dW}{\sqrt{4\lambda dt}}, \tag{4.12}$$

where dW is a Wiener increment (see Chapter 2). In Appendix C, we motivate this relation. The outcome is thus a Gaussian random variable with mean $\langle \hat{A} \rangle_c$ and two-time correlator $\mathcal{C}_z(t,t') = \delta(t-t')/4\lambda$, which we derived using Eq. (2.5) and the fact that $dW(t)/dt = \xi(t)$ is a white noise process when $dt \to 0$ (see Chapter 2). Note that the strength of the noise scales as $1/\lambda$.

We now derive the stochastic master equation. By expanding Eq. (4.7) to first order in dt, and using Eqs. (4.3), (4.12), and the Itô rule, we get [16, 78]

$$\frac{\hat{K}(z)\hat{\rho}_c\hat{K}^\dagger(z)}{p_t(z)} = \hat{\rho}_c + \lambda dt \mathcal{D}[\hat{A}]\hat{\rho}_c + \sqrt{\lambda} dW \{\hat{A} - \langle \hat{A} \rangle_c, \hat{\rho}_c\}, \tag{4.13}$$

where the time arguments were omitted for brevity. From this linearization, we find the Belavkin equation [113] (see also Refs. [15, 16, 78])

$$d\hat{\rho}_c = dt\mathcal{L}\hat{\rho}_c + \lambda dt \mathcal{D}[\hat{A}]\hat{\rho}_c + \sqrt{\lambda} dW \{\hat{A} - \langle \hat{A} \rangle_c, \hat{\rho}_c\}, \tag{4.14}$$

which is a stochastic master equation because of the Wiener increment dW. This equation is an unravelling of Eq. (4.9). The first term on the rhs describes the time evolution of the system, the second term describes measurement backaction, and the third term describes how the randomness of the measurement induces noise into the system. We note that the equation is nonlinear in $\hat{\rho}_c$ because of the average $\langle \hat{A} \rangle_c$ in the anti-commutator in the noise term. This is in contrast to the von Neumann (3.9) and Lindblad (3.15) equations, and is a result from the nonlinear transformation that describes a quantum measurement, see Eqs. (4.2) and (4.7). Note that the Belavkin equation (4.14) reduces to Eq. (4.9) when averaging over all possible trajectories of $\boldsymbol{z}$. The last term drops out because the noise dW at time t is independent of $\hat{\rho}_c(t)$, see Appendix A.

While this theory accurately describes the dynamics of a continuously measured quantum system, Eq. (4.12) is often a simplified description of the output of a detector. For instance, z contains white noise, and its variance thus diverges, $\langle z^2(t) \rangle - \langle z(t) \rangle^2 = \mathcal{C}_z(t,t) = \delta(0)/4\lambda$, which is physically unrealistic[5], see the discussion on white noise in Chapter 2. Note that the circuitry of any detector has a finite bandwidth, restricting the range of frequencies in the noise of the observed signal. The bandwidth blocks higher frequencies of the noise, resulting in a finite variance of the output. Additionally, the bandwidth introduces a finite delay time in the output. To solve these issues, we introduce a realistic

[5]In some cases, white noise is a good approximation, and leads to reasonable results. For instance, see the Wiseman-Milburn equation (4.19) below.

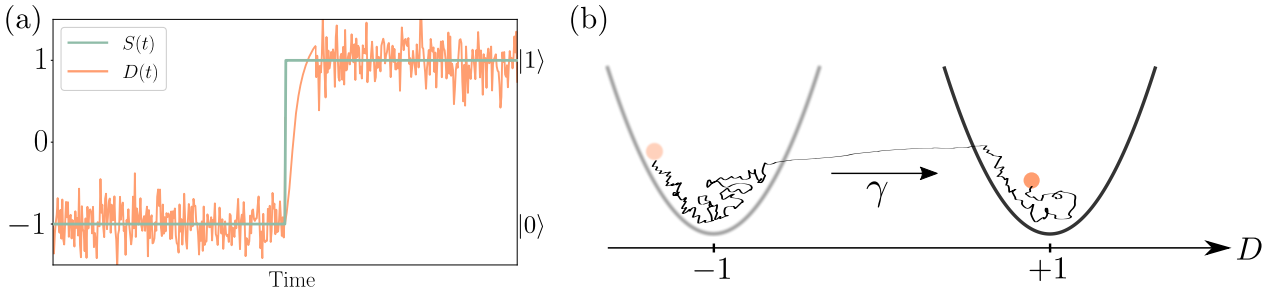

Figure 4.2: (a) Time traces of the system state $S(t)$ and the outcome $D(t)$ as observed on the detector screen during the state transition $|0\rangle \to |1\rangle$ for the example two-level system in Eq. (4.4). Due to the finite bandwidth γ, the detector signal lags behind the system state [note the finite rise time of $D(t)$]. (b) Illustration of D as a Browninan particle in a harmonic potential during the same state transition as in (a). As the transition occurs, the potential moves from -1 to $+1$. The particle follows with speed γ.

detector model, including a finite bandwidth. By $D(t)$, we denote the outcome observed on the detector screen. This variable is related to $z(t)$ via [15, 108, 114–119]

$$D(t) = \int_{t_0}^{t} ds\gamma e^{-\gamma(t-s)} z(s), \tag{4.15}$$

where γ is the bandwidth of the detector (see Fig. 4.4) and t_0 is the time where the measurement began. By differentiating Eq. (4.15) with respect to time, and employing Eq. (4.12), we get the Langevin equation

$$\dot{D}(t) = \gamma \left[\langle \hat{A} \rangle_c - D(t) \right] + \frac{\gamma}{\sqrt{4\lambda}} \xi(t), \tag{4.16}$$

using that $\xi(t) = \lim_{dt\to 0} dW/dt$, as discussed in Chapter 2. That is, $D(t)$ is an Ornstein-Uhlenbeck process with Itô equation

$$dD = \gamma \left(\langle \hat{A} \rangle_c - D \right) dt + \frac{\gamma}{\sqrt{4\lambda}} dW, \tag{4.17}$$

and thus describes a noisy relaxation towards $\langle \hat{A} \rangle_c$ on a timescale set by $1/\gamma$, i.e., the response time, or delay, of the detector. The two-time correlator of $D(t)$ is given by $\mathcal{C}_D(t,t') = (\gamma/8\lambda)e^{-\gamma|t-t'|}$, resulting in the finite variance $\langle D^2(t)\rangle - \langle D(t)\rangle^2 = \mathcal{C}_D(t,t) = \gamma/8\lambda$, see Chapter 2. In Fig. 4.2(a), we visualize $D(t)$ for the example two-level system in Eq. (4.4) undergoing the transition $|0\rangle \to |1\rangle$. Note the finite rise (response) time of the detector. Figure 4.2(b) illustrates how the outcome D may be thought of as a Brownian particle in a harmonic potential, see discussion in Chapter 2. When the system jumps $|0\rangle \to |1\rangle$, the potential is moved instantly from -1 to 1, and the detector outcome follows with speed γ. Note that $D(t) \to z(t)$ by taking $\gamma \to \infty$, i.e., when the bandwidth becomes infinitely large, diverging frequencies will be present in the noise spectrum, and the delay of the detector vanishes.

The Belavkin equation (4.14) together with Eq. (4.17) are the basic elements to model continuous measurements of quantum systems. Note that there are infinitely many realizations

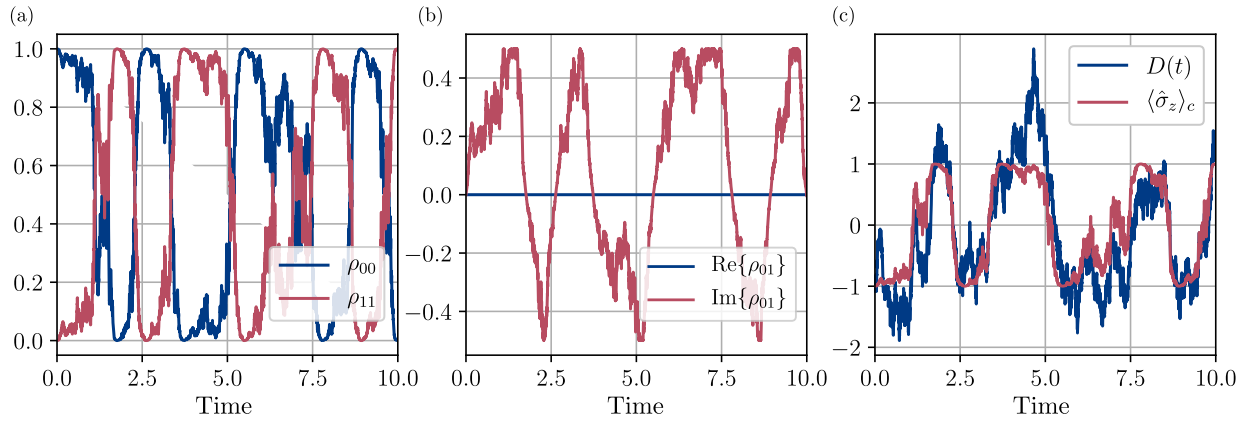

Figure 4.3: A solution to the Belavkin equation (4.14) and Eq. (4.17) for a qubit when measuring the Pauli-Z operator $\hat{\sigma}_z = |1\rangle\langle 1| - |0\rangle\langle 0|$. The qubit has Hamiltonian $\hat{H} = g\hat{\sigma}_x$, where $\hat{\sigma}_x$ is the Pauli-X operator. (a) The leftmost panel visualizes the diagonal density matrix elements $\rho_{aa} = \langle a|\hat{\rho}_c(t)|a\rangle$ of the conditioned density matrix $\hat{\rho}_c(t)$. (b) The middle panel shows the real and imaginary parts of the off-diagonal density matrix element $\rho_{01} = \langle 0|\hat{\rho}_c(t)|1\rangle$. (c) The rightmost panel is the corresponding time trace of the detector signal $D(t)$ [see Eq. (4.17)], and the expectation value $\langle\hat{\sigma}_z\rangle_c = \mathrm{tr}\{\hat{\sigma}_z\hat{\rho}_c\}$. Here we used $\gamma/g = 2$, $\lambda/g = 1/2$, and $dt/g = 10^{-3}$.

of the noise process dW, implying that there are infinitely many solutions to the Belavkin equation. Each solution defines a quantum trajectory $\hat{\rho}_c(t)$. In Fig. 4.3, we show such a trajectory for a qubit, illustrating how noise is induced into our state of knowledge (the density matrix) given that we observed the trajectory of $D(t)$ in the rightmost panel.

4.3 Quantum feedback control

An important application of measurements is feedback control, where the recorded information is used to control the dynamics of a system, see Fig. 4.4. Typically, this is referred to as measurement-based feedback control, but we will simply use the term feedback control[6]. The idea of controlling physical systems became particularly important during the industrial revolution, and has numerous applications in mechanical and electrical engineering [43]. The idea of using feedback control in quantum systems emerged during the 1980s, and has lead to several theoretical and experimental developments [15–17]. With the fast development and miniaturization of electronics during the past decades, quantum feedback control is currently of substantial interest. On the one hand, feedback is expected to play an important role in the development of quantum technologies, like quantum computers. And on the other, feedback is interesting from a fundamental perspective, exploring the limits of quantum control, e.g., in the field of quantum thermodynamics [11].

In this section, we introduce the basics of continuous quantum feedback control. We be-

[6]In fact, the term feedback can, for instance, refer to control strategies where the dynamics of one subsystem is controlling the dynamics of another subsystem. In quantum systems, this is referred to as coherent feedback control, see, for instance, Refs. [120, 121].

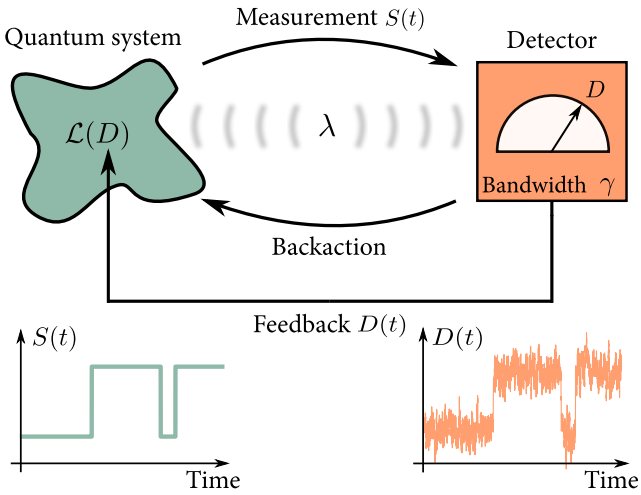

Figure 4.4: A general setup for continuous feedback control. An open quantum system is continuously measured by a detector with bandwidth γ. The measurement strength λ quantifies the backaction and uncertainty of the measurement. Based on the measurement outcome D, feedback is continuously applied on the system, controlling the system Liouvillian $\mathcal{L}(D)$. In the bottom, two typical trajectories of the system state and the corresponding measurement outcome are visualized. Figure taken from Paper II.

gin by extending the Belavkin equation (4.14) to include feedback – this equation constitutes the theoretical basis for modeling feedback in quantum systems. Then we introduce Markovian feedback, discussing two special scenarios where it is possible to derive Markovian master equations for feedback-controlled systems.

Mathematically, feedback is implemented by letting the dynamics depend on the measurement, i.e., by replacing $\mathcal{L} \to \mathcal{L}[f(\boldsymbol{D})]$ in Eq. (4.7), where $\boldsymbol{D}$ is the full trajectory of outcomes and $f(\cdot)$ is a function representing any arbitrary processing of the measured signal before being fed back to the system. The Belavkin equation (4.14) is modified by the same replacement of the Liouville superoperator. Together with Eq. (4.17), the Belavkin equation is the basic tool for modeling any continuous feedback protocol, and is useful for simulating individual trajectories $\hat{\rho}_c(t)$ of a controlled system. However, from such trajectories it can be difficult to distinguish general trends in the dynamics. Such trends are most easily understood by averaging the Belavkin equation over all possible trajectories of $\boldsymbol{D}$. In general, it is difficult to compute this average, as $\mathcal{L}[f(\boldsymbol{D})]$ can have a complicated dependence on $\boldsymbol{D}$. Therefore, we are often restricted to numerical simulations, giving limited qualitative insight of the dynamics. However, for Markovian feedback, where the feedback protocol only depends on the latest observed outcome D, i.e., $f(\boldsymbol{D}) \to D$, there are two scenarios where the average can be computed analytically. Both scenarios lead to deterministic Markovian master equations for the unconditioned state $[\hat{\rho}_t = \langle \hat{\rho}_c(t) \rangle_{\boldsymbol{D}}]$ that often have analytical solutions.

The first scenario is linear feedback with infinite detector bandwidth ($\gamma \to \infty$), resulting in feeding back the outcome z [Eq. (4.12)]. In this scenario, the Liouville superoperator depends linearly on z, $\mathcal{L}(z) = \mathcal{L}_0 + z\mathcal{K}$, where $\mathcal{L}_0$ describes the system dynamics in the

absence of feedback, and $\mathcal{K}$ is a Liouville superoperator describing the feedback forces. The Belavkin equation for this scenario is found by linearizing the time evolution in Eq. (4.7) in dt (using the Itô rule), $e^{\mathcal{L}(z)dt} \approx \mathbb{1} + dt\mathcal{L}_0 + \langle\hat{A}\rangle_c dt\mathcal{K} + dt\mathcal{K}^2/8\lambda + dW\mathcal{K}/\sqrt{4\lambda}$, resulting in

$$\begin{aligned} d\hat{\rho}_c = dt\mathcal{L}_0\hat{\rho}_c + \lambda dt\mathcal{D}[\hat{A}]\hat{\rho}_c + \frac{dt}{2}\mathcal{K}\{\hat{A},\hat{\rho}_c\} \\ + \frac{dt}{8\lambda}\mathcal{K}^2\hat{\rho}_c + dW\left[\sqrt{\lambda}\{\hat{A} - \langle\hat{A}\rangle_c, \hat{\rho}_c\} + \frac{1}{\sqrt{4\lambda}}\mathcal{K}\hat{\rho}_c\right]. \end{aligned} \tag{4.18}$$

Averaging over all possible trajectories $\boldsymbol{z}$, we get the Wiseman-Milburn equation [15, 122]

$$\partial_t\hat{\rho} = \mathcal{L}_0\hat{\rho} + \lambda\mathcal{D}[\hat{A}]\hat{\rho} + \frac{1}{2}\mathcal{K}\{\hat{A},\hat{\rho}\} + \frac{1}{8\lambda}\mathcal{K}^2\hat{\rho}, \tag{4.19}$$

which is a central result in the field of quantum feedback control. The first and second terms on the rhs correspond to Eq. (4.9). The third term describes how the feedback forces act on the system. The fourth term, originating from the noise term dW in $\mathcal{L}(z)$, describes how measurement noise is fed back to the system and causes diffusion in the dynamics [15]. When λ is large, this diffusion effect is reduced, as the detector noise becomes small – the magnitude of the noise scales as $1/\lambda$ as discussed in Sec. 4.2. This equation has been applied in numerous contexts, including stabilizing qubit states [123], manipulating entanglement [124–129], retarding decoherence [130, 131], producing squeezed states [132–135], and charging quantum batteries [136].

The second scenario is a generalization of the first, using an arbitrary $\mathcal{L}(D)$, where the dependence on D is arbitrary (it can be nonlinear as well as linear). This scenario assumes a finite bandwidth, and, therefore, the Liouvillian depends on D instead of z. For bookkeeping purposes, we assume that $\mathcal{L}(D) \sim \Gamma$, where Γ has the unit of inverse time. With a large separation $\gamma \gg \Gamma, \lambda$, i.e., when the response time of the detector is much faster than the system, we find the following Markovian master equation,

$$\partial_t\hat{\rho} = \left[\mathcal{L}_0 + \lambda\mathcal{D}[\hat{A}] + \gamma^{-1}\mathcal{L}_{\text{corr}}\right]\hat{\rho}, \tag{4.20}$$

where $\mathcal{L}_0$ is the feedback-controlled dynamics in the limit of an infinitely fast detector, and $\mathcal{L}_{\text{corr}}$ is a correction term for a small but finite response time γ^{-1} of the detector. This master equation is one of the central results of Paper II, and we refer the reader to that paper for a detailed derivation and discussion. In that paper, we also provide general formulas for calculating $\mathcal{L}_0$ and $\mathcal{L}_{\text{corr}}$. We stress that this equation can describe any Markovian, continuous feedback protocol. Finally, we note that this equation reduces to the Wiseman-Milburn equation (4.19) when $\mathcal{L}(D)$ depends linearly on D and $\gamma \to \infty$, highlighting the relation between the two equations.

Chapter 5

Thermodynamics of small systems

Thermodynamics was established as a theory during the 19th and early 20th centuries, largely driven by the desire to optimize steam and heat engines. The theory describes transfers of energy and matter in large macroscopic systems close to equilibrium. In particular, the theory provides bounds on what can be observed in nature. Typically, the systems consist of $\sim 10^{23}$ particles, which makes it impossible to model the motion of every particle. Instead, the theory is formulated in terms of macroscopic variables such as volume, conductivity, temperature, pressure, etc. Thermodynamics was later complemented with statistical mechanics, providing a link between microscopic and macroscopic variables.

During the past 30 years or so, the theory of thermodynamics has been expanded to small, non-equilibrium systems on the micro- and nanoscale. The expansion contains mainly three components; stochastic, information, and quantum thermodynamics.

Stochastic thermodynamics [1–10] deals with small, fluctuating systems far from equilibrium. Building on the prominent discoveries of the Jarzynski relation [137, 138] and Crooks' fluctuation theorem [139, 140], the last 30 years have resulted in many general laws applicable to non-equilibrium systems. As such, stochastic thermodynamics extends its conventional (macroscopic) counterpart beyond close-to-equilibrium scenarios. By defining quantities such as work, heat, and entropy at the level of single microscopic trajectories, it is possible to understand how fluctuations affect the thermodynamics of small systems. In particular, the second law is generalized in terms of fluctuation theorems, stating that entropy production is a fluctuating quantity which only needs to be non-negative on average. This stands in contrast to classical thermodynamics, where entropy should always increase, and where fluctuations are negligible. Stochastic thermodynamics is thus particularly good at describing the thermodynamics of small systems such as colloidal particles [141], DNA molecules [142], molecular motors [143], and nanosized electronic systems [144, 145], where

fluctuations play an important role.

With the increased ability to control and measure small systems in real time [146] came the possibility of exploring measurement-based feedback control. In fact, the acquisition and processing of information come with a thermodynamic cost. This is famously illustrated by Maxwell's demon [22–24], where the acquisition of information about the velocities of gas molecules can be used to rectify their thermal fluctuations, seemingly violating the second law of thermodynamics. By considering the thermodynamics of information processing, i.e., accounting for the energy and entropy required to gather, store, and erase information, one finds that Maxwell's demon does not violate the second law. This was first realized by Bennett [147], who argued, based on the Landauer principle [148], that the apparent violation is resolved when the demon erases its memory, increasing the entropy of its environment, thus restoring the second law. During the past decades, the thermodynamics of information [21, 149, 150] has been incorporated into stochastic thermodynamics. This has resulted in several generalizations of the second law, showing that processes like Maxwell's demon are not thermodynamically forbidden. In fact, several experimental implementations of the demon have been demonstrated over the last decade [25–29, 31–34, 54, 151].

Quantum thermodynamics (QTD) [11–14] deals with quantum systems coupled to thermal environments. At its core, the theory aims at defining work, heat, and entropy in the quantum realm. Interestingly, as shown below, the laws of thermodynamics may be derived from quantum theory. Similar to stochastic thermodynamics, QTD deals with questions regarding the fundamental bounds of nature, including fluctuation theorems [7] and thermodynamic uncertainty relations [38], which hold far from equilibrium. In addition to this, the thermodynamics of quantum measurements and feedback control has recently attracted interest [40–42]. While QTD is closely linked with the fundamental properties of nature, the field is expected to play an important role in the development of new technologies. With constant miniaturization and the development of quantum computers, it is likely that future technologies must take quantum thermodynamic aspects into account in their design. Relevant for both the fundamental and applied point of views are quantum thermal machines [13], where temperature biases are used to perform useful tasks, such as cooling [152] or generating entanglement [39].

In this chapter, we begin by introducing some of the results from classical thermodynamics in Sec. 5.1 that will be important for comparison in the subsequent sections. Section 5.2 is devoted to stochastic thermodynamics, and defines entropy, work, and heat on the level of single microscopic trajectories. Especially, we introduce fluctuation theorems. Section 5.3 introduces information thermodynamics, and we discuss a selection of results that are important for understanding the thermodynamics of Maxwell's demon. Section 5.4 introduces quantum thermodynamics. We show how the first and second law emerge from quantum theory, discuss open quantum systems, and introduce the absolute basics of entanglement.

5.1 Classical thermodynamics

With classical thermodynamics, we can describe the energetics and dynamics of macroscopic systems that are in equilibrium. With linear response theory, it is possible to get some insights into non-equilibrium thermodynamics, but the results are only valid close to equilibrium. In this section, we shortly review the laws of thermodynamics as a reference for the discussion in the upcoming sections.

The zeroth law of thermodynamics states that if two systems (A and B) are in thermal equilibrium with a third system (C), then A and B are in thermal equilibrium with each other.

The first law of thermodynamics reads

$$\Delta E = W + Q, \tag{5.1}$$

stating that a change in internal energy ΔE of a system can be decomposed into work W and heat Q. While work is energy that is provided macroscopically, heat is energy that is transferred by microscopic degrees of freedom. Here we use the sign convention $W > 0$ ($W < 0$) when work is done on (by) the system. Similarly, $Q > 0$ ($Q < 0$) when heat is absorbed (released) by the system.

The second law of thermodynamics states that the entropy S of an isolated system (not exchanging energy or particles with its environment) never decreases. Mathematically, we write

$$\Delta S \geq 0. \tag{5.2}$$

If the system makes a transition between two states for which $\Delta S = 0$, the process is said to be reversible, and the system can jump back and forth between these states without restriction. A system transition with $\Delta S > 0$ is said to be irreversible. That is, if the transition $x_0 \to x_1$, between system states x_0 and x_1, increases the entropy, the reverse process, $x_1 \to x_0$, is prohibited by the second law, and will never be observed. This notion of reversibility will be widened in Sec. 5.2 when we study thermodynamics on the microscopic scale.

An equilibrium state can be described by the function $E(S, V, N)$ for the internal energy E, where S is entropy, V the volume of the system, and N the number of particles of a given species. To avoid clutter, we only write out these three variables, but E could, in principle, depend on other variables as well. Let us assume that we perform an experiment where we cannot measure the entropy, but only have access to the temperature T, as well as V and N. In this case, it is difficult to describe our observations with $E(S, V, N)$. Instead, we can make use of the Legendre transform [153] to make the following change of variables, $S, V, N \to T, V, N$. Mathematically, this is done by introducing the Helmholtz

free energy (typically referred to as the free energy) as

$$F = E - ST, \tag{5.3}$$

where $F(T, V, N)$ depends on the temperature instead of the entropy. The free energy is a thermodynamic potential, which means that it can be used to reconstruct all information that we can derive from $E(S, V, N)$. Note that the second law implies that the free energy should be minimized in an isolated system, i.e., $\Delta F \leq 0$. Another example of a thermodynamic potential is the Gibbs free energy $G = E - ST + pV$ which depends on T, p (pressure), and N.

Before closing this section, we write down an alternative formulation of the second law. We consider a system that is in contact with an equilibrium heat bath at constant temperature T. By assuming that the bath is much larger than the system, the system can only weakly perturb the bath. Additionally, we assume that the bath relaxation time (to return to equilibrium) due to a small perturbation is much faster than the system timescale, such that the bath effectively remains in equilibrium at all times. We now drive the system between two equilibrium states. Since the bath effectively is in equilibrium, the bath and system are uncorrelated, and the total entropy change can be written as $\Delta S_{\rm tot} = \Delta S_{\rm sys} + \Delta S_{\rm B} \geq 0$, where $\Delta S_{\rm sys}$ and $\Delta S_{\rm B}$ are the entropy changes associated to the system and the bath, respectively. As the bath is much larger than the system, the entropy production associated to the bath can be written as $\Delta S_{\rm B} = -Q/T$, with Q being the heat absorbed or released by the system. By using the first law, we can express the second law as

$$W \geq \Delta F. \tag{5.4}$$

This establishes a minimal bound on the work that we need to do on the system to drive it between the two states. Alternatively, by defining the extracted work as $W_{\rm ext} = -W$, having a positive sign when the system does work on its environment, we find the upper bound $W_{\rm ext} \leq -\Delta F$. The change in free energy thus puts a fundamental limit on how much work that can be extracted from a system. Note that equality only holds for reversible processes, where the driving is quasistatic.

5.2 Stochastic thermodynamics

In this section, we discuss stochastic thermodynamics by studying systems described by Markovian rate equations [154], but the results are general, and are typically applicable for other systems as well – for instance, systems obeying Langevin dynamics [4]. The content of this section is relevant for Papers I, II, and VI.

We consider a system with discrete states x, each with an energy ε_x and number of particles n_x. For the purposes of this thesis, we involve only one particle species, but the results can

be extended to include several species. The energies can be controlled by an external, time dependent control variable $\lambda(t)$, such that $\varepsilon_x = \varepsilon_x[\lambda(t)]$. The control variable could, for instance, be an electric field. Here we assume that n_x is fixed for all states x, and cannot be controlled externally. The system is coupled to an arbitrary number of equilibrium reservoirs, labeled with indexes ν, having well-defined temperatures T_ν and chemical potentials μ_ν [see Fig. 5.1(a)]. The system exchanges energy and particles with the reservoirs. The reservoirs are assumed to be so large that the system can only perturb the reservoirs weakly, and that their thermal relaxation time is so short compared to the system timescale that the reservoirs effectively remain in equilibrium at all times. To describe the system dynamics, we will use the following Markovian rate equation,

$$\dot{p}_x(t) = \sum_{x'} \sum_{\nu} \left[M^{(\nu)}_{xx'} p_{x'}(t) - M^{(\nu)}_{x'x} p_x(t) \right], \tag{5.5}$$

where $p_x(t)$ is the probability to occupy state x at time t (typically, we will not write out the time dependence unless necessary), and $M^{(\nu)}_{xx'} = M^{(\nu)}_{xx'}[\lambda(t)]$ is the transition rate for the transition $x' \to x$ mediated by reservoir ν. As indicated, the transition rates will, in general, be dependent on $\lambda(t)$, but to avoid clutter, we will only write out the explicit dependence on $\lambda(t)$ when necessary.

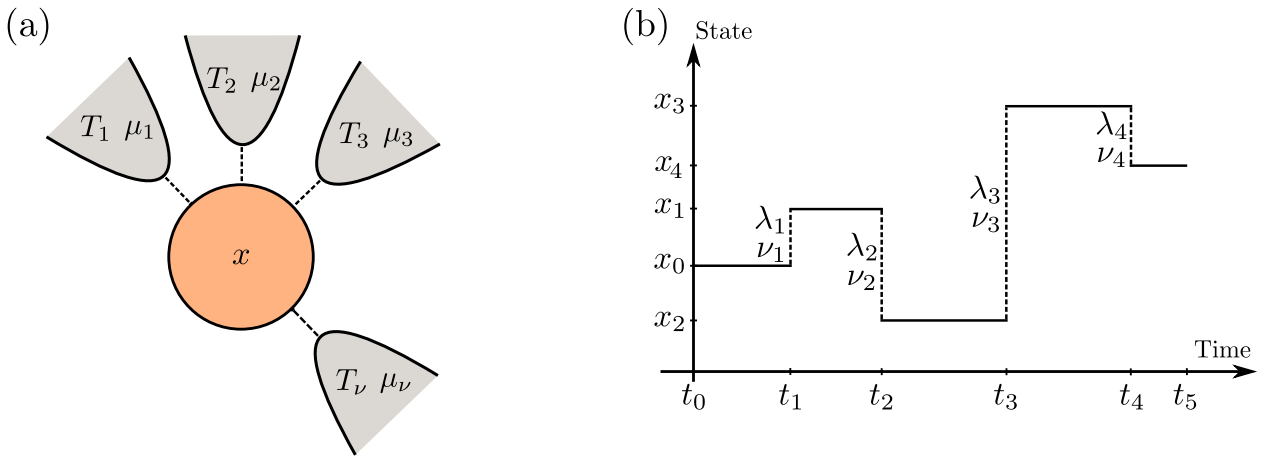

Figure 5.1: (a) A microscopic system in state x coupled to an arbitrary number of equilibrium reservoirs with which the system can exchange energy and particles. Each reservoir has a well-defined temperature T_ν and chemical potential μ_ν. (b) Example trajectory of the system state [see trajectory definition in Eq. (5.10)]. Each state transition $x_{j-1} \to x_j$ is mediated by a reservoir ν_j for a fixed control parameter λ_j. Note that the control parameter can vary continuously between transitions.

To incorporate thermodynamics into our model, we assume that the transition rates obey local detailed balance, i.e.,

$$\ln\left(\frac{M^{(\nu)}_{xx'}}{M^{(\nu)}_{x'x}}\right) = \frac{\varepsilon_{x'} - \varepsilon_x - \mu_\nu(n_{x'} - n_x)}{k_B T_\nu}, \tag{5.6}$$

where k_B is the Boltzmann constant. This assumption is justified as long as the timescale of $\lambda(t)$ is much slower than the thermal relaxation time of the reservoirs, such that the system

effectively interacts with equilibrium reservoirs at all times. To understand the origin and physical meaning of local detailed balance, we begin to consider the case where the system only interacts with one single reservoir. In the long time limit, the system thermalizes with the bath, and reaches an equilibrium distribution

$$p_x^{(\mathrm{eq})} = \frac{e^{-(\varepsilon_x - \mu_\nu n_x)/k_B T_\nu}}{Z}, \qquad Z = \sum_x e^{-(\varepsilon_x - \mu_\nu n_x)/k_B T_\nu}, \tag{5.7}$$

with Z being the partition function. In equilibrium, there should, on average, be no net flow of energy or particles. The probability current $J^{(\nu)}_{xx'} = M^{(\nu)}_{xx'} p_{x'} - M^{(\nu)}_{x'x} p_x$ should, therefore, vanish, giving the detailed balance condition

$$M^{(\nu)}_{xx'} p^{(\mathrm{eq})}_{x'} = M^{(\nu)}_{x'x} p^{(\mathrm{eq})}_{x}, \tag{5.8}$$

and we recover Eq. (5.6). We thus see that the local detailed balance condition leads to a proper description of thermalization[1], where we recover the equilibrium (Boltzmann) distribution from statistical mechanics.

In the presence of several reservoirs, all with different temperatures and chemical potentials, the situation is different. All reservoirs will try to impose an equilibrium distribution on the system, but will fail due to the presence of the other reservoirs. Because of this, there will, on average, be a net flow of energy and particles between the system and the reservoirs, and the stationary probability currents $J^{(\nu)}_{xx'} \neq 0$. This is referred to as a non-equilibrium steady state. As we, on a general level, do not know either the stationary distribution $p_x^{(\mathrm{st})}$ nor the stationary currents $J^{(\nu)}_{xx'}$, it is at this point difficult to justify that the local detailed balance condition holds also for non-equilibrium scenarios. For now, we claim that it holds, and show in the upcoming paragraphs that it leads to a thermodynamically consistent definition of a non-equilibrium entropy, motivating why local detailed balance should hold for both equilibrium and non-equilibrium scenarios.

Once we know the distribution $p_x(t)$, we can calculate the average energy $E = \sum_x \varepsilon_x p_x$ and the average number of particles $N = \sum_x n_x p_x$ of the system. The average energy changes at a rate

$$\dot{E} = \dot{W} + \dot{W}_{\mathrm{chem}} + \dot{Q}, \tag{5.9}$$

where $\dot{W} = \sum_x p_x(t) \partial_t \varepsilon_x[\lambda(t)] = \sum_x p_x(t) \dot{\lambda}(t) \partial_\lambda \varepsilon_x[\lambda(t)]$ is the external work applied on the system, $\dot{W}_{\mathrm{chem}} = \sum_\nu \sum_{xx'} \mu_\nu n_x J^{(\nu)}_{xx'}$ is the chemical work rate associated with the particle exchange between system and reservoirs, and $\dot{Q} = \sum_\nu \sum_{xx'} (\varepsilon_x - \mu_\nu n_x) J^{(\nu)}_{xx'}$ is the system heat current. Equation (5.9) thus shows that the first law of thermodynamics holds for the average system energy E. Note that the additional chemical work term was baked into one single term in Eq. (5.1).

[1] This corresponds to the zeroth law of thermodynamics.

We now define system trajectories. Since the state of the system fluctuates randomly over time, two separate measurements of the state trajectory would yield different results, see the example trajectory in Fig. 5.1(b). To fully understand how these fluctuations affect the thermodynamics of the system, we need to properly define work, heat, and entropy on the level of single system trajectories. We define a trajectory starting in state x_0 at time t_0 with control parameter λ_0 and ending in state x_{n-1} at time t_n with control parameter λ_n as

$$X = \{(t_j, \lambda_j, \nu_j, x_j)\}_{j=1}^{n-1}, \tag{5.10}$$

where t_j specifies the time when the system jumps to a new state x_j, by doing the transition $x_{j-1} \to x_j$, λ_j is the value of the control parameter when the transition occurs, and ν_j is the reservoir responsible for the transition. Note that the control variable $\lambda(t)$ varies continuously between transitions, but as we will see, we only need to care about its value at the times the system undergoes transitions. The rate of external work applied on the system at time t is given by $\partial_t \varepsilon_x[\lambda(t)] = \dot{\lambda}(t)\partial_\lambda \varepsilon_x[\lambda(t)]$ if the system is in state x. If the system remains in this state during the interval $[t, t+\Delta t]$, the work applied on the system is given by $\int_t^{t+\Delta t} ds \dot{\lambda}(s)\partial_\lambda \varepsilon_x[\lambda(s)] = \varepsilon_x[\lambda(t+\Delta t)] - \varepsilon_x[\lambda(t)]$. That is, we only need to know the initial and final position of the energy level. The external work applied along trajectory X may thus be written as

$$w[X] = \sum_{j=0}^{n-1} \left[\varepsilon_{x_j}(t_{j+1}) - \varepsilon_{x_j}(t_j)\right]. \tag{5.11}$$

For transition $x_{j-1} \to x_j$ mediated by reservoir ν_j at time t_j, the system heat is given by $\varepsilon_{x_j}(t_j) - \varepsilon_{x_{j-1}}(t_j) - \mu_{\nu_j}(n_{x_j} - n_{x_{j-1}})$, and along X, we get the trajectory heat

$$q[X] = \sum_{j=1}^{n-1} \left[\varepsilon_{x_j}(t_j) - \varepsilon_{x_{j-1}}(t_j) - \mu_{\nu_j}(n_{x_j} - n_{x_{j-1}})\right]. \tag{5.12}$$

With this definition, we follow our convention that $q[X] > 0$ when the system absorbs heat, and $q[X] < 0$ when releasing heat. The chemical work done on the system along X reads

$$w_{\text{chem}}[X] = \sum_{j=1}^{n-1} \mu_{\nu_j}(n_{x_j} - n_{x_{j-1}}). \tag{5.13}$$

Adding these contributions together, we get the first law of stochastic thermodynamics,

$$w[X] + w_{\text{chem}}[X] + q[X] = \varepsilon_{x_{n-1}}(t_n) - \varepsilon_{x_0}(t_0), \tag{5.14}$$

resembling Eq. (5.1)[2].

[2]The definitions in Eqs. (5.11)-(5.13) agree with the definitions of conventional thermodynamics. Close to equilibrium, a small change of energy can be written as $dE = TdS - pdV + \mu dn$, where we may define heat $dQ = TdS$, mechanical work $dW_{\text{mech}} = -pdV$, and chemical work $dW_{\text{chem}} = \mu dn$. Note that the heat can be calculated as $dQ = dE - \mu dn$, when the volume is constant ($dV = 0$), which corresponds to the situation where $\lambda(t)$ is constant in the description above (during heat exchanges with the bath).

Next we want to define a non-equilibrium entropy for the system. We aim to use the Shannon entropy

$$S_{\mathrm{sys}}(t) = -k_B \sum_x p_x(t) \ln[p_x(t)], \tag{5.15}$$

and show that it gives reasonable results. If we interpret $S_{\mathrm{sys}}(t)$ as the system entropy at time t, averaged over all possible trajectories X, we can define a stochastic entropy [155]

$$s_{\mathrm{sys}}(t) = -k_B \ln[p_x(t)], \tag{5.16}$$

evaluated at time t when the system state is x. Averaging over all possible trajectories X, we recover the Shannon entropy $S_{\mathrm{sys}}(t) = \langle s_{\mathrm{sys}}(t) \rangle_X$. To evaluate whether these definitions give sensible results, it is useful to study the entropy change related to a single transition $x' \to x$ mediated by reservoir ν. During this jump, the system exchanges heat with the reservoir, which can be calculated as $q^{(\nu)}_{xx'} = \varepsilon_x - \varepsilon_{x'} - \mu_\nu(n_x - n_{x'})$. As the reservoir is in equilibrium, the change of entropy in the reservoir is given by

$$\Delta s^{(\mathrm{res})}_{xx'} = -\frac{q^{(\nu)}_{xx'}}{T_\nu} = k_B \ln\left(\frac{M^{(\nu)}_{xx'}}{M^{(\nu)}_{x'x}}\right), \tag{5.17}$$

where we used the local detailed balance condition in Eq. (5.6). From our definition of stochastic entropy (5.16), the change in system entropy can be written as

$$\Delta^{(\mathrm{sys})}_{xx'} = k_B \ln\left(\frac{p_{x'}}{p_x}\right), \tag{5.18}$$

and we find the total change of entropy

$$\Delta s^{(\mathrm{tot})}_{xx'} = \Delta s^{(\mathrm{sys})}_{xx'} + \Delta s^{(\mathrm{res})}_{xx'} = k_B \ln\left(\frac{M^{(\nu)}_{xx'} p_{x'}}{M^{(\nu)}_{x'x} p_x}\right). \tag{5.19}$$

From the definition of the Shannon entropy (5.15) and the definition of the rate equation (5.5), the average system entropy production may be written as

$$\dot{S}_{\mathrm{sys}}(t) = \frac{k_B}{2} \sum_\nu \sum_{xx'} J^{(\nu)}_{xx'} \ln\left(\frac{M^{(\nu)}_{xx'} p_{x'}(t)}{M^{(\nu)}_{x'x} p_x(t)}\right) - \frac{k_B}{2} \sum_\nu \sum_{xx'} J^{(\nu)}_{xx'} \ln\left(\frac{M^{(\nu)}_{xx'}}{M^{(\nu)}_{x'x}}\right), \tag{5.20}$$

where the factor of $1/2$ accounts for counting each jump twice in the double sums. With the help of Eqs. (5.17) and (5.19), we identify the total entropy production rate

$$\dot{S}_{\mathrm{tot}}(t) = \frac{k_B}{2} \sum_\nu \sum_{xx'} J^{(\nu)}_{xx'} \ln\left(\frac{M^{(\nu)}_{xx'} p_{x'}(t)}{M^{(\nu)}_{x'x} p_x(t)}\right), \tag{5.21}$$

and the reservoir entropy production rate

$$\dot{S}_{\mathrm{res}}(t) = \frac{k_B}{2} \sum_{\nu} \sum_{xx'} J^{(\nu)}_{xx'} \ln \left(\frac{M^{(\nu)}_{xx'}}{M^{(\nu)}_{x'x}} \right), \tag{5.22}$$

such that $\dot{S}_{\mathrm{tot}}(t) = \dot{S}_{\mathrm{sys}}(t) + \dot{S}_{\mathrm{res}}(t)$. First, we note that $J^{(\nu)}_{xx'}$ and $\ln[M^{(\nu)}_{xx'} p_{x'}(t) / M^{(\nu)}_{x'x} p_x(t)]$ always have the same sign, implying that $\dot{S}_{\mathrm{tot}} \geq 0$ at all times. Second, when all reservoirs have the same temperatures and chemical potentials, i.e., being in thermal equilibrium, we get the stationary condition in Eq. (5.8), and $\dot{S}_{\mathrm{tot}}(t)$ vanishes in the long time limit when the system has thermalized to the reservoirs. Finally, the detailed balance condition in Eq. (5.6) implies that the entropy production rate in the reservoirs reads

$$\dot{S}_{\mathrm{res}}(t) = \frac{1}{2} \sum_{\nu} \sum_{xx'} J^{(\nu)}_{xx'} \frac{\left(-q^{(\nu)}_{xx'} \right)}{T_\nu}, \tag{5.23}$$

as we would expect for a set of equilibrium reservoirs. These results show that the Shannon entropy (5.15) is a sensible candidate for being a non-equilibrium entropy, and that the assumption of local detailed balance (5.6) leads to a reasonable expression for the reservoir entropy production.

We can now define a trajectory entropy production for X in Eq. (5.10) as [155]

$$\Delta s_{\mathrm{tot}}[X] = k_B \ln \left[\frac{p_{x_0}(t_0)}{p_{x_{n-1}}(t_n)} \right] + k_B \sum_{j=1}^{n-1} \ln \left(\frac{M^{(\nu_j)}_{x_j x_{j-1}}}{M^{(\nu_j)}_{x_{j-1} x_j}} \right), \tag{5.24}$$

where we used Eqs. (5.17) and (5.18).

With the definitions from the previous paragraphs, it is possible to introduce a non-equilibrium free energy. To this end, we consider a system exchanging energy with a single reservoir at temperature T – we neglect particle exchanges between the system and the reservoir for simplicity. With the first and second law for averages, Eqs. (5.9) and (5.21), we get that $\dot{W} \geq \dot{F}$, where we introduced the (trajectory averaged) non-equilibrium free energy $F = E - S_{\mathrm{sys}} T$. By integrating over time, we get the non-equilibrium inequality

$$W \geq \Delta F, \tag{5.25}$$

resembling the classical equilibrium case in Eq. (5.4). This motivates us to define a stochastic free energy $f = \varepsilon_x - T s_{\mathrm{sys}}$, with ε_x being the energy of the occupied system state x, and $s_{\mathrm{sys}} = -k_B \ln(p_x)$ the stochastic entropy of the system. In equilibrium, we have $p_x = \exp\{(F^{(\mathrm{eq})} - \varepsilon_x)/k_B T\}$, where $F^{(\mathrm{eq})}$ is the equilibrium free energy of the system, implying that $f^{(\mathrm{eq})} = F^{(\mathrm{eq})}$, such that the stochastic equilibrium free energy coincides

with the equilibrium free energy. Driving the system along an arbitrary trajectory X thus gives us the total trajectory entropy production

$$T\Delta s_{\rm tot}[X] = w[X] - \Delta f[X], \tag{5.26}$$

where $w[X]$ is the work applied along the trajectory, and $\Delta f[X]$ is the difference in stochastic free energy between the initial and final states of trajectory X. To obtain this relation, we used Eqs. (5.6), (5.11), (5.14), (5.18), and (5.24). If the initial and final states are in thermal equilibrium, we get $\Delta f[X] = \Delta F^{(\rm eq)}$, which is independent on the initial and final states – note that the equilibrium free energy $F^{(\rm eq)} = -k_B T \ln(Z)$, such that $\Delta F^{(\rm eq)} = k_B T \ln[Z(t_0)/Z(t_n)]$, which only depends on $\lambda(t)$ at t_0 and t_n.

We have now reached the heart of stochastic thermodynamics; fluctuation theorems. To begin, we define a forward trajectory X of the system as specified in Eq. (5.10). To carry out calculations, we discretize time into N steps and define a time increment $\delta t = (t_n - t_0)/N$. Between two system transitions, let us say t_{j-1} and t_j, we get $N_j = (t_j - t_{j-1})/\delta t$ time increments. Since time is discretized, the jump $x_{j-1} \to x_j$ occurs at $t_j - \delta t$, such that the system dwells in x_{j-1} during $N_j - 1$ timesteps before making the transition. By using the definitions of Markov processes (see Chapter 2), and that transition probabilities can be calculated as $P(x_j|x_{j-1}) = M^{(\nu)}_{x_j x_{j-1}} \delta t$, the probability of observing the forward trajectory reads

$$P[X] = [P(x_{n-1}|x_{n-1})]^{N_n} \left[\prod_{j=0}^{n-2} M^{(\nu_{j+1})}_{x_{j+1} x_j}(\lambda_{j+1}) \delta t [P(x_j|x_j)]^{N_{j+1}-1} \right] p_{x_0}(t_0), \tag{5.27}$$

where $P(x|x)$ is the probability to dwell in state x during a time interval δt, and $p_{x_0}(t_0)$ is the probability to initially occupy x_0. To derive a fluctuation theorem, we must define a time reversed trajectory as well, where we consider the time reversed versions of both the system state and the control protocol. The time reversed trajectory of X is given by

$$X^{\rm tr} = \{t_{n-j}, \lambda_{n-j}, \nu_{n-j}, x_{n-j-1}\}_{j=1}^{n-1}, \tag{5.28}$$

starting in x_{n-1} at t_n with control variable λ_n, and ending in x_0 at t_0 with control variable λ_0, passing through the same system states and values of the control parameter as in the forward trajectory, but in reversed order. Note that this corresponds to a scenario where both x and λ are even under time reversal. The trajectory work and heat are odd under the time reversed operation, i.e., $w[X^{\rm tr}] = -w[X]$, $q[X^{\rm tr}] = -q[X]$. The probability of observing the time reversed trajectory reads

$$P^{\rm tr}[X^{\rm tr}] = \left[\prod_{j=0}^{n-2} [P(x_j|x_j)]^{N_{j+1}-1} M^{(\nu_{j+1})}_{x_j x_{j+1}}(\lambda_{j+1}) \delta t \right] [P(x_{n-1}|x_{n-1})]^{N_n} \tilde{p}_{x_{n-1}}(t_n), \tag{5.29}$$

where the superscript 'tr' on $P^{\rm tr}$ expresses the fact that we consider a time reversed experiment. Note that the initial distribution $\tilde{p}_{x_{n-1}}(t_n)$ of $X^{\rm tr}$ not necessarily coincides with the final distribution $p_{x_{n-1}}(t_n)$ to be in x_{n-1} at time t_n in the forward trajectory X. Experimentally, these distributions are typically different as the experimenter first runs a series of forward experiments, and then performs a series of backward experiments (time-reversing the driving). The distributions thus depend on the preparation of the experiment. The special case where the distributions coincide can, for example, be achieved by either letting the forward (backward) trajectory end (start) in a stationary state for a fixed control parameter, or letting the system thermalize to some environment after (before) the driving in the forward (backward) experiment.

Here we consider the situation where $\tilde{p}_{x_{n-1}}(t_n) = p_{x_{n-1}}(t_n)$, and use the definitions of Eqs. (5.27), (5.29), and (5.24) to find the detailed fluctuation theorem

$$\frac{P[X]}{P^{\rm tr}[X^{\rm tr}]} = e^{\Delta s_{\rm tot}[X]/k_B}. \tag{5.30}$$

This theorem relates the probabilities of observing the forward and time reversed trajectories with the entropy production of the forward trajectory $\Delta s_{\rm tot}[X]$ as defined in Eq. (5.24). For trajectories where $P[X] = P^{\rm tr}[X^{\rm tr}]$, $\Delta s_{\rm tot}[X] = 0$, and there is no bias towards either of the trajectories, implying full microscopic reversibility. For $\Delta s_{\rm tot}[X] > 0$, $P[X] > P^{\rm tr}[X^{\rm tr}]$, and there is a bias towards observing the forward trajectory. We stress that there still is a finite probability to observe the time reversed trajectory, but it is less likely. When $\Delta s_{\rm tot}[X]/k_B \gg 1$, $P^{\rm tr}[X^{\rm tr}]$ becomes vanishingly small compared to $P[X]$, indicating absolute microscopic irreversibility. By averaging over all possible trajectories X, the detailed fluctuation theorem (5.30) implies an integral fluctuation theorem

$$\left\langle e^{-\Delta s_{\rm tot}[X]/k_B} \right\rangle = 1, \tag{5.31}$$

where the average is taken with respect to $P[X]$, and $\sum_X P^{\rm tr}[X^{\rm tr}] = 1$. Jensen's inequality further provides the second law of stochastic thermodynamics,

$$\langle \Delta s_{\rm tot}[X] \rangle \geq 0. \tag{5.32}$$

That is, averaged over all possible trajectories, the entropy must be non-negative. This coincides with the conventional second law of thermodynamics. Further note that as $0 < e^{-\Delta s_{\rm tot}[X]/k_B} < 1$ for all trajectories with $\Delta s_{\rm tot}[X] > 0$, it is necessary that there exist trajectories with $\Delta s_{\rm tot}[X] < 0$ such that the average in Eq. (5.31) holds. We thus understand that these fluctuation theorems are generalizations of the second law that hold for microscopic systems far from equilibrium. In particular, we note that the second law is probabilistic on the microscopic scale, allowing for observations of trajectories with negative entropy production. It is only on average that the entropy production must be non-negative.

When driving a system coupled to a single reservoir between two equilibrium states[3], Eqs. (5.26) and (5.31) can be used to recover the Jarzynski relation [137]

$$\left\langle e^{-w[X]/k_BT} \right\rangle = e^{-\Delta F^{(\mathrm{eq})}/k_BT}. \tag{5.33}$$

The power of this relation lies in its ability to determine the free energy difference $\Delta F^{(\mathrm{eq})}$ between two equilibrium states by performing measurements on a non-equilibrium system. The Jarzynski relation further implies (by Jensen's inequality) that $\langle w[X] \rangle \geq \Delta F^{(\mathrm{eq})}$, a generalization of Eq. (5.4).

Finally, we make some remarks. First, fluctuation theorems can be obtained by considering alternative time reversed trajectories as well. The scenario discussed here, when restricting ourselves to a system and a driving that are even under time reversal, is a special case. In fact, it is possible to derive fluctuation theorems for systems and control protocols that are odd under time reversal [10]. Note that this introduces several subtleties in the derivations. The reason for studying the special case of even functions under time reversal is because of its direct applicability on the results derived in Paper II. Second, during the course of the last decades, many of the non-equilibrium theorems of stochastic thermodynamics have been verified in various experimental platforms, see Ref. [146] for a review.

5.3 Information thermodynamics

The purpose of this section is to introduce and review some of the results from information thermodynamics to clearly motivate why Maxwell's demon does not violate the second law. Maxwell's demon is a central topic of Papers I and III, but is also relevant for Paper II.

To begin, we will shortly review some key concepts from information theory that will be useful throughout this section. Our average uncertainty of a random variable X with distribution $p(x)$ can be quantified via the (information theoretic) Shannon entropy

$$H[p(x)] = -\sum_x p(x) \ln[p(x)]. \tag{5.34}$$

We call this the "information theoretic entropy" since it differs by a factor of k_B from the one defined in Eq. (5.15). In the case where $p(x) = 1$ for one specific x, our uncertainty vanishes. That is, we will always know the value of X. When X is uniformly distributed over N different values, each with probability $p(x) = 1/N$, the Shannon entropy is maximized, corresponding to maximal uncertainty about X. Second, for two distributions $p(x)$

[3]In fact, we only need to require that the initial state of the forward trajectory and the initial state of the backward trajectory are equilibrium states. Above we stated that also the final state of the forward trajectory needs to be in equilibrium – we did this to simplify the derivation.

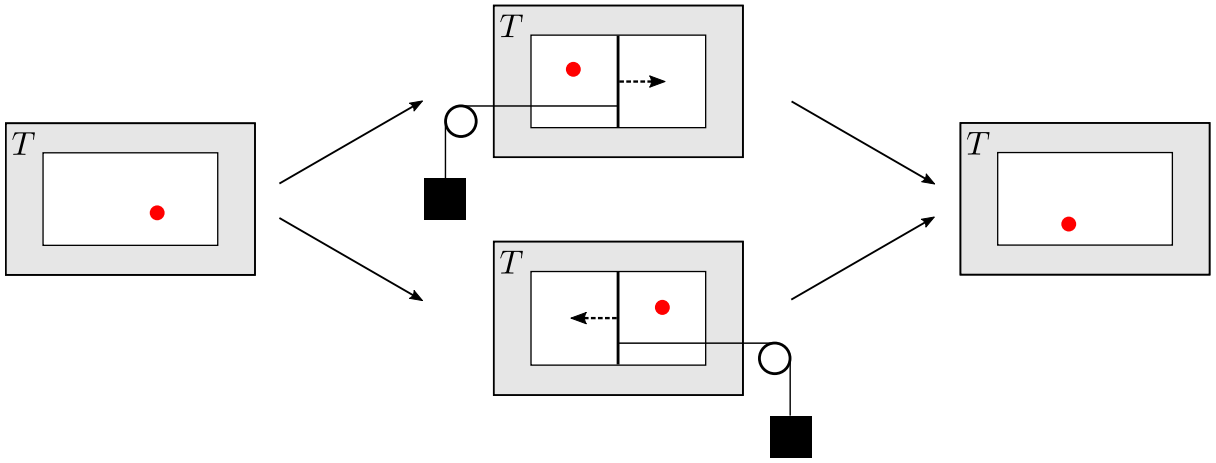

Figure 5.2: Illustration of the Szilard engine. A container with a single gas particle is in contact with a heat bath at temperature T. (left) Initially, the gas is in thermal equilibrium. (middle) A demon (experimenter) inserts a partition in the middle of the container, and measures on which side the particle is. Depending on the outcome, the demon applies feedback by attaching a weight on the same side of the partition as the particle is located. Via isothermal expansion, the gas can lift the weight, extracting $k_B T \ln(2)$ of work from the bath (dashed arrow). (right) As the expansion finishes, the gas returns to its initial state.

and $q(x)$ defined over the same outcomes x, we introduce the Kullback-Leibler divergence

$$D(p||q) = \sum_x p(x) \ln \left[\frac{p(x)}{q(x)} \right] . \tag{5.35}$$

We note that $D(p||q) \geq 0$, with equality if $p(x)$ and $q(x)$ are the same distribution. The Kullback-Leibler divergence can thus be used as a measure of how similar two distributions are. It vanishes for identical distributions and takes finite values otherwise. Finally, we define the mutual information between two random variables X and Y as

$$I[X:Y] = \sum_{x,y} p(x,y) \ln \left[\frac{p(x,y)}{p(x)p(y)} \right] , \tag{5.36}$$

where $p(x,y)$ is the joint distribution of the random variables, and $p(x)$ and $p(y)$ are the marginal distributions for X and Y, respectively. By definition, the mutual information coincides with the Kullback-Leibler divergence for $p(x,y)$ and $p(x)p(y)$, and we thus get that $I[X:Y] \geq 0$. The mutual information gives a measure on how correlated the variables X and Y are. If they are completely uncorrelated, $p(x,y) = p(x)p(y)$ and $I[X:Y] = 0$. Therefore, the mutual information is useful in measurement theory where the correlation between a system observable X and the measurement outcomes Y is of interest.

We now turn to Maxwell's demon. To illustrate the issues of apparent violations of the second law, we will study the Szilard engine – a simplified version of Maxwell's demon. Its working cycle is visualized in Fig. 5.2. A single gas particle is trapped inside a container of fixed volume, and is in contact with a heat bath of temperature T. That is, the gas

is initially in thermal equilibrium. A demon (or experimenter) inserts a partition in the middle of the container, and measures whether the particle is on the left or the right side of the partition. Based on the outcome, the demon performs feedback by attaching a weight to the partition. By quasistatic, isothermal expansion, the gas particle can lift the weight, extracting work

$$W_{\text{ext}} = -W = \int_{V_{\text{tot}}/2}^{V_{\text{tot}}} p dV = k_B T \ln(2), \tag{5.37}$$

where V_{tot} is the volume of the container, and $p = k_B T/V$ is the pressure of the gas at volume V and temperature T (ideal gas law for one particle). Finally, the demon removes the partition, and lets the particle return to its initial state. As the container returns to its initial state, the first law ensures that the bath must have provided an amount of heat $Q = k_B T \ln(2)$ to the container, implying that the change of entropy in the bath $\Delta S_{\text{B}} = -Q/T$ is negative. Since the gas returns to its initial equilibrium state, the entropy of the container does not change, and the total entropy, of both bath and container, is negative, appearing as a clear violation of the second law. To resolve this issue, the demon must be treated as a physical system whose entropy increases by an amount that at least matches the decrease in the bath. To motivate why this is the case, we will now discuss the thermodynamics of measuring, storing, and erasing information.

In the Szilard engine, the gas particle is initially in an equilibrium state with probability distribution $p(x = L) = p(x = R) = 1/2$ (x denotes the state of the gas). That is, we find the particle with equal probability on either side of the container. By measuring the state of the gas, we obtain an outcome $y = L, R$, and update our knowledge of the gas according to Bayes' rule,

$$p(x|y) = \frac{p(y|x)p(x)}{p(y)}, \qquad\qquad x, y = L, R, \tag{5.38}$$

where $p(y|x)$ is the likelihood function to get outcome y given that the state is x, $p(x)$ is the initial equilibrium distribution from above, and $p(y)$ is the probability to obtain outcome y. As $p(x|y)$ does not necessarily coincide with the equilibrium distribution, a measurement typically drives the system out of equilibrium. Therefore, the act of measuring should be considered as a non-equilibrium process. To calculate the change of system entropy due to the measurement, we use the Shannon entropy (5.34). Since $H[p(x|y)] - H[p(x)]$ depends on a specific value of y, we average this over all possible outcomes, and get

$$\Delta S_{\text{sys}} = k_B \sum_y p(y) \Big(H[p(x|y)] - H[p(x)] \Big) = -k_B I[S : M], \tag{5.39}$$

where $I[S : M]$ is the mutual information between the system and the measurement outcome. Since the mutual information is non-negative, $\Delta S_{\text{sys}} \leq 0$, implying that by measuring, our uncertainty of the system must, at least, stay the same or decrease. Assuming

that the measurement does not change the internal system energy, i.e., $\Delta E = 0$, the free energy change in the system becomes

$$\Delta F = \Delta E - T\Delta S_{\rm sys} = k_B T I[S:M] \geq 0, \tag{5.40}$$

where T is the temperature of the environment of the system. The effect of the measurement is thus to increase the free energy of the system, increasing the amount of work that can be extracted isothermally. In fact, for a system initially at equilibrium and coupled to a reservoir at temperature T, the following inequality holds true when feedback-controlling the system based on a single measurement [156]

$$W \geq -k_B T I[S:M] + \Delta F. \tag{5.41}$$

Here W is the average system work, and ΔF the change in free energy of the system. This generalizes the result in Eq. (5.25) to feedback-controlled systems. If $\Delta F = 0$, we get the following upper bound for the extracted work,

$$W_{\rm ext} = -W \leq k_B T I[S:M]. \tag{5.42}$$

That is, the decrease in uncertainty about the system sets the limit on how much work that can be extracted by doing feedback. For the Szilard engine, we have $p(x = L) = p(x = R) = 1/2$ in thermal equilibrium. For an error free measurement, the likelihood function is given by $p(y = L|x = L) = p(y = R|x = R) = 1$, and $p(y = L|x = R) = p(y = R|x = L) = 0$. We thus get that $I[S:M] = \ln(2)$. That is, the measurement obtains one bit of information. In the end of the cycle, the system returns to its initial state and $\Delta F = 0$. Therefore, the work that can be extracted by the Szilard engine obeys $W_{\rm ext} \leq k_B T \ln(2)$, providing an upper bound on how much work that is possible to extract. This inequality was saturated in Eq. (5.37).

We now consider the work required to do a measurement. The information acquired during the measurement will be stored in a memory M. Again, we obtain some outcome y that has probability distribution $p(y)$. The memory is in contact with a heat bath at temperature T. Initially, the system, the memory, and the bath are uncorrelated, and the memory is in thermal equilibrium. To perform the measurement, the memory interacts with the system. By assuming that this interaction does not involve any heat exchange, the average work [with respect to $p(y)$] performed on M during the measurement is bounded by [157]

$$W_{\rm M}^{(\rm meas)} \geq -k_B T(H - I[S:M]) + \Delta F_{\rm M}, \tag{5.43}$$

where $H = H[p(y)]$ is the Shannon entropy for the measurement outcome, and $\Delta F_{\rm M}$ is the change of free energy in the memory during the measurement. This inequality states that the work on the memory must, at least, be the change of free energy in the memory, as expected from Eq. (5.25), plus an additional energetic cost due to the information acquisition. The first term obeys the inequality $0 \leq H - I[S:M] \leq H$, where the lower

bound is obtained for an error free measurement, and the upper bound when no information is extracted, i.e., when $I[S:M]=0$. We note that when $H=I[S:M]$ (error free measurement) and $\Delta F_{\rm M}=0$, $W_{\rm M}^{(\rm meas)}\geq 0$. There are thus scenarios when no energy is needed to do the measurement. Note that there also exist scenarios where the lower bound on the work is negative, meaning that work can be extracted from the memory by doing the measurement.

By assuming that M is in thermal equilibrium with its environment before resetting it to the standard state, i.e., erasing it, the average work [with respect to $p(y)$] required to erase the memory is bounded by [157]

$$W_{\rm M}^{(\rm eras)}\geq k_BTH-\Delta F_M. \tag{5.44}$$

It is interesting to study the case for which $\Delta F_{\rm M}=0$. For a measurement with two outcomes where $p(y=0)=p(y=1)=1/2$, $W_{\rm M}^{(\rm eras)}\geq k_BT\ln(2)$. That is, to erase the memory, at least $k_BT\ln(2)$ of energy is required – this is the Landauer principle [148].

Combining Eqs. (5.41), (5.43) and (5.44) results in

$$W_{\rm SM}=W+W_{\rm M}^{(\rm meas)}+W_{\rm M}^{(\rm eras)}\geq\Delta F_{\rm S}, \tag{5.45}$$

where $W_{\rm SM}$ is the average work for the combined unit of system and memory. This inequality is in agreement with the conventional second law (5.4). We thus understand that the apparent violation of the second law for the Szilard engine only appears when considering the thermodynamics of the system alone. The information processing must be performed by a physical system (demon), which must be included in the thermodynamic book-keeping. By doing accordingly, no violations of the second law are observed.

The above discussion focused on feedback processes where only one single measurement was made, and illustrated how information processing comes with a thermodynamic cost. As this thesis concentrates on continuous measurement and feedback, we will now review a few important fluctuation theorems valid for continuous information processing.

In the absence of measurement and feedback, backward or time reversed trajectories are rather straightforward to define. However, when including measurement and feedback, it is not clear how to define a backwards trajectory. In Fig. 4.2(a), we visualize a trajectory X [marked as $S(t)$] of a two-level system together with a trajectory Y [marked as $D(t)$] of the measurement outcomes from a continuous measurement. We note that the time reversed trajectories of X and Y, going from right to left in the figure, yield an unphysical picture; the measurement outcome will predict a system transition before it happens. Similarly, a feedback protocol, with measurement dependent trajectory $\Lambda(Y)$, will therefore be able to act before a system transition occurs. This motivates why there is no clear definition of backward dynamics under feedback control. In fact, the backward trajectory can be defined

in different ways. This implies that each definition leads to a different fluctuation theorem [158]. It is, however, possible to always write down a general detailed fluctuation theorem for continuous feedback control [158]

$$\frac{P_{\rm B}[X^{\rm tr},Y^{\rm tr}]}{P[X,Y]} = e^{-\sigma[X,\Lambda(Y)]-\left(I_t[X:Y]-I_t^{\rm tr}[X^{\rm tr}:Y^{\rm tr}]\right)}, \tag{5.46}$$

where $P[X,Y]$ is the probability following the forward trajectories X and Y, $P_{\rm B}[X^{\rm tr},Y^{\rm tr}]$ is the probability for the (undefined) backward experiment following backward trajectories $X^{\rm tr}$ and $Y^{\rm tr}$, $\sigma[X,\Lambda(Y)]$ is the unitless entropy production along the forward trajectory when applying feedback protocol $\Lambda(Y)$, $I_t[X:Y]$ is the transfer entropy for the forward experiment, and $I_t^{\rm tr}[X^{\rm tr}:Y^{\rm tr}]$ is the transfer entropy of the backward experiment. The power of Eq. (5.46) lies in that it is valid for any choice of backward experiment. This indicates that each choice of backward experiment implies a choice-dependent fluctuation theorem, rather than a universal theorem that holds for all scenarios.

As an instructive example, we consider the backward trajectory of Ref. [35]. The experiment is executed as follows. First, we perform the forward experiment with feedback protocol $\Lambda(Y)$. Then, we run the backward experiment by randomly choosing an outcome trajectory Y, and applying the time reversed protocol of $\Lambda(Y)$, but do not perform any feedback. For this type of experiment, one can derive the integral fluctuation theorem [35]

$$\left\langle e^{-\sigma-I_t}\right\rangle = 1. \tag{5.47}$$

Jensen's inequality implies that

$$\langle\sigma\rangle \geq -\langle I_t\rangle. \tag{5.48}$$

This is a generalization of the second law, showing that under continuous measurement and feedback, it is possible to observe a negative system entropy production. As mentioned above, including the thermodynamics of the feedback-controller would give a non-negative total entropy production. One may also find a generalized Jarzynski relation [35]

$$\left\langle e^{-(w-\Delta F)/k_BT-I_t}\right\rangle = 1, \tag{5.49}$$

where w is the system work, and ΔF the free energy change of the system. For the average work, we get

$$\langle w\rangle \geq -k_BT\langle I_t\rangle + \Delta F, \tag{5.50}$$

resembling the single measurement inequality in Eq. (5.41).

Before closing this section, we review the special case where the presence of feedback control modifies the local detailed balance as [159]

$$\ln\left(\frac{M_{xx'}^{(\nu)}}{M_{x'x}^{(\nu)}}\right) = \frac{\varepsilon_{x'}-\varepsilon_x-\mu_\nu(n_{x'}-n_x)}{k_BT_\nu} + f_{xx'}^{(\nu)}. \tag{5.51}$$

Here $f^{(\nu)}_{xx'}$ is a feedback parameter assumed to be independent on the system energies ε_x. In the absence of feedback, $f^{(\nu)}_{xx'} = 0$, we recover the standard local detailed balance. It is assumed that the timescale of the feedback is much faster than the system, but much slower than the thermal relaxation time of the reservoirs. Again, so that the system always interacts with equilibrium reservoirs. This type of modified local detailed balance condition may arise in various situations, for instance in Paper II for the classical toy model. It was also was observed in Ref. [160]. A difference from the cases discussed above is that we do not consider any trajectory for the measurement outcomes or the control protocol – measurement and feedback are effectively incorporated into the rates $M^{(\nu)}_{xx'}$. The modified local detailed balance (5.51) leads to the integral fluctuation theorem [159]

$$\left\langle e^{-(\Delta S_{\rm tot}+I)/k_B} \right\rangle = 1, \tag{5.52}$$

where I is an information term depending on the feedback parameters $f^{(\nu)}_{xx'}$. In the absence of feedback, the information term vanishes, and we recover the standard fluctuation theorem for non-equilibrium systems (5.31). With Jensen's inequality, we get

$$\langle \Delta S_{\rm tot} \rangle \geq -\langle I \rangle, \tag{5.53}$$

similar to Eq. (5.48). Again, the entropy production is bounded from below by an information term.

5.4 Quantum thermodynamics

In this section, we begin by showing how the laws of thermodynamics emerge from quantum theory. We closely follow the lecture notes of Ref. [161]. This is followed by a discussion on how to calculate work and heat in open quantum systems, and we use the double quantum dot (DQD) as an example. Finally, we briefly discuss quantum thermal machines and entanglement. The results of this section are important for the theoretical modeling in Papers II-V.

Emergence of thermodynamics from quantum theory

In this section, we show how the first and second laws of thermodynamics emerge from quantum theory. We begin by introducing a few concepts that will be important throughout the chapter; the von Neumann entropy, the quantum relative entropy, and the thermal state.

The von Neumann entropy of a state $\hat{\rho}$ is given by

$$S_{\rm vN}(\hat{\rho}) = -k_B \,{\rm tr}\{\hat{\rho}\ln(\hat{\rho})\} \geq 0, \tag{5.54}$$

and can be seen as a quantum extension of the Shannon entropy (5.34). In fact, in the eigenbasis $\{|\lambda_j\rangle\}$ of $\hat{\rho}$, where $\hat{\rho}|\lambda_j\rangle = \lambda_j|\lambda_j\rangle$ with $0 \leq \lambda_j \leq 1$ and $\sum_j \lambda_j = 1$, the von Neumann entropy reduces to the Shannon entropy for the distribution $\{\lambda_j\}$, i.e., $S_{\rm vN}(\hat{\rho}) = -k_B \sum_j \lambda_j \ln(\lambda_j) = k_B H[\{\lambda_j\}]$. For a state that changes over time according to a unitary transformation $\hat{U}(t,t_0)$, with $\hat{\rho}(t) = \hat{U}(t,t_0)\hat{\rho}(t_0)\hat{U}^\dagger(t,t_0)$, the von Neumann entropy is stationary,

$$\partial_t S_{\rm vN}[\hat{\rho}(t)] = 0, \qquad \Big(S_{\rm vN}[\hat{\rho}(t_0)] = S_{\rm vN}[\hat{\rho}(t)]\Big). \tag{5.55}$$

This property follows from the fact that the eigenvalues of the density matrix do not change over time[4]. Thus, the information (or unceratinty) in the distribution $\{\lambda_j\}$ is preserved. However, for dissipative dynamics (non-unitary), the eigenvalues do change over time, reflecting that information is lost during the evolution.

The quantum relative entropy is defined as

$$S(\hat{\rho}||\hat{\sigma}) = {\rm tr}\{\hat{\rho}\ln(\hat{\rho})\} - {\rm tr}\{\hat{\rho}\ln(\hat{\sigma})\} = -k_B^{-1} S_{\rm vN}(\hat{\rho}) - {\rm tr}\{\hat{\rho}\ln(\hat{\sigma})\} \geq 0 \tag{5.56}$$

for density matrices $\hat{\rho}$ and $\hat{\sigma}$. This quantity provides a measure of how similar the two states are. For $\hat{\rho} = \hat{\sigma}$, $S(\hat{\rho}||\hat{\sigma}) = 0$. If $[\hat{\rho},\hat{\sigma}] = 0$, the density matrices share the same eigenbasis, and the quantum relative entropy coincides with the Kullback-Leibler divergence (5.35), i.e., $S(\hat{\rho}||\hat{\sigma}) = D(\{p_j\}||\{q_j\})$, where $\{p_j\}$ and $\{q_j\}$ are the eigenvalues of $\hat{\rho}$ and $\hat{\sigma}$, respectively.

A system with Hamiltonian $\hat{H}$ and particle number operator $\hat{N}$ is in a thermal state, in the grand canonical ensemble, if its density matrix is written as

$$\hat{\tau} = \frac{e^{-(\hat{H}-\mu\hat{N})/k_B T}}{Z}, \tag{5.57}$$

where T is temperature, μ chemical potential, and $Z = {\rm tr}\left\{e^{-(\hat{H}-\mu\hat{N})/k_B T}\right\}$ is the partition function. Note that the thermal state maximizes the von Neumann entropy for fixed $\langle\hat{H}\rangle$ and $\langle\hat{N}\rangle$ [12, 161][5].

Here we study the thermodynamics of scenarios similar to Fig. 3.1, where an open quantum system weakly interacts with several large heat baths in thermal equilibrium. The Hamilton

[4]If $\hat{\rho}(t_0) = \sum_j \lambda_j(t_0)|\lambda_j(t_0)\rangle\langle\lambda_j(t_0)|$, we find $\hat{\rho}(t) = \sum_j \lambda_j(t_0)|\lambda_j(t)\rangle\langle\lambda_j(t)|$, where $|\lambda_j(t)\rangle = \hat{U}(t,t_0)|\lambda_j(t_0)\rangle$, with $\delta_{jk} = \langle\lambda_j(t)|\lambda_k(t)\rangle$ given that $\langle\lambda_j(t_0)|\lambda_k(t_0)\rangle = \delta_{jk}$. That is, under a unitary transformation, the eigenvalues of a density matrix do not change.

[5]The following proof is provided by Ref. [161]. Consider an arbitrary state $\hat{\rho}$ for which $\langle\hat{H}\rangle = {\rm tr}\{\hat{H}\hat{\rho}\} = {\rm tr}\{\hat{H}\hat{\tau}\}$ and $\langle\hat{N}\rangle = {\rm tr}\{\hat{N}\hat{\rho}\} = {\rm tr}\{\hat{N}\hat{\tau}\}$. By using the quantum relative entropy, we find $S_{\rm vN}(\hat{\rho}) \leq -{\rm tr}\{\hat{\rho}\ln(\hat{\tau})\} = S_{\rm vN}(\hat{\tau})$. The last equality follows from explicit calculation, showing that the thermal state maximizes the von Neumann entropy.

operator of the total setup (including both system and baths) reads

$$\hat{H}(t) = \hat{H}_S(t) + \sum_\alpha \left(\hat{H}_\alpha + \hat{H}_{\alpha S} \right), \tag{5.58}$$

where $\hat{H}_S(t)$ is the Hamiltonian of the system, $\hat{H}_\alpha$ the Hamiltonian of bath α, and $\hat{H}_{\alpha S}$ the interaction Hamiltonian of the system and bath α. The time evolution of the setup is determined by Eq. (3.9). In addition, we have the particle number operators $\hat{N}_S$ and $\hat{N}_\alpha$ for the system and bath α, respectively. To make sure that particle conservation holds, we assume that

1. $[\hat{N}_S + \sum_\alpha \hat{N}_\alpha, \hat{H}(t)] = 0$ (global conservation),
2. $[\hat{N}_S, \hat{H}_S(t)] = 0$ (local conservation system),
3. $[\hat{N}_\alpha, \hat{H}_\alpha] = 0$ (local conservation baths).

For weak system-bath couplings, it is reasonable to assume that changes of energy in the system-bath couplings are negligibly small compared to changes of energy in system and baths. Therefore, we put

$$\partial_t \langle \hat{H}_{\alpha S} \rangle = -i \,\mathrm{tr} \left\{ [\hat{H}_{\alpha S}, \hat{H}_S(t) + \hat{H}_\alpha] \hat{\rho}(t) \right\} = 0, \tag{5.59}$$

where $\hat{\rho}(t)$ is the density matrix of the total setup, and we used $\langle \hat{O} \rangle = \mathrm{tr}\{\hat{O}\hat{\rho}(t)\}$ for an arbitrary operator $\hat{O}$. For open systems that weakly interact with their environment, it is, as we saw in Chapter 3 and Appendix D, reasonable to work with an effective description where correlations between system and baths are negligible, i.e.,

$$\hat{\rho}_S(t) \bigotimes_\alpha \hat{\tau}_\alpha, \tag{5.60}$$

with $\hat{\rho}_S(t) = \mathrm{tr}_E\{\hat{\rho}(t)\}$ being the reduced state of the system (the 'E' denotes a partial trace over the bath degrees of freedom), and $\hat{\tau}_\alpha = e^{-(\hat{H}_\alpha - \mu_\alpha \hat{N}_\alpha)/k_B T_\alpha}/Z_\alpha$ the thermal state of bath α with temperature T_α and chemical potential μ_α. In reality, this description might not be fully accurate, as weak correlations between system and baths can build up. However, it is often a good approximation due to the weak coupling. At the initial time t_0, we assume that no correlations exist, such that $\hat{\rho}(t_0) = \hat{\rho}_S(t_0) \bigotimes_\alpha \hat{\tau}_\alpha$.

The energy of the total setup is given by

$$E(t) = \langle \hat{H}(t) \rangle = \langle \hat{H}_S(t) \rangle + \sum_\alpha \left(\langle \hat{H}_\alpha \rangle + \langle \hat{H}_{\alpha S} \rangle \right). \tag{5.61}$$

By taking the time derivative, we find

$$\dot{E}(t) = P_S(t) + \mathrm{tr}\{\hat{H}_S(t)\partial_t\hat{\rho}(t)\} + \sum_\alpha \partial_t\langle\hat{H}_\alpha\rangle, \tag{5.62}$$

where $P_S(t) = \langle\partial_t\hat{H}_S(t)\rangle$ is the external power provided to the system, the second term is the change of energy due to internal changes of the system, and the last term is the change of energy in the baths. We note that the two last terms must cancel, as the energy of the whole setup only can change due to the external driving (that is, system and baths cannot create or destroy energy, only exhange it). The last two terms can thus only differ by a sign, reflecting that the energy that flows between system and baths must be conserved. The energy current associated with bath α can be written as

$$\partial_t\langle\hat{H}_\alpha\rangle = \partial_t\langle\hat{H}_\alpha - \mu_\alpha\hat{N}_\alpha\rangle + \mu_\alpha\partial_t\langle\hat{N}_\alpha\rangle. \tag{5.63}$$

Here we identify the heat current $\dot{Q}_\alpha^{(B)} = \partial_t\langle\hat{H}_\alpha - \mu_\alpha\hat{N}_\alpha\rangle$ and the chemical power $P_\alpha^{(B)} = \mu_\alpha\partial_t\langle\hat{N}_\alpha\rangle$. This interpretation of heat current and power can be motivated by Eq. (5.9) from stochastic thermodynamics. The superscript '(B)' indicates that $\dot{Q}_\alpha^{(B)}$, $P_\alpha^{(B)} > 0$ when energy enters the bath. By explicit calculation, the second term of Eq. (5.62) can be written as

$$\mathrm{tr}\{\hat{H}_S(t)\partial_t\hat{\rho}(t)\} = -i\sum_\alpha\Big(\langle[\hat{H}_S(t) - \mu_\alpha\hat{N}_S, \hat{H}_{\alpha S}]\rangle + \mu_\alpha\langle[\hat{N}_S, \hat{H}_{\alpha S}]\rangle\Big), \tag{5.64}$$

where we identify $\dot{Q}_\alpha^{(B)} = i\langle[\hat{H}_S(t) - \mu_\alpha\hat{N}_S, \hat{H}_{\alpha S}]\rangle$ and $P_\alpha^{(B)} = i\mu_\alpha\langle[\hat{N}_S, \hat{H}_{\alpha S}]\rangle$.

The first law of thermodynamics for the system can now be stated,

$$\partial_t\langle\hat{H}_S(t)\rangle = P_S(t) + \sum_\alpha\Big(P_\alpha + \dot{Q}_\alpha\Big), \tag{5.65}$$

where we introduced $P_\alpha = -P_\alpha^{(B)}$ and $\dot{Q}_\alpha = -\dot{Q}_\alpha^{(B)}$, such that $P_\alpha, \dot{Q}_\alpha > 0$ when energy enters the system. In accordance with the conventional first law of thermodynamics (5.1), changes of energy are due to work $\big(P_S(t), P_\alpha\big)$ or heat $(\dot{Q}_\alpha)$.

For entropy, it is tempting to use the von Neumann entopy for the entire setup (including both system and baths). However, as shown in Eq. (5.55), the von Neumann entropy is stationary for unitary evolution, suggesting that all processes of the setup are reversible. This is not realistic. As an example, we consider a quantum dot coupled to electron reservoirs at a low temperature T, see Fig. 5.3. When applying a large voltage bias $\mu_L - \mu_R = eV$ across the system, electrons will flow unidirectionally from the left to right reservoir. The reversed process is never observed, meaning that the entropy of the setup must increase. According to the definitions in stochastic thermodynamics, the entropy production rate

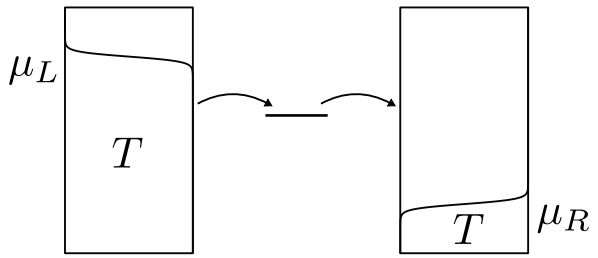

Figure 5.3: Quantum dot coupled to electron reservoirs at a low temperature T. By applying a large voltage bias $\mu_L - \mu_R = eV$, electrons are unidirectionally transported from left to right. As the reversed process is not observed, the entropy must increase.

reads $\dot{S}_{\rm tot} = -(\dot{Q}_L + \dot{Q}_R)/T$ (in steady state), see Eqs. (5.21) and (5.23). The indexes 'L' and 'R' refer to the left and right reservoir. It is desirable to find a similar relation for a quantum version of the second law.

This can be achieved by using the quantum relative entropy. The second law may be defined with the quantum relative entropy as (proof in Appendix F)

$$\Delta S(t) = k_B S(\hat{\rho}(t)||\hat{\rho}_S(t)\bigotimes_\alpha \hat{\tau}_\alpha) = S_{\rm vN}[\hat{\rho}_S(t)] - S_{\rm vN}[\hat{\rho}_S(t_0)] - \sum_\alpha \frac{\dot{Q}_\alpha}{T_\alpha} \geq 0, \quad (5.66)$$

which is ensured to be positive by the definition of the quantum relative entropy. The heat exchanged with bath α is given by $\hat{Q}_\alpha = -\,{\rm tr}\{(\hat{H}_\alpha - \mu_\alpha \hat{N}_\alpha)[\hat{\rho}(t) - \hat{\rho}(t_0)]\}$. The change of entropy can thus be interpreted as the distance between the true system state and the effective state (5.60). This choice of entropy production is satisfying, as it resembles the definitions in stochastic thermodynamics, where the first two terms correspond to the change of entropy in the system, while the last term corresponds to the change of entropy in the baths.

From Eq. (5.66), we find the entropy production rate

$$\Sigma = \partial_t \Delta S(t) = \partial_t S_{\rm vN}[\hat{\rho}_S(t)] - \sum_\alpha \frac{\dot{Q}_\alpha}{T_\alpha}. \quad (5.67)$$

In contrast to Eq. (5.66), Σ is not ensured to be non-negative. Note that $\Delta S(t)$ not necessarily increases monotonically over time, as system-bath correlations in $\hat{\rho}(t)$ may change with time. This means that $\hat{\rho}(t)$ sometimes gets closer to the uncorrelated effective state $\hat{\rho}_S(t)\bigotimes_\alpha \hat{\tau}_\alpha$, giving rise to the non-monotonic behavior. However, for large, weakly coupled baths, $\Delta S(t)$ is expected to increase monotonically, ensuring $\Sigma \geq 0$ [162].

Open systems

In Chapter 3, we remarked that it is a formidable task to model the combined dynamics of both an open system and its environment. Typically, we only know the dynamics of the

system density matrix $\hat{\rho}_S(t)$. Therefore, our definitions of heat and work in the previous subsection are hard to calculate, as many of the computations rely on knowing $\hat{\rho}(t)$. Here we show how these quantities may be calculated when only having access to $\hat{\rho}_S(t)$.

An open system, weakly coupled to a set of heat baths, evolves according to the Lindblad equation

$$\partial_t \hat{\rho}_S(t) = -i[\hat{H}_S, \hat{\rho}_S(t)] + \sum_\alpha \mathcal{L}_\alpha \hat{\rho}_S(t) \equiv \mathcal{L}\hat{\rho}_S(t), \tag{5.68}$$

where $\mathcal{L}_\alpha$ describes the coupling to bath α. Here we consider the case where the Hamiltonian is time independent (a time dependent Hamiltonian does not necessarily imply a stationary state of the Lindblad equation). We further assume there is a unique stationary state $\hat{\rho}_{\rm ss}$ for which $[\hat{H}_S, \hat{\rho}_{\rm ss}] = 0$ and $\mathcal{L}_\alpha \hat{\rho}_{\rm ss} = 0$.

If all baths are in equilibrium, all having the same temperature T and chemical potential μ, the system should thermalize, and the stationary state would be the thermal state[6]

$$\hat{\rho}_{\rm ss} \to \hat{\tau}^{(S)} = \frac{e^{-(\hat{H}_S - \mu \hat{N}_S)/k_B T}}{Z^{(S)}}. \tag{5.69}$$

This establishes the zeroth law of thermodynamics.

The average energy of the system reads $E(t) = \mathrm{tr}\{\hat{H}_S \hat{\rho}(t)\}$. By explicit calculation, we find the first law [cf. Eq. (5.65)]

$$\dot{E}(t) = \sum_\alpha \left(P_\alpha + \dot{Q}_\alpha \right), \tag{5.70}$$

where we identified the chemical power and heat current exchanged with bath α as

$$P_\alpha = \mu_\alpha \,\mathrm{tr}\{\hat{N}_S \mathcal{L}_\alpha \hat{\rho}_S(t)\}, \qquad \dot{Q}_\alpha = \mathrm{tr}\{(\hat{H}_S - \mu_\alpha \hat{N}_S)\mathcal{L}_\alpha \hat{\rho}_S(t)\}. \tag{5.71}$$

As before, for $P_\alpha, \dot{Q}_\alpha > 0$, energy is entering the system. For a time dependent Hamiltonian, we get an additional term in the first law for the external power [cf. Eq. (5.65)]. With the thermal state $\hat{\tau}_\alpha^{(S)} = e^{-(\hat{H}_S - \mu_\alpha \hat{N}_S)/k_B T_\alpha}/Z_\alpha^{(S)}$, for temperature T_α and chemical potential μ_α, satisfying $\mathcal{L}_\alpha \tau_\alpha = 0$, we can write $\hat{H}_S - \mu_\alpha \hat{N}_S = -k_B T_\alpha [\ln(\hat{\tau}_\alpha^{(S)}) + \ln(Z_\alpha^{(S)})]$. The heat current can thus be written as

$$\dot{Q}_\alpha = -k_B T_\alpha \,\mathrm{tr}\{\ln(\hat{\tau}_\alpha^{(S)}) \mathcal{L}_\alpha \hat{\rho}_S(t)\}, \tag{5.72}$$

where we used that $\mathcal{L}_\alpha$ is trace preserving.

[6]The superscript 'S' refers to the system, to distinguish it from the thermal state for the baths, see previous pages.

For the second law, we use the entropy production rate in Eq. (5.67). We find that

$$\begin{aligned}\Sigma &= \partial_t S_{\mathrm{vN}}[\hat{\rho}_S(t)] - \sum_\alpha \frac{\dot{Q}_\alpha}{T_\alpha} \\ &= k_B \sum_\alpha \mathrm{tr}\left\{\mathcal{L}_\alpha \hat{\rho}_S(t)\left(\ln(\hat{\tau}_\alpha^{(S)}) - \ln[\hat{\rho}_S(t)]\right)\right\} \geq 0,\end{aligned} \tag{5.73}$$

where we used $\partial_t S_{\mathrm{vN}}[\hat{\rho}_S(t)] = -k_B\,\mathrm{tr}\{\mathcal{L}_\alpha \hat{\rho}_S(t)\ln[\hat{\rho}_S(t)]\}$ [70] and Eq. (5.72). The entropy production rate is ensured to be non-negative by Spohn's inequality [163], which relies on that $\mathcal{L}_\alpha \hat{\tau}_\alpha^{(S)} = 0$. We note that the second law may be violated when using local Lindblad equations [164], but is ensured to hold for global Lindblad equations [74][7]. As the local approach is widely used and is central in this thesis, it is desirable to understand when it is valid. Several studies have addressed this question [74, 165–168]. Trushechkin and Volovich showed that the local model emerges from the global model as its zeroth order contribution when treating the couplings between subsystems perturbatively [165]. In particular, they showed that no violations of the second law for the local model are observed as long as higher order terms in the perturbation scheme can be neglected. Hewgill et. al. note that the definition of heat current in Eq. (5.72) gives rise to terms that are responsible for the violation of the second law [166]. By redefining heat, in accordance with a collisional framework, the authors argue that the problematic terms can be identified as work, and should thus not enter the second law (5.67), ensuring that no violations occur. Potts, Kalaee, and Wacker introduce a framework for deriving local master equations that are thermodynamically consistent [74]. Finally, Kalaee and Wacker show that non-negative entropy production is ensured by introducing effective energy levels at which the transfer of energy occurs [167, 168]. There is thus no general consensus yet on how to treat this problem, but up to every individual researcher.

Thermodynamics of the DQD

As an example of the thermodynamic consistency of local master equations, we study the DQD (see Chapter 3). In particular, we show that the local dynamics of the DQD determined by Eq. (3.20) are compliant with the laws of thermodynamics, provided that the equation is used in its regime of validity.

We begin by noting that the transition rates for electrons to enter and leave the DQD [see Eq. (3.20)] are evaluated at $\bar{\epsilon} = (\epsilon_L + \epsilon_R)/2$, rather than at the bare local energies ϵ_L and ϵ_R. For large detuning $|\epsilon_L - \epsilon_R|$, this is not physically sensible – it appears as if

[7] Often a system is made up of many coupled subsystems. In a local description, the baths couple to the local states of the subsystems. Typically, this description is valid when the couplings between subsystems are weak. For global descriptions, the baths couple to the delocalized eigenstates of the entire network of subsystems. This description works well if the couplings between subsystems are strong.

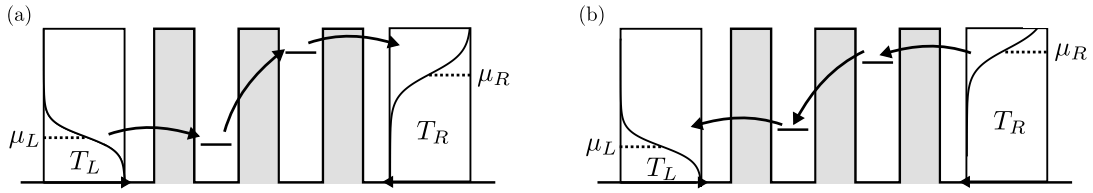

Figure 5.4: A DQD where the electron reservoirs couple locally to the respective dot levels. We visualize two thermodynamically inconsistent electron trajectories for large detuning $|\epsilon_L - \epsilon_R|$. In (a), energy appears to be created, and in (b), energy appears to be destroyed. The figure suggests that $\epsilon_L \simeq \epsilon_R$ is required for thermodynamic consistency.

electrons are being transported at energies far from the local levels. This suggests that the master equation (3.20) only give reasonable results when the detuning is small, i.e., when $\epsilon_L \simeq \epsilon_R$. An additional argument for this is depicted in Fig. 5.4, where it appears as energy can be created or destroyed in the local description when having a large detuning[8]. We thus expect that Eq. (3.20) is valid when the levels are close to each other. We now show that this leads to a thermodynamically consistent description.

To be compliant with the zeroth law, we expect that

$$\hat{\tau}^{(\mathrm{DQD})} = \frac{e^{-(\hat{H}_{\mathrm{DQD}} - \mu\hat{N})/k_B T}}{Z^{(\mathrm{DQD})}} \tag{5.74}$$

is the stationary state of Eq. (3.20) when $T_L = T_R = T$ and $\mu_L = \mu_R = \mu$. Here $\hat{N} = |L\rangle\langle L| + |R\rangle\langle R|$ is the number operator of the DQD. As $[\hat{H}_{\mathrm{DQD}}, \hat{N}] = 0$, we find that $[\hat{H}_{\mathrm{DQD}}, \hat{\tau}^{(\mathrm{DQD})}] = 0$. Additionally, we find, for $\epsilon_L = \epsilon_R$,

$$\mathcal{L}_\alpha \hat{\tau}^{(\mathrm{DQD})} = \mathcal{O}(g/k_B T), \tag{5.75}$$

where $\mathcal{L}_\alpha = \gamma_\alpha(\bar{\epsilon})\mathcal{D}[\hat{\sigma}_\alpha^\dagger] + \kappa_\alpha(\bar{\epsilon})\mathcal{D}[\hat{\sigma}_\alpha]$. This means that $\hat{\tau}^{(\mathrm{DQD})}$ is the stationary state of (3.20) if $g \ll k_B T$. Note that this coincides with Eq. (3.21) when $\epsilon_L = \epsilon_R$. For $\epsilon_L \neq \epsilon_R$, we find that $\mathcal{L}_\alpha \hat{\tau}^{(\mathrm{DQD})} \neq 0$. In conclusion, the master equation (3.20) correctly describes thermalization when $\epsilon_L = \epsilon_R$ and $g \ll k_B T$. Therefore, we continue to work with $\epsilon_L = \epsilon_R = \epsilon$.

For the first law (5.65), the chemical power reads

$$P_\alpha = \mu_\alpha \dot{n}_\alpha, \tag{5.76}$$

where μ_α is the chemical potential of bath α, and

$$\dot{n}_\alpha = \gamma_\alpha(\epsilon)\rho_{00} - \kappa_\alpha(\epsilon)\rho_{\alpha\alpha} \tag{5.77}$$

[8]We note that it is reasonable to expect some transport for disaligned levels in the local description due to the lifetime broadening of the levels.

is the particle current between dot α and bath α, with ρ_{ab} being the density matrix elements in Eq. (3.22). Note that the current is positive (negative) when electrons enter (leave) the DQD. The heat current (5.71) is given by

$$\dot{Q}_\alpha = (\epsilon - \mu_\alpha)\dot{n}_\alpha. \tag{5.78}$$

For $\epsilon_L \neq \epsilon_R$, an additional term, proportional to $\mathrm{Re}\{\rho_{LR}\}$, appears in the heat current. This term can give rise to violations of the second law [166]. In total, the first law (5.65) tells us that the energy of the DQD changes due to particle exchanges with the baths.

The second law can be proven by making use of Spohn's inequality as in Eq. (5.73). This proof relies on the fact that $\mathcal{L}_\alpha \hat{\tau}_\alpha^{(\mathrm{DQD})} \simeq 0$, with $\hat{\tau}_\alpha^{(\mathrm{DQD})} = e^{-(\hat{H}_{\mathrm{DQD}} - \mu_\alpha \hat{N})/k_B T_\alpha} / Z_\alpha^{(\mathrm{DQD})}$, as long as $g \ll k_B T_\alpha$.

To summarize, with $\epsilon_L = \epsilon_R$ and $g \ll k_B T_\alpha$, the local master equation (3.20) is thermodynamically consistent. Additionally, we stress that local master equations, in general, should be treated with care as they may violate the laws of thermodynamics.

Thermal machines and entanglement

An interesting type of system in quantum thermodynamics is the thermal machine. Similar to conventional thermodynamics, such machines make use of heat flows to perform useful tasks, such as cooling, producing work, or keeping time [13]. An important difference from the conventional machines is that the systems are quantum. Therefore, they can perform tasks that conventional machines cannot. For instance, generating entanglement.

In Ref. [39], it was shown that a simple autonomous machine[9], with two coupled qubits interacting with thermal baths at different temperatures, could generate weak entanglement in its stationary state by letting a heat current [169] flow through the machine. Several studies have later shown how to amplify the entanglement, including population inversion in the baths [170], heralding the stationary state [171, 172], and using feedback control [173] (Paper IV). It has also been shown that using a voltage bias, rather than a temperature bias, can be beneficial [174]. However, non of these studies showed that it is possible to deterministically generate maximal entanglement in autonomous machines. In fact, Paper V does show that this is possible for a specific setup. In the remainder of this section, we introduce the basics of (bipartite) entanglement. This is important for Papers IV and V.

As mentioned above, entanglement is a special type of state that is unique to quantum physics. It can be seen as a form of correlation that cannot be described by classical models.

[9]The terminology 'autonomous machines' refers to systems whose Hamiltonian is time independent. Coherent interactions are spontaneous rather than externally driven. Interdot tunneling in DQDs is an autonomous process.

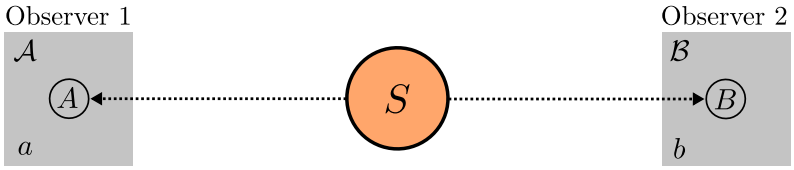

Figure 5.5: The source S prepares particles A and B, and sends them to observers 1 and 2. Observer 1 (2) measures observable $\mathcal{A}$ ($\mathcal{B}$) and obtains outcome a (b).

As such, entanglement acts as a hallmark highlighting the fundamental differences between quantum and classical physics. Besides being a fundamental curiosity, entanglement is the central resource for many applications in quantum information processing, including superdense coding [175], quantum teleportation [176], and quantum cryptography [177]. The remainder of this chapter is structured as follows. We begin by introducing the definition of entanglement and the Bell states. This is followed by a motivation of why entanglement is different from classical physics. At last, we discuss various ways of quantifying entanglement.

A pure bipartite system, with subsystems A and B, is entangled if its state vector cannot be written as the product

$$|\psi_A\rangle \otimes |\psi_B\rangle \,, \tag{5.79}$$

where $|\psi_A\rangle$ and $|\psi_B\rangle$ are the state vectors for the individual subsystems. If the state takes the form of Eq. (5.79), it is said to be separable. Similarly, mixed bipartite systems are said to be entangled if they cannot be written as

$$\sum_j p_j \hat{\rho}_A^{(j)} \otimes \hat{\rho}_B^{(j)}, \qquad\qquad \sum_j p_j = 1, \tag{5.80}$$

where $\hat{\rho}_A^{(j)}$ and $\hat{\rho}_B^{(j)}$ are density matrices for subsystems A and B, respectively.

An important set of entangled states in bipartite systems consisting of two qubits, A and B, are the Bell (or maximally entangled) states,

$$|\Psi_\pm\rangle = \frac{|01\rangle \pm |10\rangle}{\sqrt{2}}, \qquad\qquad |\Phi_\pm\rangle = \frac{|00\rangle \pm |11\rangle}{\sqrt{2}}, \tag{5.81}$$

with $|jk\rangle = |j\rangle_A \otimes |k\rangle_B \, \big(j,k=0,1\big)$, where $|j\rangle_{A(B)}$ is a basis state for qubit A (B). It can be verified by explicit calculation that these states cannot be written as in Eq. (5.79).

To understand why entanglement is inherently quantum, we consider the thought experiment illustrated in Fig. 5.5. A source (S) prepares two particles, A and B, and sends them to the spatially separated observers 1 and 2. Observer 1 obtains A, while observer 2 obtains B. Observer 1 (2) randomly chooses an observable $\mathcal{A}$ ($\mathcal{B}$) to measure, performs the measurement, and obtains outcome a (b). Note that the observers choose observables independently. By repeating the experiment many times, we can calculate the probability

distribution $p(a, b|\mathcal{A}, \mathcal{B})$ for obtaining a and b given that $\mathcal{A}$ and $\mathcal{B}$ were measured. Any correlations between the outcomes are encoded in this distribution.

To describe the experiment classically, the model must take local realism into account. This corresponds to two criteria [19]:

1. Physical systems are only directly (instantaneously) influenced by their immediate environment[10] (locality).
2. Physical systems have definite properties that exist independent of observation (realism).

Criterion 1 tells us that the choice of observable and the action of measuring by either observer cannot influence the other observer's measurement. Therefore, if we observe correlations between a and b, they must originate from the preparation of the particles. To encode this into the model, we introduce a local hidden variable λ that pre-determines what outcomes that will be observed (criterion 2). The distribution of outcomes can be calculated according to

$$\begin{aligned} p(a, b|\mathcal{A}, \mathcal{B}) &= \int d\lambda p(a, b|\mathcal{A}, \mathcal{B}, \lambda) p(\lambda) \\ &= \int d\lambda p(a|\mathcal{A}, \lambda) p(b|\mathcal{B}, \lambda) p(\lambda), \end{aligned} \tag{5.82}$$

where $p(\lambda)$ is a probability distribution for the hidden variable λ. Note that we assumed independence of the measurements in the second equality (locality). This means that all correlations between the measurements are caused by the hidden variable. Note that if there was no dependence on λ, we would get $p(a, b|\mathcal{A}, \mathcal{B}) = p(a|\mathcal{A})p(b|\mathcal{B})$, indicating that the outcomes are uncorrelated. To test whether this model accurately describes the physics of the experiment, one can use $p(a, b|\mathcal{A}, \mathcal{B})$ to derive bounds on the correlations between a and b. Violations of these bounds in an actual realization of the experiment imply that the model is inaccurate. Such bounds are referred to as Bell inequalities [178]. The most famous one is the CHSH (Clauser, Horne, Shimony, Holt) inequality [179]. It is given by

$$\mathcal{S} = \langle \mathcal{A}_1 \mathcal{B}_1 \rangle + \langle \mathcal{A}_1 \mathcal{B}_2 \rangle + \langle \mathcal{A}_2 \mathcal{B}_1 \rangle - \langle \mathcal{A}_2 \mathcal{B}_2 \rangle \leq 2, \tag{5.83}$$

where $\mathcal{A}_1, \mathcal{A}_2$ are observables of particle A, and $\mathcal{B}_1, \mathcal{B}_2$ are observables of particle B, all with outcomes ± 1. The expectation values are calculated as

$$\langle \mathcal{A}\mathcal{B} \rangle = \sum_{a,b=\pm 1} ab \cdot p(a, b|\mathcal{A}, \mathcal{B}). \tag{5.84}$$

[10] Environments far away can still influence the system, but their forces cannot propagate faster than the speed of light, and are thus influencing the system with a delay (rather than instantly).

We now study the thought experiment from a quantum perspective. Imagine that the source produces the Bell state $|\Psi_+\rangle$. By using the formula $\langle \mathcal{AB} \rangle = \langle \Psi_+ | \hat{\mathcal{A}} \otimes \hat{\mathcal{B}} | \Psi_+ \rangle$, together with the observables $\hat{\mathcal{A}}_1 = \hat{\sigma}_x$, $\hat{\mathcal{A}}_2 = \hat{\sigma}_z$, $\hat{\mathcal{B}}_1 = (\hat{\sigma}_x + \hat{\sigma}_z)/\sqrt{2}$, and $\hat{\mathcal{B}}_2 = (\hat{\sigma}_x - \hat{\sigma}_z)/\sqrt{2}$ [180], one can show that $\mathcal{S} = 2\sqrt{2}$, demonstrating a violation of the CHSH inequality[11]. The assumptions of local realism are thus not obeyed by quantum mechanics, showing that quantum and classical theory are fundamentally different. Entanglement is a hallmark highlighting this. Realizations of the thought experiment have shown similar violations of the CHSH inequality, and strongly confirm the predictions of quantum theory [181].

We close this section by discussing how entanglement can be quantified. The definitions in Eqs. (5.79) and (5.80) tell us how to distinguish entangled and separable states. However, it can be hard to use these definitions in practice, especially for mixed states. To this end, it is useful to introduce entanglement monotones. A general monotone $E(\hat{\rho})$ takes a state $\hat{\rho}$ as input and returns a numerical value. Besides this, the monotone should obey various properties, and among these, it is common to mention [81]

1. $E(\hat{\rho}) = 0$ for separable states,
2. $E(\hat{\rho}) > 0$ for entangled states,
3. $E(\hat{\rho})$ does not increase by performing local operations and classical communication (LOCC).

A more detailed discussion on properties can be found in Ref. [81]. Various monotones can be found in the literature, but here we focus on a bipartite monotone called concurrence. The concurrence is calculated via [182]

$$\mathcal{C}(\hat{\rho}) = \max\{0, \sqrt{\lambda_1} - \sqrt{\lambda_2} - \sqrt{\lambda_3} - \sqrt{\lambda_4}\}, \tag{5.85}$$

where $\lambda_1 > \lambda_2 > \lambda_3 > \lambda_4$ are the eigenvalues of the operator $\hat{\rho}(\hat{\sigma}_y \otimes \hat{\sigma}_y)\hat{\rho}^*(\hat{\sigma}_y \otimes \hat{\sigma}_y)$, with * denoting the elementwise complex conjugate in the $\{|00\rangle, |01\rangle, |10\rangle, |11\rangle\}$-basis. Note that $0 \leq \mathcal{C}(\hat{\rho}) \leq 1$, where 0 corresponds to separable states and 1 to the Bell states.

While the concurrence can correctly identify all entangled states, it does not provide any information about how useful the entanglement is from an operational point of view [170]. To this end, one can test whether the entanglement can violate the CHSH inequality or perform quantum teleportation. Let us focus on bipartite qubit systems with density matrices

[11] This is the largest possible violation of the CHSH inequality in quantum mechanics, and is achieved by all Bell states.

on the form (see Paper IV)

$$\hat{\rho} = \begin{pmatrix} \rho_{00} & 0 & 0 & 0 \\ 0 & \rho_{01} & \alpha & 0 \\ 0 & \alpha^* & \rho_{10} & 0 \\ 0 & 0 & 0 & \rho_{11} \end{pmatrix}, \tag{5.86}$$

in the $\{|00\rangle, |01\rangle, |10\rangle, |11\rangle\}$-basis, with $\rho_{00}+\rho_{01}+\rho_{10}+\rho_{11} = 1$ and $|\alpha| \leq \sqrt{\rho_{01}\rho_{10}}$. For this state, the lhs of the CHSH inequality can be computed with [170]

$$\mathcal{S} = 2\sqrt{8\alpha^2 + (2\Delta - 1)^2 - \min\{4\alpha^2, (2\Delta - 1)^2\}}, \tag{5.87}$$

where $\Delta = \rho_{01} + \rho_{10}$. For $\mathcal{S} > 2$, the state is said to be nonlocal, as the correlations cannot be reproduced by a classical model obeying local realism. For the Bell states $|\Psi_\pm\rangle$, we get $\mathcal{S} = 2\sqrt{2}$ as expected (see above). To quantify how well $\hat{\rho}$ can perform quantum teleportation, one can calculate the teleportation fidelity [170]

$$f(\hat{\rho}) = \frac{1 + 2F(\hat{\rho})}{3}, \tag{5.88}$$

where

$$F(\hat{\rho}) = \begin{cases} \alpha + \frac{\Delta}{2}, & \text{if } 1 + 2\alpha - 2\Delta \leq 0, \\ \max\{\alpha + \frac{\Delta}{2}, \frac{1-\Delta}{2}\}, & \text{otherwise.} \end{cases} \tag{5.89}$$

For maximally entangled states, $f(\hat{\rho}) = 1$, meaning that the teleportation works perfectly. A classical implementation of the teleportation protocol can at best achieve $f(\hat{\rho}) = 2/3$, implying that $\hat{\rho}$ contains useful entanglement when $F(\hat{\rho}) > 1/2$ [170].

Chapter 6

Outlook

In Paper II, we derived a quantum Fokker-Planck master equation (QFPME) – a general tool for describing continuous, Markovian feedback control in quantum systems. Currently, there is limited knowledge on the thermodynamic consistency of this equation. A first investigation can be found in Ref. [183]. Establishing a thermodynamically consistent framework for the QFPME would strengthen its position as a reliable tool for modeling quantum feedback control. For instance, using the equation for deriving a second law of thermodynamics including both system and detector would be an interesting avenue to pursue. This could provide complementary insights into information thermodynamics, establishing bounds on the entropy production in feedback-controlled systems. In Paper III, we explored various energetic contributions in the QFPME. However, we did not find a simple analytical method for calculating the work performed by applying feedback. Instead, we inferred the work numerically from energy conservation. Future studies should investigate if a simple analytical method exists. Recently, thermodynamic uncertainty relations for feedback-controlled quantum systems were presented [42]. The relations were derived for continuous quantum jump detection as well as continuous noisy measurements. An interesting extension would be to include a noisy detector with finite bandwidth, similar to the QFPME.

Until now, the QFPME has been used by assuming that the dynamics of the system obeys a Lindblad master equation. It is thus not clear for what hierarchy of timescales that this assumption holds. For instance, does the type of dynamics, i.e., local or global, put restrictions on the measurement strength or the detector bandwidth? Such a study would clarify the regime of validity of the QFPME. Another open question revolves around the description of performing measurements in a local basis when the dynamics of the system is global. The measurement would necessarily drive the dynamics towards a local description. It is not clear how to model such a cross-over within the QFPME formalism. Finding

answers to these questions would clarify what scenarios the QFPME can be applied in. Additionally, the QFPME has not yet been used to describe experimental data. This would strengthen the credibility of the equation.

The QFPME describes Markovian feedback scenarios where the latest measurement outcome is directly fed back to the system. A natural extension would be to derive a similar equation for a non-Markovian setup, where the whole signal of outcomes is used. Additionally, one may add a processing stage in the loop, where the signal is manipulated before being fed back. For instance, one could design feedback protocols relying on estimates of system properties. This could be useful for studying adaptive estimation strategies as the one proposed in Paper VI.

References

[1] M. Campisi, P. Hänggi, and P. Talkner. Colloquium: Quantum fluctuation relations: Foundations and applications. *Rev. Mod. Phys.*, 83:771, 2011.

[2] C. Jarzynski. Equalities and inequalities: Irreversibility and the second law of thermodynamics at the nanoscale. *Annu. Rev. Condens. Matter Phys.*, 2:329, 2011.

[3] C. Bustamante, J. Liphardt, and F. Ritort. The nonequilibrium thermodynamics of small systems. *Phys. Today*, 8:43, 2005.

[4] U. Seifert. Stochastic thermodynamics, fluctuation theorems and molecular machines. *Rep. Prog. Phys.*, 75:126001, 2012.

[5] R. J. Harris and G. M. Schütz. Fluctuation theorems for stochastic dynamics. *J. Stat. Mech.: Theory Exp.*, 2007:P07020, 2007.

[6] M. Esposito. Stochastic thermodynamics under coarse graining. *Phys. Rev. E*, 85:041125, 2012.

[7] M. Esposito, U. Harbola, and S. Mukamel. Nonequilibrium fluctuations, fluctuation theorems, and counting statistics in quantum systems. *Rev. Mod. Phys.*, 81:1665–1702, Dec 2009.

[8] U. Seifert. Stochastic thermodynamics: principles and perspectives. *Eur. Phys. J. B*, 64:423, 2008.

[9] C. Van den Broeck and M. Esposito. Ensemble and trajectory thermodynamics: A brief introduction. *Physica A: Statistical Mechanics and its Applications*, 418:6–16, 2015. Proceedings of the 13th International Summer School on Fundamental Problems in Statistical Physics.

[10] L. Peliti and S. Pigolotti. *Stochastic thermodynamics - an introduction*. Princton University Press, 2021.

[11] S. Vinjanampathy and J. Anders. Quantum thermodynamics. *Contemp. Phys.*, 57(4):545–579, 2016.

[12] F. Binder, L. A. Correa, C. Gogolin, J. Anders, and G. Adesso, editors. *Thermodynamics in the quantum regime*. Springer, 2018.

[13] M. T. Mitchison. Quantum thermal absorption machines: refrigerators, engines and clocks. *Contemp. Phys.*, 60(2):164–187, 2019.

[14] S. Deffner and S. Campbell. *Quantum thermodynamics: An introduction to the thermodynamics of quantum information*. IOP Publishing, 2019.

[15] H. M. Wiseman and G. J. Milburn. *Quantum measurement and control*. Cambridge Univeristy Press, 2010.

[16] K. Jacobs. *Quantum measurement theory and its applications*. Cambridge University Press, 2014.

[17] J. Zhang, Y.-X. Liu, R.-B. Wu, K. Jacobs, and F. Nori. Quantum feedback: Theory, experiments, and applications. *Phys. Rep.*, 679:1–60, 2017.

[18] J. P. Dowling and G. J. Milburn. Quantum technology: the second quantum revolution. *Philos. Trans. R. Soc. A*, 361(1809):1655–1674, 2003.

[19] M. A. Nielsen and I. L. Chuang. *Quantum information and quantum computation*. Cambridge University Press, 2010.

[20] J. M. Horowitz and T. R. Gingrich. Thermodynamic uncertainty relations constrain non-equilibrium fluctuations. *Nat. Phys.*, 16:15, 2020.

[21] J. M. R. Parrondo, J. M. Horowitz, and T. Sagawa. Thermodynamics of information. *Nat. Phys.*, 11:131, 2015.

[22] J. C. Maxwell. *Theory of heat*. Longmans, Green, and Co., 1871.

[23] H. S. Leff and A. F. Rex, editors. *Maxwell's Demon 2 Entropy, Classical and Quantum Information, Computing*. CRC Press, Boca Raton, 2002.

[24] K. Maruyama, F. Nori, and V. Vedral. Colloquium: The physics of Maxwell's demon and information. *Rev. Mod. Phys.*, 81:1, 2009.

[25] V. Serreli, C. F. Lee, E. R. Kay, and D. A. Leigh. A molecular information ratchet. *Nature*, 445:523, 2007.

[26] S. Toyabe, T. Sagawa, M. Ueda, E. Muneyuki, and M. Sano. Experimental demonstration of information-to-energy conversion and validation of the generalized Jarzynski equality. *Nat. Phys.*, 6:988, 2010.

[27] J. V. Koski, V. F. Maisi, J. P. Pekola, and D. V. Averin. Experimental realization of a Szilard engine with a single electron. *Proc. Natl. Acad. Sci. U.S.A.*, 111:13786, 2014.

[28] K. Chida, S. Desai, K. Nishiguchi, and A. Fujiwara. Power generator driven by Maxwell's demon. *Nat. Commun.*, 8:15310, 2017.

[29] A. Kumar, T.-Y. Wu, F. Giraldo, and D. S. Weiss. Sorting ultracold atoms in a three-dimensional optical lattice in a realization of Maxwell's demon. *Nature*, 561:83, 2018.

[30] M. Ribezzi-Crivellari and F. Ritort. Large work extraction and the Landauer limit in a continuous Maxwell demon. *Nat. Phys.*, 15:660, 2019.

[31] M. D. Vidrighin, O. Dahlsten, M. Barbieri, M. S. Kim, V. Vedral, and I. A. Walmsley. Photonic Maxwell's demon. *Phys. Rev. Lett.*, 116:050401, 2016.

[32] N. Cottet, S. Jezouin, L. Bretheau, P. Campagne-Ibarcq, Q. Ficheux, J. Anders, A. Auffèves, R. Azouit, P. Rouchon, and B. Huard. Observing a quantum Maxwell demon at work. *Proc. Natl. Acad. Sci. U.S.A.*, 114:7561, 2017.

[33] Y. Masuyama, K. Funo, Y. Murashita, A. Noguchi, S. Kono, Y. Tabuchi, R. Yamazaki, M. Ueda, and Y. Nakamura. Information-to-work conversion by Maxwell's demon in a superconducting circuit quantum electrodynamical system. *Nat. Commun.*, 9:1291, 2018.

[34] M. Naghiloo, J. J. Alonso, A. Romito, E. Lutz, and K. W. Murch. Information gain and loss for a quantum Maxwell's demon. *Phys. Rev. Lett.*, 121:030604, 2018.

[35] T. Sagawa and M. Ueda. Nonequilibrium thermodynamics of feedback control. *Phys. Rev. E*, 85:021104, 2012.

[36] P. P. Potts and P. Samuelsson. Thermodynamic uncertainty relations including measurement and feedback. *Phys. Rev. E*, 100:052137, 2019.

[37] T. Van Vu and Y. Hasegawa. Uncertainty relation under information measurement and feedback control. *J. Phys. A: Math. Theor.*, 53, 2020.

[38] Y. Hasegawa. Thermodynamic uncertainty relation for general open quantum systems. *Phys. Rev. Lett.*, 126:010602, Jan 2021.

[39] J. Bohr Brask, G. Haack, N. Brunner, and M. Huber. Autonomous quantum thermal machine for generating steady-state entanglement. *New J. Phys.*, 17(11):113029, nov 2015.

[40] G. Manzano and R. Zambrini. Quantum thermodynamics under continuous monitoring: A general framework. *AVS Quantum Science*, 4(2):025302, 2022.

[41] K. Prech and P. P. Potts. Quantum fluctuation theorem for arbitrary measurement and feedback schemes. *arXiv:2306.12281*, 2023.

[42] Yoshihiko Hasegawa. Quantum thermodynamic uncertainty relation under feedback control. *arXiv:2312.07407*, 2023.

[43] K. J. Åström and R. M. Murray. *Feedback systems - An Introduction for Scientists and Engineers*. Princton University Press, 2008.

[44] D. Risté, M. Dukalski, C. A. Watson, G. De Lange, M. J. Tiggelman, Y. M. Blanter, K. W. Lehnert, R. N. Schouten, and L. DiCarlo. Deterministic entanglement of superconducting qubits by parity measurement and feedback. *Nature*, 502(7471):350–354, 2013.

[45] A. D. Ludlow, M. M. Boyd, J. Ye, E. Peik, and P. O. Schmidt. Optical atomic clocks. *Rev. Mod. Phys.*, 87:637–701, Jun 2015.

[46] W. P. Smith, J. E. Reiner, L. A. Orozco, S. Kuhr, and H. M. Wiseman. Capture and release of a conditional state of a cavity QED system by quantum feedback. *Phys. Rev. Lett.*, 89:133601, Sep 2002.

[47] C. Sayrin, I. Dotsenko, X. Zhou, B. Peaudecerf, T. Rybarczyk, S. Gleyzes, P. Rouchon, M. Mirrahimi, H. Amini, M. Brune, J.-M. Raimond, and S. Haroche. Real-time quantum feedback prepares and stabilizes photon number states. *Nature*, 477(7362):73–77, 2011.

[48] R. Vijay, C. Macklin, D. H. Slichter, S. J. Weber, K. W. Murch, R. Naik, A. N. Korotkov, and I. Siddiqi. Stabilizing Rabi oscillations in a superconducting qubit using quantum feedback. *Nature*, 490(7418):77–80, 2012.

[49] Z. K. Minev, S. O. Mundhada, S. Shankar, P. Reinhold, R. Gutiérrez-Jáuregui, R. J. Schoelkopf, M. Mirrahimi, H. J. Carmichael, and M. H. Devoret. To catch and reverse a quantum jump mid-flight. *Nature*, 570:200–204, 2019.

[50] W. G. van der Wiel, S. De Franceschi, J. M. Elzerman, T. Fujisawa, S. Tarucha, and L. P. Kouwenhoven. Electron transport through double quantum dots. *Rev. Mod. Phys.*, 75:1–22, Dec 2002.

[51] J. P. Pekola. Towards quantum thermodynamics in electronic circuits. *Nat. Phys.*, 11:118, 2015.

[52] B. Küng, C. Rössler, M. Beck, M. Marthaler, D. S. Golubev, Y. Utsumi, T. Ihn, and K. Ensslin. Irreversibility on the level of single-electron tunneling. *Phys. Rev. X*, 2:011001, 2012.

[53] D. Barker, S. Lehmann, L. Namazi, M. Nilsson, C. Thelander, K. A. Dick, and V. F. Maisi. Individually addressable double quantum dots formed with nanowire polytypes and identified by epitaxial markers. *Appl. Phys. Lett.*, 114, 2019.

[54] D. Barker, M. Scandi, S. Lehmann, C. Thelander, K. A. Dick, M. Perarnau-Llobet, and V. F. Maisi. Experimental verification of the work fluctuation-dissipation relation for information-to-work conversion. *Phys. Rev. Lett.*, 128:040602, Jan 2022.

[55] Annby-Andersson, B. A General Formalism for Continuous Feedback Control in Quantum Systems. *Lund University*, 2022. Licentiate Thesis.

[56] J. B. Johnson. Thermal agitation of electricity in conductors. *Phys. Rev.*, 32:97–109, Jul 1928.

[57] H. Nyquist. Thermal agitation of electric charge in conductors. *Phys. Rev.*, 32:110–113, Jul 1928.

[58] Y. M. Blanter and M. Büttiker. Shot noise in mesoscopic conductors. *Phys. Rep.*, 336:1, 2000.

[59] C. W. Gardiner. *Handbook of stochastic methods*. Springer Berlin, 1985.

[60] K. Jacobs. *Stochastic processes for physicists - understanding noisy nystems*. Cambridge University Press, 2010.

[61] O. Vasicek. An equilibrium characterization of the term structure. *J. Financ. Econ.*, 5(2):177–188, 1977.

[62] S.M. Kay. *Fundamentals of statistical signal processing: estimation theory*. Prentice-Hall, Inc., 1993.

[63] G. Cowan. *Statistical data analysis*. Oxford University Press, 1998.

[64] H. Cramer. *Mathematical methods of statistics*. Princeton University Press, 1954.

[65] C.R. Rao. Information and the accuracy attainable in the estimation of statistical parameters. In S. Kotz and N. L. Johnson, editors, *Breakthroughs in Statistics: Foundations and Basic Theory*, page 235–247. Springer, 1992.

[66] J. Rubio, J. Anders, and L. A. Correa. Global quantum thermometry. *Phys. Rev. Lett.*, 127:190402, Nov 2021.

[67] A.W. van der Vaart. *Asymptotic Statistics*. Cambridge University Press, 1998.

[68] G. Grynberg, A. Aspect, and C. Fabre. *Introduction to quantum optics - From a semi-classical approach to quantized light*. Cambridge University Press, 2010.

[69] D. F. Walls and G. J. Milburn. *Quantum optics*. Springer Science & Business Media, 2007.

[70] H.P. Breuer and F. Petruccione. *The theory of open quantum systems*. Oxford Univeristy Press, 2002.

[71] A. Rivas and S. F. Huelga. *Open quantum systems - an introduction*. Springer, 2012.

[72] G. Lindblad. On the generators of quantum dynamical semigroups. *Commun. Math. Phys.*, 48:119–130, 1976.

[73] V. Gorini, A. Kossakowski, and E. C. G. Sudarshan. Completely positive dynamical semigroups of N−level systems. *J. Math. Phys.*, 17:821, 1976.

[74] P. P. Potts, A. A. S. Kalaee, and A. Wacker. A thermodynamically consistent markovian master equation beyond the secular approximation. *New J. Phys.*, 23(12):123013, dec 2021.

[75] P. P. Hofer, M. Perarnau-Llobet, L. D. M. Miranda, G. Haack, R. Silva, J. Bohr Brask, and N. Brunner. Markovian master equations for quantum thermal machines: local versus global approach. *New J. Phys.*, 19(12):123037, dec 2017.

[76] H. Carmichael. *An Open Systems Approach to Quantum Optics*. Springer, 1993.

[77] G. T. Landi, M. J. Kewming, M. T. Mitchison, and P. P. Potts. Current fluctuations in open quantum systems: Bridging the gap between quantum continuous measurements and full counting statistics.

[78] K. Jacobs and D. A. Steck. A straightforward introduction to continuous quantum measurement. *Contemp. Phys.*, 47(5):279–303, 2006.

[79] G. De Sousa, P. Bakhshinezhad, B. Annby-Andersson, P. Samuelsson, P. P. Potts, and C. Jarzynski. Continuous feedback protocols for cooling and trapping a quantum harmonic oscillator. *(in preparation)*, 2024.

[80] M. Schlosshauer. *Decoherence and the quantum to classical transition*. Springer, 2007.

[81] E. Andersson and P. Öhberg, editors. *Quantum Information and Coherence*. Springer, 2014.

[82] G. Kurizki S. Pellegrin V.M. Akulin, A. Sarfati, editor. *Decoherence, Entanglement and Information Protection in Complex Quantum Systems*. Springer, 2004.

[83] S. Singh, É. Roldán, I. Neri, I. M. Khaymovich, D. S. Golubev, V. F. Maisi, J. T. Peltonen, F. Jülicher, and J. P. Pekola. Extreme reductions of entropy in an electronic double dot. *Phys. Rev. B*, 99:115422, 2019.

[84] M. T. Mitchison, M. P. Woods, J. Prior, and M. Huber. Coherence-assisted single-shot cooling by quantum absorption refrigerators. *New J. of Phys.*, 17(11):115013, 2015.

[85] S. Nakajima. On quantum theory of transport phenomena: Steady diffusion. *Prog. Theor. Phys.*, 20(6):948, 12 1958.

[86] R. Zwanzig. Ensemble method in the theory of irreversibility. *J. Chem. Phys.*, 33(5):1338–1341, 1960.

[87] D. Mandal and C. Jarzynski. Analysis of slow transitions between nonequilibrium steady states. *J. Stat. Mech: Theory Exp.*, 2016(6):063204, 2016.

[88] M. Scandi and M. Perarnau-Llobet. Thermodynamic length in open quantum systems. *Quantum*, 3:197, October 2019.

[89] L. S. Levitov, H. Lee, and G. B. Lesovik. Electron counting statistics and coherent states of electric current. *J. Math. Phys.*, 37:4845, 1996.

[90] D. A. Bagrets and Yu. V. Nazarov. Full counting statistics of charge transfer in coulomb blockade systems. *Phys. Rev. B*, 67:085316, Feb 2003.

[91] G. Schaller. *Open quantum systems far from equilibrium*, volume 881. Springer, 2014.

[92] C. Matthiesen, M. J. Stanley, M. Hugues, E. Clarke, and M. Atatüre. Full counting statistics of quantum dot resonance fluorescence. *Sci. Rep.*, 4, 2014.

[93] J. D. Cohen, S. M. Meenehan, G. S. MacCabe, S. Gröblacher, A. H. Safavi-Naeini, F. Marsili, M. D. Shaw, and O Painter. Phonon counting and intensity interferometry of a nanomechanical resonator. *Nature*, 520:522–525, 2015.

[94] S. Gustavsson, R. Leturcq, B. Simovič, R. Schleser, T. Ihn, P. Studerus, K. Ensslin, D. C. Driscoll, and A. C. Gossard. Counting statistics of single electron transport in a quantum dot. *Phys. Rev. Lett.*, 96:076605, 2006.

[95] T. Fujisawa, T. Hayashi, R. Tomita, and Y. Hirayama. Bidirectional counting of single electrons. *Science*, 312:1634, 2006.

[96] C. Fricke, F. Hohls, W. Wegscheider, and R. J. Haug. Bimodal counting statistics in single-electron tunneling through a quantum dot. *Phys. Rev. B*, 76:155307, Oct 2007.

[97] C. Flindt, C. Fricke, F. Hohls, T. Novotny, K. Netočný, T. Brandes, and R. J. Haug. Universal oscillations in counting statistics. *Proc. Natl. Acad. Sci. U.S.A.*, 106(25):10116–10119, 2009.

[98] N. Ubbelohde, C. Fricke, C. Flindt, F. Hohls, and R. J. Haug. Measurement of finite-frequency current statistics in a single-electron transistor. *Nat. Commun.*, 3, 2012.

[99] Y. V. Nazarov. *Quantum noise in mesoscopic physics*, volume 97. Springer Science & Business Media, 2003.

[100] Y.V. Nazarov and M. Kindermann. Full counting statistics of a general quantum mechanical variable. *Eur. Phys. J. B*, 35:413–420, 2003.

[101] A. Gut. *An Intermediate Course in Probability*. Springer, 2009.

[102] H. E. Daniels. Saddlepoint approximations in statistics. *Ann. Math. Stat.*, 25(4):631–650, 1954.

[103] H. Touchette. The large deviation approach to statistical mechanics. *Phys. Rep.*, 478(1):1–69, 2009.

[104] F. Brange, P. Menczel, and C. Flindt. Photon counting statistics of a microwave cavity. *Phys. Rev. B*, 99:085418, Feb 2019.

[105] A. Hofmann, V.F. Maisi, J. Basset, C. Reichl, W. Wegscheider, T. Ihn, K. Ensslin, and C. Jarzynski. Heat dissipation and fluctuations in a driven quantum dot. *Phys. Status Solidi B*, 254:1600546, 2017.

[106] J. M. Elzerman, R. Hanson, L. H. Willems van Beveren, B. Witkamp, L. M. K. Vandersypen, and L. P. Kouwenhoven. Single-shot read-out of an individual electron spin in a quantum dot. *Nature*, 430:431–435, 2004.

[107] L. Rippe, B. Julsgaard, A. Walther, Yan Ying, and S. Kröll. Experimental quantum-state tomography of a solid-state qubit. *Phys. Rev. A*, 77:022307, Feb 2008.

[108] M. Sarovar, C. Ahn, K. Jacobs, and G. J. Milburn. Practical scheme for error control using feedback. *Phys. Rev. A*, 69:052324, May 2004.

[109] A. Bednorz, W. Belzig, and A. Nitzan. Nonclassical time correlation functions in continuous quantum measurement. *New J. Phys.*, 14, 2012.

[110] B. Misra and E. C. G. Sudarshan. The zeno's paradox in quantum theory. *J. Math. Phys.*, 18:756–763, Dec 1977.

[111] M. B. Mensky. *Quantum measurements and decoherence - models and phenomenology*. Springer Science & Business Media, 2000.

[112] H. M. Wiseman. Quantum theory of continuous feedback. *Phys. Rev. A*, 49:2133–2150, Mar 1994.

[113] V. P. Belavkin. Non-demolition measurement and control in quantum dynamical systems. In A. Blaquiere, S. Diner, and G. Lochak, editors, *Information Complexity and Control in Quantum Physics*, pages 311–329, Vienna, 1987. Springer Vienna.

[114] P. Warszawski and H. M. Wiseman. Quantum trajectories for realistic photodetection: I. General formalism. *J. Opt. B: Quantum and Semiclassical Optics*, 5(1):1–14, nov 2002.

[115] P. Warszawski and H. M. Wiseman. Quantum trajectories for realistic photodetection: II. Application and analysis. *J. Opt. B: Quantum and Semiclassical Optics*, 5(1):15–28, nov 2002.

[116] M. Sarovar, H.-S. Goan, T. P. Spiller, and G. J. Milburn. High-fidelity measurement and quantum feedback control in circuit QED. *Phys. Rev. A*, 72:062327, Dec 2005.

[117] Z. Liu, L. Kuang, K. Hu, L. Xu, S. Wei, L. Guo, and X.-Q. Li. Deterministic creation and stabilization of entanglement in circuit QED by homodyne-mediated feedback control. *Phys. Rev. A*, 82:032335, Sep 2010.

[118] T. A. Wheatley, D. W. Berry, H. Yonezawa, D. Nakane, H. Arao, D. T. Pope, T. C. Ralph, H. M. Wiseman, A. Furusawa, and E. H. Huntington. Adaptive optical phase estimation using time-symmetric quantum smoothing. *Phys. Rev. Lett.*, 104:093601, Mar 2010.

[119] W. Feng, P. Wang, X. Ding, L. Xu, and X.-Q. Li. Generating and stabilizing the Greenberger-Horne-Zeilinger state in circuit QED: Joint measurement, Zeno effect, and feedback. *Phys. Rev. A*, 83:042313, Apr 2011.

[120] S. Lloyd. Coherent quantum feedback. *Phys. Rev. A*, 62:022108, Jul 2000.

[121] M. Ernzer, M. Bosch Aguilera, M. Brunelli, G.-L. Schmid, T. M. Karg, C. Bruder, P. P. Potts, and P. Treutlein. Optical coherent feedback control of a mechanical oscillator. *Phys. Rev. X*, 13:021023, May 2023.

[122] H. M. Wiseman and G. J. Milburn. Quantum theory of optical feedback via homodyne detection. *Phys. Rev. Lett.*, 70:548–551, Feb 1993.

[123] J. Wang and H. M. Wiseman. Feedback-stabilization of an arbitrary pure state of a two-level atom. *Phys. Rev. A*, 64:063810, Nov 2001.

[124] J. Wang, H. M. Wiseman, and G. J. Milburn. Dynamical creation of entanglement by homodyne-mediated feedback. *Phys. Rev. A*, 71:042309, Apr 2005.

[125] N. Yamamoto. Parametrization of the feedback Hamiltonian realizing a pure steady state. *Phys. Rev. A*, 72:024104, Aug 2005.

[126] S. Mancini and J. Wang. Towards feedback control of entanglement. *Eur. Phys. J. D*, 32:257–260, 2005.

[127] J.-G. Li, J. Zou, B. Shao, and J.-F. Cai. Steady atomic entanglement with different quantum feedbacks. *Phys. Rev. A*, 77:012339, Jan 2008.

[128] A. R. R. Carvalho, A. J. S. Reid, and J. J. Hope. Controlling entanglement by direct quantum feedback. *Phys. Rev. A*, 78:012334, Jul 2008.

[129] Y. Li, B. Luo, and H. Guo. Entanglement and quantum discord dynamics of two atoms under practical feedback control. *Phys. Rev. A*, 84:012316, Jul 2011.

[130] P. Tombesi and D. Vitali. Macroscopic coherence via quantum feedback. *Phys. Rev. A*, 51:4913–4917, Jun 1995.

[131] P. Goetsch, P. Tombesi, and D. Vitali. Effect of feedback on the decoherence of a Schrödinger-cat state: A quantum trajectory description. *Phys. Rev. A*, 54:4519–4527, Nov 1996.

[132] H. M. Wiseman and G. J. Milburn. Squeezing via feedback. *Phys. Rev. A*, 49:1350–1366, Feb 1994.

[133] P. Tombesi and D. Vitali. Physical realization of an environment with squeezed quantum fluctuations via quantum-nondemolition-mediated feedback. *Phys. Rev. A*, 50:4253–4257, Nov 1994.

[134] H. M. Wiseman. In-loop squeezing is like real squeezing to an in-loop atom. *Phys. Rev. Lett.*, 81:3840–3843, Nov 1998.

[135] L. K. Thomsen, S. Mancini, and H. M. Wiseman. Spin squeezing via quantum feedback. *Phys. Rev. A*, 65:061801, Jun 2002.

[136] M. T. Mitchison, J. Goold, and J. Prior. Charging a quantum battery with linear feedback control. *Quantum*, 5:500, July 2021.

[137] C. Jarzynski. Nonequilibrium equality for free energy differences. *Phys. Rev. Lett.*, 78:2690, 1997.

[138] C. Jarzynski. Equilibrium free-energy differences from nonequilibrium measurements: A master-equation approach. *Phys. Rev. E*, 56:5018–5035, Nov 1997.

[139] G. E. Crooks. Entropy production fluctuation theorem and the nonequilibrium work relation for free energy differences. *Phys. Rev. E*, 60:2721, 1999.

[140] G. E. Crooks. Path-ensemble averages in systems driven far from equilibrium. *Phys. Rev. E*, 61:2361–2366, Mar 2000.

[141] J. R. Gomez-Solano, A. Petrosyan, S. Ciliberto, R. Chetrite, and K. Gawedzki. Experimental verification of a modified fluctuation-dissipation relation for a micron-sized particle in a nonequilibrium steady state. *Phys. Rev. Lett.*, 103:040601, Jul 2009.

[142] A. Mossa, M. Manosas, N. Forns, J. M. Huguet, and F. Ritort. Dynamic force spectroscopy of DNA hairpins: I. Force kinetics and free energy landscapes. *J. Stat. Mech.: Theory Exp.*, 2009(02):P02060, feb 2009.

[143] K. Hayashi, H. Ueno, R. Iino, and H. Noji. Fluctuation theorem applied to F1-ATPase. *Phys. Rev. Lett.*, 104:218103, May 2010.

[144] J. V. Koski, T. Sagawa, O-P. Saira, Y. Yoon, A. Kutvonen, P. Solinas, M. Möttönen, T. Ala-Nissila, and J. P. Pekola. Distribution of entropy production in a single-electron box. *Nat. Phys.*, 9:644–648, 2013.

[145] A. Hofmann, V.F. Maisi, J. Basset, C. Reichl, W. Wegscheider, T. Ihn, K. Ensslin, and C. Jarzynski. Heat dissipation and fluctuations in a driven quantum dot. *Phys. Status Solidi B*, 254, 2013.

[146] S. Ciliberto. Experiments in stochastic thermodynamics: Short history and perspectives. *Phys. Rev. X*, 7:021051, 2017.

[147] C. H. Bennett. The thermodynamics of computation – A review. *Int. J. Theor. Phys.*, 21:905, 1982.

[148] R. Landauer. Irreversibility and heat generation in the computing process. *IBM J. Res. Dev.*, 5:183, 1961.

[149] T. Sagawa. Thermodynamics of information processing in small systems. *Prog. Theor. Phys.*, 127:1, 2012.

[150] J. Goold, M. Huber, A. Riera, L. del Rio, and P. Skrzypczyk. The role of quantum information in thermodynamics—a topical review. *J. Phys. A*, 49(14):143001, feb 2016.

[151] J. V. Koski, V. F. Maisi, T. Sagawa, and J. P. Pekola. Experimental observation of the role of mutual information in the nonequilibrium dynamics of a Maxwell demon. *Phys. Rev. Lett.*, 113:030601, 2014.

[152] M. A. Aamir, P. J. Suria, J. A. M. Guzmán, C. Castillo-Moreno, J. M. Epstein, N. Yunger Halpern, and S. Gasparinetti. Thermally driven quantum refrigerator autonomously resets superconducting qubit. *arXiv: 2305.16710*, 2023.

[153] H. B. Callen. *Thermodynamics and an introduction to thermostatistics*. John Wiley and Sons, 1985.

[154] M. Esposito and C. Van den Broeck. Three faces of the second law. I. Master equation formulation. *Phys. Rev. E*, 82:011143, 2010.

[155] U. Seifert. Entropy production along a stochastic trajectory and an integral fluctuation theorem. *Phys. Rev. Lett.*, 95:040602, Jul 2005.

[156] T. Sagawa and M. Ueda. Second law of thermodynamics with discrete quantum feedback control. *Phys. Rev. Lett.*, 100:080403, 2008.

[157] T. Sagawa and M. Ueda. Minimal energy cost for thermodynamic information processing: Measurement and information erasure. *Phys. Rev. Lett.*, 102:250602, Jun 2009.

[158] P. P. Potts and P. Samuelsson. Detailed fluctuation relation for arbitrary measurement and feedback schemes. *Phys. Rev. Lett.*, 121:210603, 2018.

[159] M. Esposito and G. Schaller. Stochastic thermodynamics for "Maxwell demon" feedbacks. *EPL*, 99(3):30003, 2012.

[160] G. Schaller, C. Emary, G. Kiesslich, and T. Brandes. Probing the power of an electronic Maxwell's demon: single-electron transistor monitored by a quantum point contact. *Phys. Rev. B*, 84:085418, 2011.

[161] P. P. Potts. Introduction to quantum thermodynamics (lecture notes). *arXiv:1906.07439*, 2019.

[162] M. Esposito, K. Lindenberg, and C. van den Broeck. Entropy production as correlation between system and reservoir. *New J. Phys.*, 12(1):013013, jan 2010.

[163] H. Spohn. Entropy production for quantum dynamical semigroups. *J. Math. Phys.*, 19(5):1227–1230, 1978.

[164] A. Levy and R. Kosloff. The local approach to quantum transport may violate the second law of thermodynamics. *EPL*, 107(2):20004, jul 2014.

[165] A. S. Trushechkin and I. V. Volovich. Perturbative treatment of inter-site couplings in the local description of open quantum networks. *EPL*, 113(3):30005, feb 2016.

[166] A. Hewgill, G. De Chiara, and A. Imparato. Quantum thermodynamically consistent local master equations. *Phys. Rev. Res.*, 3:013165, Feb 2021.

[167] A. A. S. Kalaee and A. Wacker. Positivity of entropy production for the three-level maser. *Phys. Rev. A*, 103:012202, Jan 2021.

[168] A. Wacker. Nonresonant two-level transitions: Insights from quantum thermodynamics. *Phys. Rev. A*, 105:012214, Jan 2022.

[169] S. Khandelwal, N. Palazzo, N. Brunner, and G. Haack. Critical heat current for operating an entanglement engine. *New J. Phys.*, 22(7):073039, jul 2020.

[170] J. Bohr Brask, F. Clivaz, G. Haack, and A. Tavakoli. Operational nonclassicality in minimal autonomous thermal machines. *Quantum*, 6:672, March 2022.

[171] A. Tavakoli, G. Haack, M. Huber, N. Brunner, and J. Bohr Brask. Heralded generation of maximal entanglement in any dimension via incoherent coupling to thermal baths. *Quantum*, 2:73, June 2018.

[172] A. Tavakoli, G. Haack, N. Brunner, and J. Bohr Brask. Autonomous multipartite entanglement engines. *Phys. Rev. A*, 101:012315, Jan 2020.

[173] G. F. Diotallevi, B. Annby-Andersson, P. Samuelsson, A. Tavakoli, and P. Bakhshinezhad. Steady-state entanglement production in a quantum thermal machine with continuous feedback control. *arXiv:2309.07696*, 2023.

[174] K. Prech, P. Johansson, E. Nyholm, G. T. Landi, C. Verdozzi, P. Samuelsson, and P. P. Potts. Entanglement and thermokinetic uncertainty relations in coherent mesoscopic transport. *Phys. Rev. Res.*, 5:023155, Jun 2023.

[175] C. H. Bennett and S. J. Wiesner. Communication via one- and two-particle operators on Einstein-Podolsky-Rosen states. *Phys. Rev. Lett.*, 69:2881–2884, Nov 1992.

[176] C. H. Bennett, G. Brassard, C. Crépeau, R. Jozsa, A. Peres, and W. K. Wootters. Teleporting an unknown quantum state via dual classical and Einstein-Podolsky-Rosen channels. *Phys. Rev. Lett.*, 70:1895–1899, Mar 1993.

[177] A. K. Ekert. Quantum cryptography based on Bell's theorem. *Phys. Rev. Lett.*, 67:661–663, Aug 1991.

[178] J. S. Bell. On the Einstein Podolsky Rosen paradox. *Physics*, 1(3):195, 1964.

[179] J. F. Clauser, M. A. Horne, A. Shimony, and R. A. Holt. Proposed experiment to test local hidden-variable theories. *Phys. Rev. Lett.*, 23:880–884, Oct 1969.

[180] Tavakoli, A. Quantum Correlations and Communications. *University of Geneva*, 2020. PhD thesis.

[181] R. Horodecki, P. Horodecki, M. Horodecki, and K. Horodecki. Quantum entanglement. *Rev. Mod. Phys.*, 81:865–942, Jun 2009.

[182] W. K. Wootters. Entanglement of formation of an arbitrary state of two qubits. *Phys. Rev. Lett.*, 80:2245–2248, Mar 1998.

[183] Aschwanden, J. The thermodynamics of continuous feedback control: Case studies based on the quantum Fokker-Planck master equation. *University of Basel*, 2023. Master Thesis.

Scientific publications

Author contributions

The order of authors on each paper should be interpreted as follows. The position of the last author reflects that the author coordinated as well as supervised the project, and came up with the initial idea. Authors listed towards the end often took the role as supervisor and/or contributed with expert knowledge in the analysis of the results. The first author carried out most of the calculations, and often wrote the bulk of the manuscript. The remaining authors contributed with smaller calculations and/or took part in the analysis of the results.

Co-authors are abbreviated as follows: Peter Samuelsson (PS), Patrick P. Potts (PPP), Pharnam (Faraj) Bakhshinezhad (PB), Debankur Bhattacharyya (DB), Daniel Holst (DH), Guilherme De Sousa (GDS), Christopher Jarzynski (CJ), Giovanni Francesco Diotallevi (GFD), Armin Tavakoli (AT), Shishir Khandelwal (SK), Andreas Wacker (AW), Julia Boeyens (JB), Stefan Nimmrichter (SN), and Mohammad Mehboudi (MM).

Paper I: Maxwell's demon in a double quantum dot with continuous charge detection

PPP came up with the idea of the project. I performed all calculations under the supervision of PS and PPP, and wrote the manuscript. PPP derived Eq. (17) and the results of Sec. III E. All authors contributed to the analysis of the results and the revision of the manuscript.

Paper II: Quantum Fokker-Planck Master Equation for Continuous Feedback Control

PPP came up with the idea of the project. I and PPP derived the quantum Fokker-Planck master equation, and the leading order contribution in the separation of timescales expan-

sion. PPP, DB, GDS, and CJ developed two separate techniques for finding the correction term in the separation of timescales expansion. All authors derived results for the classical toy model. I and PPP derived the results for the quantum toy model. I wrote the bulk of the manuscript. PS and I wrote the introduction. PS wrote the abstract. All authors contributed to the analysis of the results and took part in revising the manuscript.

Paper III: Maxwell's demon across the quantum-to-classical transition

PPP came up with the idea of the project. I, DB, GDS, and DH performed all analytical and numerical calculations. DB implemented and performed the trajectory simulations. I produced all the figures with help from DB. I and DB wrote the first draft of the manuscript. All authors contributed to the analysis of the results and the revision of the manuscript.

Paper IV: Steady-state entanglement production in a quantum thermal machine with continuous feedback control

AT came up with the idea of using feedback and the QFPME to increase the entanglement of the studied system. I and PB came up with the idea of the feedback protocol. GFD derived the results in his master thesis under my supervision, with support from PS, PB, and AT. I and PB wrote the bulk of the manuscript with the help of GFD. AT wrote the abstract. I and AT co-wrote the introduction. All authors contributed to the analysis of the results and revised the manuscript.

Paper V: Maximal steady-state entanglement in autonomous quantum thermal machines

The idea of the project resulted from initial calculations by GFD. These were analyzed by myself, AT, GFD and SK. AT lead, coordinated and supervised the project. SK did all calculations, wrote the manuscript and made the final versions of the figures. I and GFD independently double checked the calculations for the three-qubit setup. I drew the first drafts of Figs. 1 and 4. AW benchmarked the results with independent methods. All authors contributed to the analysis of the results and the revision of the manuscript.

Paper VI: Probe thermometry with continuous measurements

I, PB and MM, as well as JB and SN came up with the idea of the project independently. Later, we merged our groups. MM lead and coordinated the project. JB and MM performed the numerical calculations. These were benchmarked with independent calcula-

tions by myself and PB. JB, MM, SN, and PPP derived all analytical results. All authors contributed in writing the manuscript. I wrote the first draft of section 6. All authors participated in the analysis and took part in revising the manuscript.

Appendix 

Appendix A

Proof: $\langle f(X)dW \rangle = 0$

In Chapter 2, we introduced the Itô stochastic differential equation

$$dX(t) = a[X(t)]dt + b[X(t)]dW(t), \tag{A.1}$$

where the stochastic process $X(t)$ and the Wiener increment $dW(t)$ at time t are statistically independent. Due to this independence, we argued that averages $\langle f[X(t)]dW(t)\rangle$ should vanish as $\langle dW(t)\rangle = 0$. Here, we show that this is true. We evaluate

$$\begin{aligned}\langle f[X(t)]dW(t)\rangle &= \int \mathfrak{D}[\boldsymbol{X}] f[X(t)]dW(t)P[\boldsymbol{X}] \\ &= \int dx_j dx_{j+1} f(x_j)dW_j P[x_j, x_{j+1}],\end{aligned} \tag{A.2}$$

where we used that $t = t_0 + jdt$, with $0 < j < n-1$, can be any time in between t_0 and $t_0 + (n-1)dt$. Note that we need to integrate over both x_j and x_{j+1} under the integral in the last equality as x_{j+1} is dependent on dW_j. To proceed, we make use of Bayes rule to rewrite $P[x_j, x_{j+1}] = P[x_{j+1}|x_j]P[x_j]$, and get

$$\begin{aligned}&\int dx_j dx_{j+1} f(x_j)dW_j P[x_j, x_{j+1}] \\ &\qquad = \int dx_j f(x_j)P[x_j] \int dx_{j+1} dW_j P[x_{j+1}|x_j].\end{aligned} \tag{A.3}$$

The conditional probability $P[x_{j+1}|x_j]$ may be found since we know that the probability distribution of dW_j is (see Chapter 2.3)

$$P[dW_j] = \frac{e^{-dW_j^2/2dt}}{\sqrt{2\pi dt}}, \tag{A.4}$$

and that $x_{j+1} = x_j + a(x_j)dt + b(x_j)dW_j$ from the Itô equation. The conditional probability is obtained via

$$\begin{aligned} P[x_{j+1}|x_j] &= \int d[dW_j]\delta\Big(x_{j+1} - [x_j + a(x_j)dt + b(x_j)dW_j]\Big)P[dW_j] \\ &= \frac{e^{-\frac{\left(x_{j+1}-[x_j+a(x_j)dt]\right)^2}{2b^2(x_j)dt}}}{\sqrt{2\pi b^2(x_j)dt}}, \end{aligned} \tag{A.5}$$

where we used that the delta function is an even function, and that $\delta(\alpha x) = \delta(x)/|\alpha|$ for a constant α. We understand that once x_j is known, x_{j+1} is a Gaussian random variable with mean $x_j + a(x_j)dt$ and variance $b^2(x_j)dt$. This mean and variance agrees with what we find from the Itô equation assuming $X(t) = x_j$ at time t. The rightmost integral in Eq. (A.3) can now be evaluated using $dW_j = [x_{j+1} - x_j - a(x_j)dt]/b(x_j)$,

$$\int dx_{j+1}dW_j P[x_{j+1}|x_j] = \int dx_{j+1}\frac{x_{j+1} - x_j - a(x_j)dt}{b(x_j)}P[x_{j+1}|x_j] = 0, \tag{A.6}$$

and we get $\langle f[X(t)]dW(t)\rangle = 0$.

Appendix B

n-resolved density matrix

To derive the n-resolved master equation (3.64), we begin by introducing the Laplace transform of the density matrix,

$$\tilde{\rho}_z = \int_0^\infty dt e^{-zt} \hat{\rho}_t, \tag{B.1}$$

where the hat and tilde indicate whether the density matrix belongs to the time domain or the Laplace domain. In Laplace space, the master equation (3.63) reads

$$\tilde{\rho}_z = \Omega(z)\hat{\rho}_0, \qquad \Omega(z) = \frac{1}{z - \mathcal{L}_0 - \mathcal{J}_+ - \mathcal{J}_-}, \tag{B.2}$$

where $\Omega(z)$ is the Laplace space propagator. Making use of the Neumann series, we can write the Laplace space propagator as an expansion in $\mathcal{J}_+ + \mathcal{J}_-$ as

$$\Omega(z) = \sum_{N=0}^{\infty} \Omega_0(z)[(\mathcal{J}_+ + \mathcal{J}_-)\Omega_0(z)]^N, \tag{B.3}$$

where $\Omega_0(z) = 1/(z - \mathcal{L}_0)$. By investigating the sum, term by term, we identify

$$\begin{aligned}
N = 0: &\quad \Omega_0(z), \\
N = 1: &\quad \Omega_0(z)\mathcal{J}_+\Omega_0(z) + \Omega_0(z)\mathcal{J}_-\Omega_0(z), \\
N = 2: &\quad \Omega_0(z)\mathcal{J}_+\Omega_0(z)\mathcal{J}_+\Omega_0(z) + \Omega_0(z)\mathcal{J}_-\Omega_0(z)\mathcal{J}_-\Omega_0(z) \\
&+ \Omega_0(z)\mathcal{J}_+\Omega_0(z)\mathcal{J}_-\Omega_0(z) + \Omega_0(z)\mathcal{J}_-\Omega_0(z)\mathcal{J}_+\Omega_0(z), \\
&\vdots
\end{aligned} \tag{B.4}$$

We see that the first term ($N = 0$) leaves the number of particles in the reservoir unchanged. The second term ($N = 1$) contains one part increasing the number of particles in the reservoir by one, and one term decreasing the number of particles by one.

The third term ($N = 2$) contains two parts where the reservoir particle number is either increased or decreased by two, and two terms where the net particle number is left unchanged. By using Eqs. (B.2) and (B.3), we note that different combinations of the terms in the sum can be interpreted as number resolved states $\tilde{\rho}_z(\pm n)$. We write $\tilde{\rho}_z(0) = [\Omega_0(z) + \Omega_0(z)\mathcal{J}_+\Omega_0(z)\mathcal{J}_-\Omega_0(z) + \Omega_0(z)\mathcal{J}_-\Omega_0(z)\mathcal{J}_+\Omega_0(z) + \dots]\hat{\rho}_0$, and $\tilde{\rho}_z(\pm 1) = [\Omega_0(z)\mathcal{J}_\pm\Omega_0(z) + \dots]\hat{\rho}_0$, where '$\dots$' denotes all possible combinations of Ω_0 and $\mathcal{J}_\pm$ that results in 0 or ± 1 particles in the reservoir. By using this recursively, we may write down similar expressions for a general $\tilde{\rho}_z(\pm n)$, and we obtain the following Laplace space relation for the number resolved density matrix,

$$\tilde{\rho}_z(n) = \Omega_0(z)\mathcal{J}_+\tilde{\rho}_z(n-1) + \Omega_0(z)\mathcal{J}_-\tilde{\rho}_z(n+1). \tag{B.5}$$

By transforming this back to the time domain, using the initial condition $\hat{\rho}_0(n) = \delta_{n,0}\hat{\rho}_0$, we get Eq. (3.64).

Appendix C

Motivation Eq. (4.12)

In this appendix, we motivate why Eq. (4.12) can be used for small dt. To simplify the discussion, we restrict ourselves to an observable with two eigenvalues, ξ_{a_1} and ξ_{a_2}. The probability distribution for observing outcome z reads

$$p(z) = \sqrt{\frac{2\lambda dt}{\pi}} \left[p_{a_1} e^{-2\lambda dt (z-\xi_{a_1})^2} + p_{a_2} e^{-2\lambda dt (z-\xi_{a_2})^2} \right], \tag{C.1}$$

where $|a_j\rangle$ ($j = 1, 2$) is the eigenstate corresponding to eigenvalue ξ_{a_j}, and $p_{a_j} = \langle a_j|\hat{\rho}|a_j\rangle$ is the probability of finding the system ($\hat{\rho}$) in state $|a_j\rangle$. We also note that the average of the measured observable is given by $\langle A\rangle = \mathrm{tr}\{\hat{A}\hat{\rho}\} = \xi_{a_1} p_{a_1} + \xi_{a_2} p_{a_2}$. We now consider two limiting cases.

First, we assume that $p_{a_1} \gg p_{a_2}$, where $\langle A\rangle \approx \xi_{a_1}$. In this limit, the second term of $p(z)$ barely contributes to the distribution, and it is reasonable to use

$$p(z) \approx \sqrt{\frac{2\lambda dt}{\pi}} e^{-2\lambda dt (z-\langle \hat{A}\rangle)^2}. \tag{C.2}$$

Second, we assume that $p_{a_1} \approx p_{a_2}$, where $\langle \hat{A}\rangle \approx (\xi_{a_1} + \xi_{a_2})/2$. If dt is small, the two Gaussians in $p(z)$ greatly overlap, and we can again use the approximation

$$p(z) \approx \sqrt{\frac{2\lambda dt}{\pi}} e^{-2\lambda dt (z-\langle \hat{A}\rangle)^2}, \tag{C.3}$$

which is a Gaussian centered in between ξ_{a_1} and ξ_{a_2}.

From these limiting cases, we understand that z, for small dt, is a Gaussian centered at $\langle \hat{A} \rangle$ with variance $1/4\lambda dt$. Therefore, we can write

$$z = \langle \hat{A} \rangle + \frac{dW}{\sqrt{4\lambda dt}}, \tag{C.4}$$

where dW is a Wiener increment with mean 0 and variance dt (see Chapter 2).

Appendix D

Derivation Eq. (3.20)

We begin by writing out the full Hamiltonian of the DQD and the baths,

$$\hat{H} = \hat{H}_{\mathrm{DQD}} + \sum_{\alpha=L,R} \left(\hat{H}_{\alpha} + \hat{H}_{\mathrm{DQD},\alpha} \right), \tag{D.1}$$

where $\hat{H}_{\mathrm{DQD}}$ is given in Eq. (3.19). The DQD Hamiltonian can be diagonalized as $\hat{H}_{\mathrm{DQD}} = E_0 \left|E_0\right\rangle\!\left\langle E_0\right| + E_1 \left|E_1\right\rangle\!\left\langle E_1\right| + E_2 \left|E_2\right\rangle\!\left\langle E_2\right|$, where

$$E_0 = 0, \qquad E_1 = \bar{\epsilon} + \sqrt{\Delta^2 + g^2}, \qquad E_2 = \bar{\epsilon} - \sqrt{\Delta^2 + g^2}, \tag{D.2}$$

with $\bar{\epsilon} = (\epsilon_L + \epsilon_R)/2$ and $\Delta = (\epsilon_L - \epsilon_R)/2$. The corresponding eigenvectors are

$$\left|E_0\right\rangle = \left|0\right\rangle, \qquad \left|E_1\right\rangle = a\left|L\right\rangle + b\left|R\right\rangle, \qquad \left|E_2\right\rangle = c\left|L\right\rangle + d\left|R\right\rangle, \tag{D.3}$$

where

$$\begin{cases} a = \dfrac{\Delta + \sqrt{g^2+\Delta^2}}{\sqrt{g^2 + \left(\Delta + \sqrt{g^2+\Delta^2}\right)^2}}, & b = \dfrac{g}{\sqrt{g^2 + \left(\Delta + \sqrt{g^2+\Delta^2}\right)^2}}, \\ c = \dfrac{\Delta - \sqrt{g^2+\Delta^2}}{\sqrt{g^2 + \left(\Delta - \sqrt{g^2+\Delta^2}\right)^2}}, & d = \dfrac{g}{\sqrt{g^2 + \left(\Delta - \sqrt{g^2+\Delta^2}\right)^2}}. \end{cases} \tag{D.4}$$

The bare bath Hamiltonians are given by

$$\hat{H}_{\alpha} = \sum_{k} \omega_{\alpha k} \hat{a}^{\dagger}_{\alpha k} \hat{a}_{\alpha k}, \tag{D.5}$$

with the fermionic annihilation (creation) operators $\hat{a}_{\alpha k}$ ($\hat{a}^{\dagger}_{\alpha k}$), annihilating (creating) an electron in mode k with energy $\omega_{\alpha k}$. These operators obey the following anti-commutation relations,

$$\left\{ \hat{a}^{\dagger}_{\alpha k}, \hat{a}_{\alpha k'} \right\} = \delta_{k k'}, \qquad \left\{ \hat{a}_{\alpha k}, \hat{a}_{\alpha k'} \right\} = 0. \tag{D.6}$$

The coupling between the DQD and bath α is described by

$$\hat{H}_{\mathrm{DQD},\alpha} = \sum_k \left(h_{\alpha k} \hat{\sigma}_\alpha^\dagger \hat{a}_{\alpha k} + h_{\alpha k}^* \hat{\sigma}_\alpha \hat{a}_{\alpha k}^\dagger \right), \tag{D.7}$$

with coupling elements $h_{\alpha k}$. We note that the coupling Hamiltonian can be written as

$$\hat{H}_{\mathrm{DQD},\alpha} = \sum_{j=0,1} \hat{S}_{\alpha j} \otimes \hat{B}_{\alpha j}, \tag{D.8}$$

where

$$\hat{S}_{\alpha 0} = \hat{\sigma}_\alpha^\dagger, \quad \hat{S}_{\alpha 1} = \hat{\sigma}_\alpha, \quad \hat{B}_{\alpha 0} = \sum_k h_{\alpha k} \hat{a}_{\alpha k}, \quad \hat{B}_{\alpha 1} = \sum_k h_{\alpha k}^* \hat{a}_{\alpha k}^\dagger. \tag{D.9}$$

This compact form simplifies the notation during the derivation.

The time evolution of the DQD and the baths is given by the von Neumann equation (3.9)

$$\partial_t \hat{\rho}_{\mathrm{tot}}(t) = -i[\hat{H}, \hat{\rho}_{\mathrm{tot}}(t)], \tag{D.10}$$

where $\hat{\rho}_{\mathrm{tot}}(t)$ is the total density matrix of both DQD and baths. To make progress, we transform the von Neumann equation to the interaction picture,

$$\partial_t \tilde{\rho}_{\mathrm{tot}}(t) = -i \sum_\alpha \left[\tilde{H}_{\mathrm{DQD},\alpha}(t), \tilde{\rho}_{\mathrm{tot}}(t) \right], \tag{D.11}$$

where operators in the interaction picture are defined as $\tilde{O}(t) = \hat{U}_{\mathrm{IP}} \hat{O} \hat{U}_{\mathrm{IP}}^\dagger$ for operators $\hat{O}$ in the Schrödinger picture and the unitary operator

$$\hat{U}_{\mathrm{IP}} = e^{i(\hat{H}_{\mathrm{DQD}} + \sum_\alpha \hat{H}_\alpha)t}. \tag{D.12}$$

The solution to Eq. (D.11) reads

$$\tilde{\rho}_{\mathrm{tot}}(t) = \tilde{\rho}_{\mathrm{tot}}(0) - i \sum_\alpha \int_0^t ds \left[\tilde{H}_{\mathrm{DQD},\alpha}(s), \tilde{\rho}_{\mathrm{tot}}(s) \right]. \tag{D.13}$$

By plugging the solution back into (D.11), and tracing over the baths, we get

$$\begin{aligned} \partial_t \tilde{\rho}(t) = &-i \sum_\alpha \mathrm{tr}_B \left\{ \left[\tilde{H}_{\mathrm{DQD},\alpha}(t), \tilde{\rho}_{\mathrm{tot}}(0) \right] \right\} \\ &- \sum_{\alpha,\beta} \int_0^t ds \, \mathrm{tr}_B \left\{ \left[\tilde{H}_{\mathrm{DQD},\alpha}(t), \left[\tilde{H}_{\mathrm{DQD},\beta}(s), \tilde{\rho}_{\mathrm{tot}}(s) \right] \right] \right\}, \end{aligned} \tag{D.14}$$

where $\mathrm{tr}_B\{\cdot\}$ denotes the partial trace over the baths, and $\tilde{\rho}(t) = \mathrm{tr}_B\{\tilde{\rho}_{\mathrm{tot}}(t)\}$ is the reduced state of the DQD (in the interaction picture). We now make two assumptions.

At time $t = 0$, we assume that there are no correlations between the DQD and the baths, such that $\hat{\rho}_{\mathrm{tot}}(0) = \hat{\rho}(0) \bigotimes_\alpha \hat{\tau}_\alpha$, where $\hat{\tau}_\alpha = \exp\Big\{-(\hat{H}_\alpha - \mu_\alpha \hat{N}_\alpha)/k_B T_\alpha\Big\}/Z_\alpha$ is the thermal state of bath α, with the chemical potential μ_α, number operator $\hat{N}_\alpha = \sum_k \hat{a}^\dagger_{\alpha k}\hat{a}_{\alpha k}$ and partition function $Z_\alpha = \mathrm{tr}\left\{\exp\left(-(\hat{H}_\alpha - \mu_\alpha \hat{N}_\alpha)/k_B T_\alpha\right)\right\}$. It is common to put $\mathrm{tr}\{\tilde{B}_{\alpha k}(t)\tau_\alpha\} = 0$, which eliminates the first term on the rhs of Eq. (D.14) [70, 91] (note that this equality holds for the operators $\hat{B}_{\alpha k}$ defined above). While this appears to put restrictions on the $\hat{B}_{\alpha k}$ operators, it can always be constructed by replacing $\hat{B}_{\alpha k} \to \hat{B}_{\alpha k} - g^{(\alpha)}_k \mathbb{1}$ and $\hat{H}_{\mathrm{DQD}} \to \hat{H}_{\mathrm{DQD}} + \sum_{\alpha,k} g^{(\alpha)}_k \hat{S}_{\alpha k} \otimes \mathbb{1}$, with $g^{(\alpha)}_k = \mathrm{tr}_B\{\hat{B}_{\alpha k}\hat{\tau}_\alpha\}$ [91]. Note that these replacements do not change the total Hamiltonian.

We also assume that $\hat{H}_{\mathrm{DQD},\alpha} \sim \mathcal{O}(\lambda)$, where λ is a book-keeping parameter representing the strength of the interaction between the DQD and the baths. To obtain a Markovian master equation, this parameter must be small, such that correlations between the DQD and the baths are weak (see Chapter 3). The density matrix on the rhs of Eq. (D.14) can thus be written as $\hat{\rho}_{\mathrm{tot}}(t) = \hat{\rho}(t) \bigotimes_\alpha \hat{\tau}_\alpha + \mathcal{O}(\lambda)$, where all DQD-bath correlations are contained in $\mathcal{O}(\lambda)$. We now plug this into (D.14) and keep all terms up to $\mathcal{O}(\lambda^2)$. This is known as the Born approximation, and results in

$$\begin{aligned}\partial_t \tilde{\rho}(t) = \sum_\alpha \sum_{kk'} \int_0^t ds \Big\{ & C^{(\alpha)}_{kk'}(t-s)\left[\tilde{S}_{\alpha k'}(s)\tilde{\rho}(s)\tilde{S}^\dagger_{\alpha k}(t) - \tilde{S}^\dagger_{\alpha k}(t)\tilde{S}_{\alpha k'}(s)\tilde{\rho}(s)\right] \\ & + C^{(\alpha)}_{kk'}(s-t)\left[\tilde{S}_{\alpha k'}(t)\tilde{\rho}(s)\tilde{S}^\dagger_{\alpha k}(s) - \tilde{\rho}(s)\tilde{S}^\dagger_{\alpha k}(s)\tilde{S}_{\alpha k'}(t)\right]\Big\},\end{aligned} \tag{D.15}$$

where we introduced the bath correlation functions

$$C^{(\alpha)}_{kk'}(t) = \mathrm{tr}\left\{\tilde{B}^\dagger_{\alpha k}(t)\hat{B}_{\alpha k'}\hat{\tau}_\alpha\right\}, \tag{D.16}$$

and used that $[C^{(\alpha)}_{kk'}(t)]^* = C^{(\alpha)}_{k'k}(-t)$. To find a Markovian description, we introduce $\tau = t - s$, and assume that $C^{(\alpha)}_{kk'}(t)$ decays to zero on a timescale τ_B that is much faster than the timescale of $\tilde{\rho}(t)$, such that $\tilde{\rho}(t)$ remains constant over τ_B. This allows us to replace $\tilde{\rho}(t-\tau) \to \tilde{\rho}(t)$ and extend the upper integration limit to ∞. This is known as the Markovian assumption, and yields the Markovian master equation

$$\begin{aligned}\partial_t \tilde{\rho}(t) = \sum_\alpha \sum_{kk'} \int_0^\infty d\tau \Big\{ & C^{(\alpha)}_{kk'}(\tau)\left[\tilde{S}_{\alpha k'}(t-\tau)\tilde{\rho}(t)\tilde{S}^\dagger_{\alpha k}(t) - \tilde{S}^\dagger_{\alpha k}(t)\tilde{S}_{\alpha k'}(t-\tau)\tilde{\rho}(t)\right] \\ & + C^{(\alpha)}_{kk'}(-\tau)\left[\tilde{S}_{\alpha k'}(t)\tilde{\rho}(t)\tilde{S}^\dagger_{\alpha k}(t-\tau) - \tilde{\rho}(t)\tilde{S}^\dagger_{\alpha k}(t-\tau)\tilde{S}_{\alpha k'}(t)\right]\Big\}.\end{aligned} \tag{D.17}$$

By explicit calculation, it is possible to show that $C^{(\alpha)}_{kk'}(t) \sim \delta_{kk'}$, and we find that

$$C^{(\alpha)}_{00}(t) = \sum_k |h_{\alpha k}|^2 e^{i\omega_{\alpha k}t} n^{(\alpha)}_{\mathrm{F}}(\omega_{\alpha k}) = \int_{-\infty}^{\infty} d\omega \rho^{(\alpha)}(\omega) n^{(\alpha)}_{\mathrm{F}}(\omega) e^{i\omega t}, \tag{D.18}$$

$$C^{(\alpha)}_{11}(t) = \sum_k |h_{\alpha k}|^2 e^{-i\omega_{\alpha k}t}[1 - n^{(\alpha)}_{\mathrm{F}}(\omega_{\alpha k})] = \int_{-\infty}^{\infty} d\omega \rho^{(\alpha)}(\omega)[1 - n^{(\alpha)}_{\mathrm{F}}(\omega)] e^{-i\omega t}, \tag{D.19}$$

where we used $[\hat{H}_\alpha, \hat{a}_{\alpha k}] = -\omega_{\alpha k}\hat{a}_{\alpha k}$, the Baker–Campbell–Hausdorff formula, and $\mathrm{tr}\{\hat{a}^\dagger_{\alpha j}\hat{a}_{\alpha k}\hat{\tau}_\alpha\} = \delta_{jk} n^{(\alpha)}_{\mathrm{F}}(\omega_{\alpha k})$ with $n^{(\alpha)}_{\mathrm{F}}(\cdot)$ being the Fermi-Dirac distribution defined in Eq. (3.18). We also introduced the spectral density of bath α as

$$\rho^{(\alpha)}(\omega) = \sum_k |h_{\alpha k}|^2 \delta(\omega - \omega_{\alpha k}). \tag{D.20}$$

Here we assume that the spectral densities are constant over all ω. Under this assumption, the bath correlation functions become the Fourier transforms of $n^{(\alpha)}_{\mathrm{F}}(\omega)$ and $1 - n^{(\alpha)}_{\mathrm{F}}(\omega)$. With the identity $\int_{-\infty}^{\infty} dx e^{i\lambda x}/(e^x + 1) = \pi[\delta(\lambda) - i/\sinh(\pi\lambda)]$, the bath correlation functions can be written as

$$C^{(\alpha)}_{00/11}(t) = \frac{\Gamma_\alpha}{2} e^{\pm i\mu_\alpha t}\left[\delta(t) - i\frac{k_B T_\alpha}{\sinh(\pi k_B T_\alpha t)}\right], \tag{D.21}$$

where we introduced the tunneling rate $\Gamma_\alpha = 2\pi\rho^{(\alpha)}(\omega)$ between the DQD and bath α. We can now identify the bath correlation time $\tau_B = \max\{1/k_B T_L, 1/k_B T_R\}$. For infinite temperatures, i.e., when the Fermi-Dirac distributions are flat, the correlation functions become Dirac delta functions and $\tau_B \to 0$. For $T_\alpha \to 0$, the second term of the correlation function decays as $1/t$, and must be taken into account when estimating τ_B.

To find the local master equation, we must perform a second Markov assumption, where we replace $\tilde{S}_{\alpha k}(t - \tau)$ with $\tilde{S}_{\alpha k}(t)$. To do this, we begin by noting that

$$\tilde{S}_{L0}(t) = a e^{iE_1 t} |E_1\rangle\langle E_0| + c e^{iE_2 t} |E_2\rangle\langle E_0|, \tag{D.22}$$

$$\tilde{S}_{R0}(t) = b e^{iE_1 t} |E_1\rangle\langle E_0| + d e^{iE_2 t} |E_2\rangle\langle E_0|, \tag{D.23}$$

where we expanded the operators in the energy eigenbasis. Observe that $\tilde{S}_{\alpha 1}(t) = \tilde{S}^\dagger_{\alpha 0}(t)$. For $\tilde{S}_{L0}(t)$, we can write

$$\begin{aligned}\tilde{S}_{L0}(t - \tau) = a e^{iE_1 t} e^{-i(\bar{\epsilon} + \sqrt{\Delta^2 + g^2})\tau} |E_1\rangle\langle E_0| \\ + b e^{iE_2 t} e^{-i(\bar{\epsilon} - \sqrt{\Delta^2 + g^2})\tau} |E_2\rangle\langle E_0|.\end{aligned} \tag{D.24}$$

The remaining operators can be expressed on a similar form. By plugging this into Eq. (D.17), we find integrals on the form

$$\frac{\Gamma_\alpha}{2}\int_0^\infty d\tau\left[\delta(\tau)-i\frac{k_BT_\alpha}{\sinh(\pi k_BT_\alpha\tau)}\right]e^{\mp i(\bar{\epsilon}-\mu_\alpha)\tau}e^{\pm i\sqrt{\Delta^2+g^2}\tau}, \tag{D.25}$$

where we used Eq. (D.21). When $\sqrt{\Delta^2+g^2}\tau_B \ll 1$ or $\sqrt{\Delta^2+g^2} \ll |\bar{\epsilon}-\mu_\alpha|$, the integrals can be approximated with

$$\frac{\Gamma_\alpha}{2}\int_0^\infty d\tau\left[\delta(\tau)-i\frac{k_BT_\alpha}{\sinh(\pi k_BT_\alpha\tau)}\right]e^{\mp i(\bar{\epsilon}-\mu_\alpha)\tau}. \tag{D.26}$$

Under this approximation, we can replace $\tilde{S}_{\alpha k}(t-\tau)\to e^{(-1)^{1-k}i\bar{\epsilon}\tau}\tilde{S}_{\alpha k}(t)$ in Eq. (D.17). Inserting this in (D.17) results in

$$\begin{aligned}\partial_t\tilde{\rho}(t)=\sum_\alpha\sum_k\Bigg(&2\,\mathrm{Re}\Big\{\gamma_{kk}^{(\alpha)}(\bar{\epsilon})\Big\}\left[\tilde{S}_{\alpha k}(t)\tilde{\rho}(t)\tilde{S}_{\alpha k}^\dagger(t)-\frac{1}{2}\left\{\tilde{S}_{\alpha k}^\dagger(t)\tilde{S}_{\alpha k}(t),\tilde{\rho}(t)\right\}\right]\\&-i\,\mathrm{Im}\Big\{\gamma_{kk}^{(\alpha)}(\bar{\epsilon})\Big\}\left[\tilde{S}_{\alpha k}^\dagger(t)\tilde{S}_{\alpha k}(t),\tilde{\rho}(t)\right]\Bigg),\end{aligned} \tag{D.27}$$

where we introduced

$$\gamma_{kk}^{(\alpha)}(\bar{\epsilon})=\int_0^\infty d\tau C_{kk}^{(\alpha)}(\tau)e^{(-1)^{1-k}i\bar{\epsilon}\tau}. \tag{D.28}$$

In particular, we note that

$$2\,\mathrm{Re}\Big\{\gamma_{00}^{(\alpha)}(\bar{\epsilon})\Big\}=\Gamma_\alpha n_{\mathrm{F}}^{(\alpha)}(\bar{\epsilon}),\qquad 2\,\mathrm{Re}\Big\{\gamma_{11}^{(\alpha)}(\bar{\epsilon})\Big\}=\Gamma_\alpha[1-n_{\mathrm{F}}^{(\alpha)}(\bar{\epsilon})], \tag{D.29}$$

which we found by using that $\int_{-\infty}^\infty d\tau\exp\{\pm i(\omega-\bar{\epsilon})\tau\}=2\pi\delta(\omega-\bar{\epsilon})$. Equation (D.27) is written on Lindblad form, and desribes the time evolution of the DQD in the interaction picture. Note that $1/\Gamma_\alpha$ determines the timescale τ_{DQD} of the density matrix in the interaction picture. For the first Markov assumption to hold, we required that $\tau_B \gg \tau_{\mathrm{DQD}}$, which is true as long as $\gamma_{kk}^{(\alpha)}(\bar{\epsilon})$ is flat around $\bar{\epsilon}$. This occurs if $k_BT_\alpha \gg \Gamma_\alpha$ or $|\bar{\epsilon}-\mu_\alpha| \gg \Gamma_\alpha$. Transforming (D.27) to the Schrödinger picture, we find

$$\begin{aligned}\partial_t\hat{\rho}(t)=&-i[\hat{H}_{\mathrm{DQD}}+\hat{H}_{\mathrm{LS}},\hat{\rho}(t)]\\&+\sum_{\alpha=L,R}\left(\Gamma_\alpha n_{\mathrm{F}}^{(\alpha)}(\bar{\epsilon})\mathcal{D}[\hat{\sigma}_\alpha^\dagger]+\Gamma_\alpha[1-n_{\mathrm{F}}^{(\alpha)}(\bar{\epsilon})]\mathcal{D}[\hat{\sigma}_\alpha]\right)\hat{\rho}(t),\end{aligned} \tag{D.30}$$

with the Lamb shift Hamiltonian

$$\hat{H}_{\mathrm{LS}}=\sum_\alpha\sum_k\mathrm{Im}\Big\{\gamma_{kk}^{(\alpha)}(\bar{\epsilon})\Big\}\hat{\sigma}_\alpha^\dagger\hat{\sigma}_\alpha, \tag{D.31}$$

shifting the bare energies of the dots. Typically, this Hamiltonian is baked into $\hat{H}_{\mathrm{DQD}}$ (or neglected), giving Eq. (3.20), which is valid for

$$\max\{k_B T_\alpha, |\bar{\epsilon} - \mu_\alpha|\} \gg \Gamma_\alpha, \sqrt{\Delta^2 + g^2}. \tag{D.32}$$

Appendix E

Ensemble averages over trajectories of jumps

For simplicity, we consider trajectories of jumps for only one jump process $dN(t)$, but the method can be generalized to K processes. We define a trajectory of jumps as

$$\gamma_n = \{dN_j\}_{j=0}^{n}, \tag{E.1}$$

where we have discretized time into n segments of length $dt = (t - t_0)/n$, such that $dN_j = dN(t_0 + jdt)$. The probability of observing this trajectory can be decomposed as (Bayes's rule)

$$P[\gamma_n] = P[dN_n|\gamma_{n-1}]P[\gamma_{n-1}], \tag{E.2}$$

where $P[dN_n|\gamma_{n-1}]$ is the conditional probability that dN_n happens given that we previously observed the trajectory γ_{n-1}. We now introduce the notation $\hat{\rho}_c(t) = \hat{\rho}(t|\gamma_{n-1}) = \hat{\rho}(t, \gamma_{n-1})/P[\gamma_{n-1}]$ to indicate that the density matrix at time t is conditioned on the full trajectory of jumps γ_{n-1} up to time t. The notation suggests that the n:th jump has not occurred yet. We can now write $P[dN_n = 1|\gamma_{n-1}] = dt\,\mathrm{tr}\{\hat{L}^\dagger \hat{L}\hat{\rho}(t|\gamma_{n-1})\}$ and $P[dN_n = 0|\gamma_{n-1}] = 1 - dt\,\mathrm{tr}\{\hat{L}^\dagger \hat{L}\hat{\rho}(t|\gamma_{n-1})\}$ for the n:th jump.

The ensemble average over all possible trajectories is defined as a path integral via

$$\mathrm{E}[\cdot] = \int \mathfrak{D}[\gamma_n]\cdot = \sum_{dN_0=0,1} \cdots \sum_{dN_n=0,1} \cdot. \tag{E.3}$$

Via this definition, we get

$$\begin{aligned} \mathrm{E}[dtdN_n] &= \int \mathfrak{D}[\gamma_n] dtdN_n P[\gamma_n] \\ &= \int \mathfrak{D}[\gamma_{n-1}] \sum_{dN_n=0,1} dtdN_n P[dN_n|\gamma_{n-1}] P[\gamma_{n-1}] \\ &= dt^2 \,\mathrm{tr}\{\hat{L}^\dagger \hat{L} \hat{\rho}(t)\} = 0, \end{aligned} \tag{E.4}$$

where we used that $\int \mathfrak{D}[\gamma_{n-1}]\hat{\rho}(t,\gamma_{n-1}) = \hat{\rho}(t)$ is the unconditioned density matrix at time t. This proves that $\mathrm{E}[dtdN_n] \propto dt^2$, as stated below Eq. (3.30).

We now prove that the ensemble average of Eq. (3.32) gives back the Lindblad equation (3.15). For one jump process, the stochastic master equation (3.32) reads

$$\begin{aligned} d\hat{\rho}_c(t) = -idt[\hat{H}, \hat{\rho}_c(t)] + dN_n \left(\frac{\hat{L}\hat{\rho}_c(t)\hat{L}^\dagger}{\mathrm{tr}\left\{\hat{L}^\dagger \hat{L} \hat{\rho}_c(t)\right\}} - \hat{\rho}_c(t) \right) \\ + dt \left(\hat{\rho}_c(t)\,\mathrm{tr}\left\{\hat{L}^\dagger \hat{L} \hat{\rho}_c(t)\right\} - \frac{1}{2}\left\{\hat{L}^\dagger \hat{L}, \hat{\rho}_c(t)\right\} \right). \end{aligned} \tag{E.5}$$

We begin by noting that our definitions provide $\mathrm{E}[\hat{\rho}_c(t+dt)] = \hat{\rho}(t+dt)$ and $\mathrm{E}[\hat{\rho}_c(t)] = \hat{\rho}(t)$, where we, for the second equality, used that $\int \mathfrak{D}[\gamma_n] = \int \mathfrak{D}[\gamma_{n-1}] \sum_{dN_n}$. The second equality implies that all terms that are linear in $\hat{\rho}_c(t)$ can use the replacement $\hat{\rho}_c(t) \to \hat{\rho}(t)$ when averaging. We further find

$$\mathrm{E}\left[dN_n \frac{\hat{L}\hat{\rho}_c(t)\hat{L}}{\mathrm{tr}\left\{\hat{L}^\dagger \hat{L} \hat{\rho}_c(t)\right\}} \right] = dt \hat{L}\hat{\rho}(t)\hat{L}^\dagger, \tag{E.6}$$

as well as

$$\mathrm{E}\left[dN_n \hat{\rho}_c(t)\right] = \int \mathfrak{D}[\gamma_{n-1}] dt \hat{\rho}(t,\gamma_{n-1})\,\mathrm{tr}\left\{\hat{L}^\dagger \hat{L} \hat{\rho}(t|\gamma_{n-1})\right\}, \tag{E.7}$$

and

$$\mathrm{E}\left[\hat{\rho}_c(t)\,\mathrm{tr}\left\{\hat{L}^\dagger \hat{L} \hat{\rho}_c(t)\right\}\right] = \int \mathfrak{D}[\gamma_{n-1}] \hat{\rho}(t,\gamma_{n-1})\,\mathrm{tr}\left\{\hat{L}^\dagger \hat{L} \hat{\rho}(t|\gamma_{n-1})\right\}. \tag{E.8}$$

Putting everything together now gives

$$d\hat{\rho}(t) = -idt[\hat{H}, \hat{\rho}(t)] + dt\left[\hat{L}\hat{\rho}(t)\hat{L}^\dagger - \frac{1}{2}\left\{\hat{L}^\dagger \hat{L}, \hat{\rho}(t)\right\}\right], \tag{E.9}$$

which is the Lindblad equation.

Appendix F

Derivation Eq. (5.66)

We derive Eq. (5.66) by assuming that the system only couples to one bath, thus simplifying the derivation. The derivation can be generalized to an arbitrary number of baths. At time t_0, the density matrix of the total setup (both system and bath) factorizes as $\hat{\rho}(t_0) = \hat{\rho}_S(t_0) \otimes \hat{\tau}$, where the bath is in the thermal state $\hat{\tau} = e^{-(\hat{H}_B - \mu\hat{N}_B)/k_BT}/Z$, with the bath Hamiltonian $\hat{H}_B$ and the bath number operator $\hat{N}_B$.

Before providing the derivation, we present two important identities. If $\hat{A}$ is defined on a Hilbert space $\mathcal{H}_A$ and $\hat{B}$ is defined on a Hilbert space $\mathcal{H}_B$, we have that

$$\ln\Big(\hat{A} \otimes \hat{B}\Big) = \ln\Big(\hat{A}\Big) \otimes \mathbb{1} + \mathbb{1} \otimes \ln\Big(\hat{B}\Big). \tag{F.1}$$

If $\hat{B}$ and $\hat{C}$ are defined on Hilbert spaces $\mathcal{H}_B$ and $\mathcal{H}_C$, and $\hat{A}$ is defined on $\mathcal{H}_B \otimes \mathcal{H}_C$, the following holds,

$$\mathrm{tr}\left\{\hat{A}\ln\Big(\hat{B}\Big) \otimes \mathbb{1}\right\} = \mathrm{tr}_{\mathcal{H}_B}\left\{\mathrm{tr}_{\mathcal{H}_C}\{\hat{A}\}\ln\Big(\hat{B}\Big)\right\}, \tag{F.2}$$

where $\mathrm{tr}_{\mathcal{H}_j}$ is the partial trace over $\mathcal{H}_j$.

Now we derive Eq. (5.66). We have

$$\begin{aligned} S[\hat{\rho}(t)||\hat{\rho}_S(t) \otimes \hat{\tau}] &= -S_{\mathrm{vN}}[\hat{\rho}(t)] - \mathrm{tr}\{\hat{\rho}(t)\ln[\hat{\rho}_S(t) \otimes \hat{\tau}]\} \\ &= -S_{\mathrm{vN}}[\hat{\rho}(t)] - \mathrm{tr}\{\hat{\rho}(t)\ln[\hat{\rho}_S(t)] \otimes \mathbb{1}\} - \mathrm{tr}\{\hat{\rho}(t)\mathbb{1} \otimes \ln(\hat{\tau})\} \\ &= -S_{\mathrm{vN}}[\hat{\rho}(t)] + S_{\mathrm{vN}}[\hat{\rho}_S(t)] + \frac{1}{k_BT}\,\mathrm{tr}\{(\hat{H}_B - \mu\hat{N}_B)\hat{\rho}(t)\} + \ln(Z) \\ &= S_{\mathrm{vN}}[\hat{\rho}_S(t)] - S_{\mathrm{vN}}[\hat{\rho}_S(t_0)] + \frac{1}{k_BT}\,\mathrm{tr}\{(\hat{H}_B - \mu\hat{N}_B)[\hat{\rho}(t) - \hat{\rho}(t_0)]\}, \end{aligned} \tag{F.3}$$

where we after the second equal sign used Eq. (F.1), after the third equal sign, we used Eq. (F.2), and in the last equality, we used that $S_{\mathrm{vN}}[\hat{\rho}(t)] = S_{\mathrm{vN}}[\hat{\rho}(t_0)]$.

Appendix G

Particle currents: from discrete to diffusive

In this appendix, we provide some more details on particle currents. In particular, we illustrate the relation between "jump currents" and diffusive currents.

For simplicity, we concentrate on unidirectional jumps here. That is, we only consider particles jumping from S to R, see Fig. 3.3. The total number of jumps at time t can be decomposed as

$$n(t) = \int_0^t dn(\tau), \tag{G.1}$$

where τ runs from 0 to t, and $dn(t) = n(t + dt) - n(t) = 0, 1$ is a point process with $P[dn(t) = 1] = \lambda dt$ and $P[dn(t) = 0] = 1 - \lambda dt$ with the average particle transition rate λ and the infinitesimal time increment dt. Note that $dn(t)$ at different times are independent. By discretizing time into N segments of length $dt = t/N$, we can calculate the charactersitic function of $n(t)$ as

$$\begin{aligned} \varphi_{n(t)}(s) &= \langle e^{isn(t)} \rangle \\ &= \langle e^{isdn(t)} \rangle^N \\ &= \left[1 + \frac{\lambda t}{N} \left(e^{is} - 1 \right) \right]^N \to e^{\lambda t \left(e^{is} - 1 \right)}, \end{aligned} \tag{G.2}$$

where the limit is taken with $N \to \infty$. This proves that $n(t)$ is a Poissonian process [101] with

$$P[n(t) = k] = \frac{(\lambda t)^k e^{-\lambda t}}{k!}. \tag{G.3}$$

As $dn(t)$ changes discontinuously between 0 and 1 for a jump, the particle current will be given by a series of δ-peaks,

$$I(t) = \frac{dn(t)}{dt} = \sum_j \delta(t - t_j), \tag{G.4}$$

where t_j corresponds to the times where a jump occurs. In Fig. 3.3(b), we illustrate such a current, but for a bidirectional process.

For $\lambda t \gg 1$, $n(t)$ is well-approximated as a Gaussian random variable. We now show this,

$$\begin{aligned} \ln\{P[n(t) = k]\} &= k \ln(\lambda t) - \ln(k!) - \lambda t \\ &\simeq k \ln\left(\frac{\lambda t}{k}\right) + (k - \lambda t) - \ln\left(\sqrt{2\pi k}\right) \\ &= -(x + \lambda t) \ln\left(1 + \frac{x}{\lambda t}\right) + x - \ln\left(\sqrt{2\pi(x + \lambda t)}\right), \end{aligned} \tag{G.5}$$

where we used Stirling's approximation in the second line, and introduced the variable $x = k - \lambda t$ in the third line. We note that $k \simeq \lambda t$ on average, which means that $x \ll 1$ and $x/\lambda t \ll 1$. By using the Taylor approximation $\ln(1 + \epsilon) \simeq \epsilon - \epsilon^2/2$, we arrive at

$$\ln\{P[n(t) = k]\} \simeq -\frac{x^2}{2\lambda t} - \ln\left(\sqrt{2\pi\lambda t}\right), \tag{G.6}$$

which gives

$$P[n(t) = k] \simeq \frac{e^{-(k-\lambda t)^2/2\lambda t}}{\sqrt{2\pi\lambda t}}, \tag{G.7}$$

proving that $n(t)$ is approximately Gaussian for $\lambda t \gg 1$. This means that we can write

$$n(t) \simeq \lambda t + \sqrt{\lambda} W(t), \tag{G.8}$$

where $W(t)$ is a Wiener process, see Chapter 2. For an infinitesimal increment, we get

$$dn(t) \simeq \lambda dt + \sqrt{\lambda} dW(t), \tag{G.9}$$

with the Wiener increment $dW(t)$. We now find the diffusive current

$$I(t) = \frac{dn(t)}{dt} \simeq \lambda + \sqrt{\lambda}\xi(t), \tag{G.10}$$

where $\xi(t) = dW(t)/dt$ is a white noise process as introduced in Chapter 2. That is, for $\lambda t \gg 1$, the current between S and R behaves diffusively. This is similar to homodyne detection, where a laser beam (local oscillator) is mixed with the output of an optical cavity, and then detected by a photo-detector. Note that the local oscillator and the output of the cavity have the same frequency. When the number of photons in the laser beam greatly exceeds the average number of photons in the cavity output, the detector records a signal with Gaussian, rather than Poissonian, noise [15, 16, 77].

Printed by Media-Tryck, Lund 2024 NORDIC SWAN ECOLABEL 3041 0903

Lund University
Faculty of Science
Department of Physics

ISBN 978-91-8104-027-2